UNIVERSIDADE DE SÃO PAULO

FACULDADE DE CIÊNCIAS FARMACÊUTICAS DE RIBEIRÃO PRETO

Avaliação da toxicidade e eficácia de ingredientes de uso tópico por métodos alternativos *in vitro*: culturas 2D, 3D e microfluídica de órgãos-em-chip

Renata Spagolla Napoleão Tavares

Ribeirão Preto
2020

Renata Spagolla Napoleão Tavares

Avaliação da toxicidade e eficácia de ingredientes de uso tópico por métodos alternativos *in vitro*: culturas 2D, 3D e microfluídica de órgãos-em-chip

Tese de Doutorado apresentada ao Programa de Pós-Graduação em Ciências Farmacêuticas da Faculdade de Ciências Farmacêuticas de Ribeirão Preto/USP para obtenção do Título de Doutor em Ciências

Área de Concentração: Medicamentos e Cosméticos.

Orientadora: Profa. Dra. Lorena Rigo Gaspar Cordeiro

Versão corrigida da Tese de Doutorado apresentada ao Programa de Pós-Graduação em Ciências Farmacêuticas em 27/05/2020. A versão original encontra-se disponível na Faculdade de Ciências Farmacêuticas de Ribeirão Preto/USP.

Ribeirão Preto
2020

TAVARES; R: S: N:	**Avaliação da toxicidade e eficácia de ingredientes de uso tópico por métodos alternativos *in vitro*: culturas 2D, 3D e microfluídica de órgãos-em-chip**	Espaço de **2,5 cm** reservado para etiqueta de localização da biblioteca	DOUTORADO FCFRPUSP 2020

FICHA CATALOGRÁFICA

Renata Spagolla Napoleão Tavares
Avaliação da toxicidade e eficácia de ingredientes de uso tópico por métodos alternativos *in vitro*: culturas 2D, 3D e microfluídica de órgãos-em-chip. Ribeirão Preto, 2020.
130 p.; 30cm.

Tese de Doutorado, apresentada à Faculdade de Ciências Farmacêuticas de Ribeirão Preto/USP – Área de concentração: Medicamentos e Cosméticos.
Orientador: Gaspar, Lorena Rigo.

1. Métodos alternativos *in vitro* 2. Modelo de pele humana 3. Microfluídica 4. Irritação 5. Fototoxicidade

FOLHA DE APROVAÇÃO

Renata Spagolla Napoleão Tavares
"Avaliação da toxicidade e eficácia de ingredientes de uso tópico por métodos alternativos *in vitro*: culturas 2D, 3D e microfluídica de órgãos-em-chip"

Tese de Doutorado apresentada ao Programa de Pós-Graduação em Ciências Farmacêuticas da Faculdade de Ciências Farmacêuticas de Ribeirão Preto/USP para obtenção do Título de Doutor em Ciências

Área de Concentração: Medicamentos e Cosméticos.

Aprovado em:

Banca Examinadora

Prof. Dr. _____

Instituição: _____ Assinatura:_____

Prof. Dr. _____

Instituição: _____ Assinatura:_____

Prof. Dr. _____

Instituição: _____ Assinatura:_____

Prof. Dr. _____

Instituição: _____ Assinatura:_____

Dedico esse trabalho ao Camilo, meu companheiro de todas as horas, minha sorte grande. A minha mãe querida, Kátia e ao meu irmão querido, Marcos. A Lorena pelos anos dedicados a esse trabalho.

AGRADECIMENTOS

Gostaria de agradecer a professora Lorena por ter me apresentado o maravilhoso mundo dos métodos *in vitro* alternativos à experimentação animal. Após o mestrado, pude criar um projeto de doutorado desafiador e inovador graças a todo o seu interesse na área da eficácia e toxicidade dos ingredientes que utilizam a pele humana como sistema de teste. Sou grata por todas as oportunidades que criamos juntas para que este pudesse ser realizado. Agradeço também a técnica e amiga Karina, a Carolina e aos alunos do laboratório, em especial a amiga Camila.

Agradeço a professora Dra Monika Schäfer-Korting, por ter me recebido na *Freie Universität* e especialmente ao *post-doc* Dr Christian Zoschke. Adorei ter trabalhado com todos do grupo! Especialmente, obrigada a técnica Carola Kapfer, a coordenadora do programa BB3Rs Dra Vívian, aos alunos Bárbara, Christian, Christofer, Anna, Rawan, Anne, Patrik, e as amigas Bianca e Letícia.

Agradeço imensamente ao Dr. Uwe Marx e ao Professor Dr Roland Lauster pela incrível oportunidade de me receberem na *Spin-off TissUse GmbH,* também em Berlim. Em especial a amiga e *partner* de pesquisa Thi Phuong Tao, foi muito bom poder aprender e conviver com você! Agradeço também as queridas Dras Annika Winter, Ilka Maschmeyer, Beren Ataç, Daniel Fausto e Katharina Schimek pelo suporte durante o projeto; e a Alexandra Lorenz, Reyk Horland e Sarah pelas negociações da transferência de tecnologia. Pela ótima convivência, um agradecimento especial a Oussama, Corinna, Anne, Juliane, Christine, Isi, Sascha, Locke, Flora, Henrico e aos demais pesquisadores da empresa.

Pelas considerações e contribuições ao trabalho durante o Exame de Qualificação, gostaria de agradecer aos professores Renata Fonseca Vianna Lopez, Marlus Chorilli e Laena Pernomian.

Obrigada aos funcionários da pós-graduação da FCFRP, Rafael, Rosana e em especial a Eleni.

Agradeço também a minha querida família sempre orgulhosa, me dando o apoio necessário. No mais, agradeço a todos que direta ou indiretamente fizeram parte deste.

O presente trabalho foi realizado com apoio da Fundação de Amparo à Pesquisa do Estado de São Paulo (FAPESP), do Conselho Nacional de Desenvolvimento de Científico e Tecnológico – Brasil (CNPq) e pela Coordenação de

Aperfeiçoamento de Pessoal de Nível Superior – Brasil (CAPES) – Código de Financiamento 001.

“Presentemente eu posso me considerar um sujeito de sorte porque apesar de muito moço me sinto são e salvo e forte e tenho comigo pensado Deus é brasileiro e anda do meu lado e assim já não posso sofrer no ano passado”

(Sujeito de sorte – Belchior)

SUMÁRIO

RESUMO

TAVARES; R. S. N. **Avaliação da toxicidade e eficácia de ingredientes de uso tópico por métodos alternativos *in vitro*: culturas 2D, 3D e micro fluídica (Organ-on-a-chip**). 2020. 155f Tese (Doutorado). Faculdade de Ciências Farmacêuticas de Ribeirão Preto – Universidade de São Paulo, Ribeirão Preto, 2020.

Os ensaios *in vitro* são aceitos como alternativos à experimentação animal, apenas se apresentarem alta reprodutibilidade e relevância para predizer a toxicidade em seres humanos. Assim, novas tecnologias, tais como tecidos tridimensionais (3D) foram desenvolvidas para preencher a lacuna entre os modelos *in vitro* bidimensionais (2D) e melhorar a correlação com os humanos. Mais recentemente, os sistemas microfluídicos órgãos-em-chip, que emulam a fisiologia do ambiente *in vivo* por permitirem a inclusão de diferentes organoides em um mesmo meio circulante, possuem maior potencial preditivo em relação à toxicidade humana e podem ser utilizadas durante a triagem de substâncias desconhecidas. O objetivo principal deste trabalho foi desenvolver e comparar a capacidade de sistemas *in vitro* de diferentes complexidades: culturas 2D, pele 3D cultivada de modo estático ou em microfluídica associada ao modelo de fígado, em predizer a toxicidade e eficácia das substâncias teste. Para tal, foi desenvolvido um modelo de pele - *Reconstructed Human Skin* (RHS). Na primeira abordagem, o modelo RHS foi aplicado para a avaliação da fototoxicidade e da atividade antioxidante da fucoxantina, isolada de alga antártica e com um conhecido potencial antioxidante nunca testado na pele humana. A fucoxantina se mostrou fototóxica em monocamadas e fotoinstável, porém quando adicionada em fotoprotetor se mostrou fotoestável. A fucoxantina não foi considerada fototóxica em modelo de pele, demonstrando a importância da presença do estrato córneo para confirmar a toxicidade de compostos desconhecidos. Ainda, se mostrou capaz de inibir as espécies reativas do oxigênio (ERO) de maneira significativa tanto em monocamadas quanto em modelo de pele, mostrando que mesmo em baixas concentrações, exerce efeito protetor contra ERO gerados pela radiação UVA. A etapa seguinte, o RHS foi miniaturizado para adequação em sistema de órgãos-em-chip e o RHS reduzido foi utilizado no ensaio de irritação cutânea da fucoxantina (OECD TG 439). Novas análises foram incluídas em paralelo para a identificação de novos biomarcadores da irritação nos tecidos; o controle positivo lauril sulfato de sódio (LSS) foi considerado irritante e a fucoxantina não; entretanto, a fucoxantina reduziu a expressão de gênica de interleucinas pró-inflamatórias (IL-6 e IL-8) quando no veículo etanol, e aumentou a expressão de NAT1, indicando sua metabolização pela pele e efeito protetor aos efeitos deletérios do etanol. Na terceira abordagem, ensaio de irritação cutânea do RHS reduzido foi avaliado tanto em cultivo estático, quanto dinâmico, para tal, o fármaco de escolha foi o antifúngico terbinafina, por se acumular na pele humana e ter potencial hepatotóxico em terapias de longo prazo. No modelo dinâmico, o RHS foi associado a modelo de fígado e o sistema foi chamado de Chip2. Tanto no RHS estático quanto no Chip2 a terbinafina não foi considerada irritante enquanto que o controle positivo LSS foi o único considerado irritante, por meio dos resultados metabólicos, de liberação de IL-6 e ainda pela análise de viabilidade celular por LDH e MTT (nos tecidos estáticos). Demonstrou também efeitos deletérios nos esferoides de fígado, mostrando ter atravessado o modelo de RHS. Entretanto, no RHS a concentração tópica de terbinafina a 5% no Chip2 aumentou a expressão de IL-1α e ainda aumentou células apoptóticas e diminuiu as proliferativas nos esferoides de fígado, aumentando também a expressão das enzimas hepáticas CYP1A2 e CYP3A4, o que prova que também atravessou o RHS para exercer os efeitos

observados no fígado. A aplicação sistêmica de 0,1% de terbinafina aumentou a expressão de EGFR apenas no RHS do Chip2 e aumentou as células apoptóticas no fígado, além de regular negativamente a albumina e regular positivamente CYP2C9, agindo como um controle hepatotóxico de terbinafina. A combinação de RHS e fígado no Chip2 em microfluídica permitiu uma resposta mais sensível do RHS observado apenas pela expressão gênica e permitiu a avaliação de efeitos hepáticos causados pelas substâncias capazes de atravessar o RHS. Em conclusão, o aumento da complexidade dos ensaios *in vitro* desenvolvidos no presente trabalho abrem novas perspectivas para a avaliação da toxicidade e da eficácia de substâncias teste, com o potencial para melhorar a predição dos estudos pré-clínicos.

Palavras-chave: Métodos alternativos *in vitro*, modelo de pele humana, microfluídica, esferoide de fígado, órgãos em chip, irritação, citotoxicidade, fototoxicidade.

ABSTRACT

TAVARES; R. S. N. **Toxicity assessment of topical ingredients by *in vitro* alternative methods: 2D, 3D and microfluidic (Organ-on-a-chip) cultures**. 2020. 155f. Thesis (Doctoral). Faculdade de Ciências Farmacêuticas de Ribeirão Preto – Universidade de São Paulo, Ribeirão Preto, 2020.

In vitro tests are accepted as alternatives to animal experimentation, only if they have high reproducibility and relevance for predicting toxicity in humans. Thus, new technologies such as three-dimensional (3D) reconstructed tissues have been developed to fill the gap between two-dimensional (2D) *in vitro* models and improve the correlation with humans. More recently, microfluidic organ-on-a-chip systems, which emulate the physiology of the *in vivo* environment by allowing the inclusion of different organoids in the same circulating medium, have greater predictive potential for human toxicity and can be used during the screening of unknown substances. The objective of this study was to develop and compare the capacity of *in vitro* systems of different complexities: 2D cultures, 3D skin cultivated in a static way or in microfluidic associated to a liver model, to predict the toxicity and efficacy of the test substances, following established protocols and internationally recommended. To this end, a reconstructed human skin (RHS) was developed In the first approach, the RHS model was applied for the evaluation of phototoxicity and antioxidant activity of fucoxanthin, isolated from Antarctic algae, with promising antioxidant activity never tested in the human skin. Fucoxanthin was shown to be phototoxic in the monolayer assay and photo unstable, but when added in a sunscreen it was shown to be photostable. Fucoxanthin was not considered phototoxic in the RHS, demonstrating the importance of the stratum corneum to confirm the toxicity of unknown compounds. It was also shown to inhibit reactive oxygen species (ROS) significantly in both monolayers and RHS, demonstrating that even at low concentrations it exerts a protective effect against ROS generated by UVA radiation. The next step, RHS was miniaturized for adaptation in an organ-chip system and the reduced RHS was used in the fucoxanthin skin irritation test (OECD TG 439). New analyses were included in parallel for the identification of new biomarkers of tissue irritation; the positive control of sodium lauryl sulfate (LSS) was considered irritant and fucoxanthin was not; however, fucoxanthin reduced the gene expression of pro-inflammatory interleukins (IL-6 and IL-8) when in the ethanol vehicle, and increased the expression of NAT1, indicating its metabolization by the skin and protective effect to the deleterious effects of ethanol. In the third approach, the reduced RHS skin irritation test was evaluated both in static and dynamic culture, for which the drug of choice was the antifungal terbinafine, as it accumulates in human skin and has hepatotoxic potential in long-term therapies. In the dynamic model, RHS was associated with the liver model and the system was called Chip2. In both static RHS and Chip2, terbinafine was not considered irritant, while the LSS positive control was the only one considered irritant, through metabolic results, IL-6 release and also through cell viability analysis by LDH and MTT (in static tissues). It also demonstrated deleterious effects on liver spheroids, showing to have passed through the RHS model. However, in RHS the topical concentration of 5% terbinafine in Chip2 increased IL-1α expression; in liver spheroids it increased apoptotic cells and decreased proliferative cells, and also increased CYP1A2 and CYP3A4 enzyme expression, proving that it also passed through RHS to exert the effects observed in the liver. The systemic application of terbinafine of 0.1% increased EGFR expression only in the RHS of Chip2 and increased the apoptotic cells in the liver, in addition to

regulating albumin negatively and regulating CYP2C9 positively, acting as a hepatotoxic control of terbinafine. The combination of RHS and liver on Chip2 in microfluidics allowed a more sensitive response of RHS observed only by gene expression and allowed the evaluation of liver effects caused by substances capable of passing through RHS. In conclusion, the increased complexity of the in vitro tests developed in this work opens new perspectives for the evaluation of the toxicity and efficacy of test substances, with the potential to improve the prediction of preclinical studies.

Keywords: Alternative methods, in vitro, human skin model, microfluidics, liver spheroid, two organs-on-a-chip, irritation, cytotoxicity.

LISTA DE FIGURAS

4.3 CAPÍTULO 3 – Avaliação de toxicidade da terbinafina por via tópica e sistêmica em condição estática versus dinâmica (organ-on-a-chip)

Artigo 3: TAVARES, R. S. N.; TAO, T. P.; MASCHMEYER, I.; SCHÄFER-KORTING, M.; ZOSCHKE, C.; WINTER, A.; MARIA-ENGLER, S. S.; MARX, U.; GASPAR, L. R.1. Toxicity of Topically Applied Drugs Beyond Skin Irritation: Static Skin Model vs Two Organs-on-a-Chip, submitted to Int J Pharmaceutics.

LISTA DE TABELAS

LISTA DE ABREVIATURAS E SIGLAS

3T3 NRU PT	3T3 *Neutral Red Uptake* - i.e. teste de fototoxicidade por captação do vermelho neutro em fibroblastos murinos 3T3
ANVISA	Agência Nacional de Vigilância Sanitária
CH_2Cl_2	Diclorometano
CLV	Cromatografia Líquida à Vacuo
CONCEA	Conselho Nacional de Controle de Experimentação Animal
DAD	Detector de Arranjos de Diodos
-dd	Duplo dupleto
DMEM	*Dulbecco's modified eagle médium*
DMSO	Dimetilsulfóxido
ECVAM	*European Union Reference Laboratory for alternatives to animal testing*
ERO	Espécies reativas do oxigênio
ESI	Ionização por "*Electrospray*"
Fx	Fucoxantina
HPLC	Cromatografia Líquida de Alta Eficiência
ICH	*International Council for Harmonization*
MeOH	Metanol
MHz	*Megahertz*
Min	Minutos
MPE	*Mean photo effect*
NADPH	*Nicotinamide adenine dinucleotide phosphate reduced*
OECD	*Organization for economic co-operation and development*
PIF	*Photo irritation fator*
RHS	*Reconstructed Human Skin*
RMN ^{13}C	*Ressonância Magnética Nuclear de Hidrogênio Treze*
RMN ^{1}H	*Ressonância Magnética Nuclear de Hidrogênio Um*
ROS	*Reactive oxigen species*
Terb	Terbinafina
UV	Ultravioleta
UVA	Ultravioleta A
UVB	Ultravioleta B
UVC	Ultravioleta C

LISTA DE SÍMBOLOS

α	Alfa
™	Trademark
®	Marca Registrada
©	Copyright
°C	Graus Celsius
µg/ mL	Microgramas por mililitro
µL	Microlitro
cis	Isômero cis
g	Grama
H1	Hidrogênio
J	Joule
mL	Mililitro
trans	Isômero *trans*
W	Watts
δ	Deslocamento químico
λ	Comprimento de onda
nm	Nanômetros
s	*Singleto*
t	*Tripleto*
-m	Multipleto
-Me	Metila
-d	*Dupleto*
eq	Posição equatorial

1. INTRODUÇÃO

No Brasil, seguindo o processo de redução da experimentação animal criado pela a Lei Arouca (Lei nº 11.794, de 8 de outubro de 2008), em 2014, o Conselho Nacional de Controle de Experimentação Animal (CONCEA) publicou duas Resoluções Normativas (RN) nº 17, 18 (03 de julho, 24 de setembro de 2014, respectivamente) que estabeleceram o prazo de cinco anos (até 2019) para a proibição do uso de animais para 17 desfechos cujos métodos alternativos para substituição do modelo animal foram validados por centros da validação e reconhecidos e publicados pela Organização para a Cooperação e Desenvolvimento Econômico (OECD). No ano seguinte, a Agência Nacional de Vigilância Sanitária (ANVISA) reconheceu os métodos pela resolução da diretoria colegiada nº35 (de 10 de agosto de 2015). Em 2021, será o prazo máximo para a substituição de mais sete métodos alternativos citados da RN nº 31 de 18 de agosto de 2016.

Este fato se deu após uma série de acontecimentos históricos iniciados pela mobilização internacional para a substituição de animais de experimentação em pesquisa na União Europeia em 1991 e estendeu-se para outros países. Desde então, muitos avanços têm sido observados nessa área, o que culminou no desenvolvimento e aceitação, pela OECD, de diferentes métodos para a redução e substituição dos ensaios em animais para a avaliação da segurança de compostos, uma vez que estes ensaios alternativos apresentam alta relevância e reprodutibilidade (HARTUNG, 2018). Em 2010, foi publicada a Diretiva Europeia (2010/63/UE) relativa à proteção dos animais utilizados para fins científicos, para cumprir a prioridade dos testes não-animais para todos os desfechos previstos na legislação da União Europeia.

Entretanto, no Brasil, para os testes que dependem de tecidos humanos reconstituídos, ainda é inadequada a burocracia envolvida na importação de tecidos comerciais ou insumos necessários para a sua produção no país. Esta questão vem sendo discutida junto à ANVISA para que a comercialização ou importação dos modelos oriundos de engenharia tecidual, como os modelos de pele, seja facilitada. Assim, protocolos internos (*in house*) de confecção desses tecidos são necessários e têm sido desenvolvidos por alguns grupos de pesquisa, mas os mesmos precisam ser validados para o uso pretendido (DE VECCHI et al., 2018; TAVARES et al., 2020).

Os sistemas de cultivo desses tecidos reconstituídos tridimensionais (3D) surgem como uma ponte para preencher a lacuna entre os modelos *in vitro* bidimendionais (2D) ou em monocamadas, e os modelos *in vivo;* ao exemplo do modelo de epiderme humana reconstituída, produzida a partir da proliferação e diferenciação de

queratinócitos humanos, que é reconhecida pela OECD para a avaliação dos desfechos de corrosão (TG 431, OECD, 2014) e irritação cutâneas (TG 439 OECD, 2015) em substituição ao modelo animal (DE VECCHI et al., 2018).

Avançando cada vez mais nas tecnologias de ponta disponíveis atualmente, os modelos 3D *in vitro* também apresentam limitações uma vez que os ensaios atuais são baseados em sua maioria em culturas estáticas (ATAÇ et al., 2013), os quais não conseguem mimetizar os arranjos complexos dos diferentes órgãos do corpo humano e suas funções (HASENBERG et al., 2015). Para isso, os modelos em chip, que são ferramentas planejadas fluidas e complexas, possuem o potencial de acelerar ainda mais a tradução de descobertas básicas em novas estratégias de tratamento mais efetivas, visto que essas propriedades de simular a fisiologia são cruciais para testes de toxicidade durante a triagem de substâncias desconhecidas (ATAÇ et al., 2013).

Os chips com múltiplos "órgãos" oferecem a oportunidade de estudar como uma substância afeta um modelo *in vitro* interconectado e perfundido, acrescido da influência de função hepática na avaliação da substância (TAVARES et al., 2020). Por esse motivo, dentre os vários órgãos, a serem associados a uma pele 3D, o fígado é o mais adequado para aplicações micro tecnológicas, visto que este possui uma microarquitetura extremamente complexa que é controlado por um preciso microambiente com interações micrométricas (YOON NO et al., 2015). Além disso, o fígado é o responsável pelo processo de desintoxicação, metabolismo de carboidratos, lipídios e proteínas, assim como a biotransformação de substâncias endógenas e exógenas (ALÉPÉE et al., 2014; YOON NO et al., 2015).

Na presente tese, desenvolvemos um rápido protocolo de pele humana reconstituída (*Reconstructed Human Skin* – RHS) cultivado em 10 dias totalmente compatível com as plataformas de órgãos-em-chip (*organ-on-a-chip)*. Utilizamos dois dos guias publicados pela OECD e reconhecidos pelo CONCEA e pela ANVISA, o de fototoxicidade em monocamadas, 2D (OECD TG 432) e o de irritação em modelo de pele 3D (OECD TG 439), bem como o ensaio de fotoirritação em modelo de pele 3D recomendado pelo Conselho Internacional de Hamonização (*Intenational Council for Hamonization* –ICH) e pré-validado pela *European Centre for the Validation of Alternative Methods* (ECVAM) (ICH, 2013).

Ainda, para os ensaios de irritação no modelo de pele, com o objetivo de obter uma visão mais detalhada sobre a toxicidade cutânea da substância teste, avaliamos a viabilidade dos tecidos de acordo com as diretrizes de ensaio da OECD nº 439 bem

como avaliação de padrões morfofisiológicos, alterações na inflamação (IL-1, IL-6, IL-8), homeostase (EGFR, HSPB1) e metabolismo (NAT1).

Para a avaliação da irritação cutânea no chip, seguimos o mesmo modelo de estudo, realizando análises além-viabilidade por MTT, tais quais as já citadas para o modelo de pele bem como as específicas ao fígado, como genes de metabolismo (CYPs), de homeostase (albumina) e perfil metabólico, para sugerir novos biomarcadores de detecção do processo de irritação e toxicidades inerentes, bem como para ampliar as informações acerca do ensaio validado.

2. REVISÃO DA LITERATURA

2.1 Contextualização dos métodos *in vitro* alternativos à experimentação animal

Desde a sua publicação em 1959, *The Principles of Humane Experimental Technique*, de Russell e Burch, que introduziu o conceito dos Três Rs (Redução, Refinamento e Substituição), as leis e práticas relacionadas ao uso de animais de laboratório em educação, pesquisa e testes têm mudado (BALLS, 2018).

A substituição dos ensaios em animais por procedimentos e estratégias de ensaio alternativos mais relevantes e mais confiáveis para prever os perigos potenciais de produtos químicos e cosméticos para os seres humanos vêm chamado a atenção de cientistas, políticos e consumidores. Esta substituição vem ocorrendo pois apesar de, em muitos casos, os experimentos em animais serem considerados padrão ouro, eles têm provado serem imprecisos devido a distância filogenética e as falhas metodológica (DEHNE; HASENBERG; MARX, 2017). Além disso, essa falha em prever a eficácia e toxicidade nos ensaios pré-clínicos leva a sérios atrasos no desenvolvimento de novos fármacos, exposição de pessoas a substâncias ineficazes e até efeitos colaterais indesejados, desperdiçando os investimentos da fase clínica, ou seja, a parte mais cara do processo de desenvolvimento de fármacos (MARX et al., 2016).

Um exemplo de substituição direta é a aplicação de um potente irritante nos olhos isolados de coelhos ao invés de aplicar diretamente nos olhos de um coelho intacto, neste caso o método *in vitro* ainda possui a mesma desvantagem do *in vivo*. Já a substituição indireta envolve uma abordagem experimental diferente, tal como o teste de fármacos em hepatócitos humanos ao invés de administrar a ratos ou cachorros, que possuem metabolismo diferente (BALLS, 2018).

Os testes de toxicidade são realizados para caracterizar os efeitos potencialmente adversos das substâncias químicas na saúde humana, na saúde animal ou no ambiente, com vista a garantir a utilização mais segura possível das substâncias químicas e dos produtos químicos que as contenham (WORTH, 2018). Em geral, os testes de toxicidade são realizados pela indústria ou por empresas de pesquisa auditadas e terceirizadas pelas indústrias, e as avaliações resultantes são submetidas às autoridades para cumprir os requisitos legais e regulamentares para a gestão de risco de produtos químicos (WORTH et al., 2014).

Todos os ensaios de toxicidade preconizados pelas agências reguladoras foram anteriormente validados e aceitos pelas organizações internacionais. A

validação pode ser entendida como o processo pelo qual se estabelece a confiabilidade e a relevância de um novo método para um fim específico (MARX et al., 2020); a confiabilidade é definida como o grau de reprodutibilidade dos resultados de um teste utilizando o mesmo protocolo intra e inter laboratórios ao longo do tempo, enquanto que relevância de um método de teste descreve a relação entre o teste e o efeito na espécie alvo e se o método de teste é significativo e útil para um propósito definido (MARX et al., 2020). Estes desenvolvimentos foram amplamente acelerados pela criação do ECVAM em 1992 e de organismos de validação nacionais semelhantes em muitos países nas décadas seguintes (MARX et al., 2020).

No Brasil, a legislação para a proteção animal começou em 1934, com uma lei contra crueldade animal, incluindo o reconhecimento e a proteção de todos os animais pelo Estado. Em seguida, uma lei sobre crimes ambientais, pela primeira vez estabeleceu o dever de respeitar os cuidados adequados com os animais por parte dos envolvidos no uso dos mesmos, incluindo o uso em experimentos ou para educação. Entretanto, foi apenas em 2008 que o Brasil adotou a lei 11.794, que especificamente regulamentou o uso de animais em laboratório para experimentação e educação. Essa lei representou um significativo avanço para o País e criou duas novas ações: a criação do CONCEA, implementado pelo Decreto 6.899 de 2009 (BRASIL, 2009), e a obrigação da criação da Comissão de Ética no Uso de Animais (CEUA) por todas as instituições que utilizassem os animais (CURREN; ESKES; CHENG, 2018).

O CONCEA é um conselho multi-institucional que representa diferentes Ministérios governamentais, associações, sociedades científicas e organizações não governamentais (ONGs), e possui dentre outras competências o dever de controlar e monitorar a implementação de métodos alternativos (CURREN; ESKES; CHENG, 2018).

Desde 2003, a ANVISA reconheceu o uso dos métodos *in vitro* como testes pré-clínicos para análise de segurança de produtos cosméticos. Este protocolo foi revisado e 2012, e incluiu vários dos métodos 3Rs validados e aceitos na União Europeia, incluindo avaliação *in silico*, métodos *in vitro*, a utilização dos dados existentes e dos princípios de extrapolação. Em especial, sugere-se a utilização de ensaios pré-clínicos *in vitro* para a avaliação do potencial de irritação e corrosão ocular, da fototoxicidade e da absorção cutânea (CURREN et al. 2019, BRASIL, 2014).

A Rede Nacional de Métodos Alternativos (ReNaMA), da qual nosso laboratório faz parte, foi criada pelo Ministério de Cultura, Tecnologia e Inovações (MCTI) e é composta por três laboratórios centrais (Instituto Nacional de Controle de Qualidade em Saúde - INCQS; Instituto Nacional de Metrologia, Qualidade e Tecnologia – INMETRO e o Laboratório Nacional de Biociências - LNBio) e aproximadamente 40 laboratórios associados, privados e de universidades públicas, que trabalham com os métodos alternativos à experimentação animal. Essa rede visa promover treinamentos para implementação dos métodos alternativos ao ensaios em animais, monitorar a proficiência dos laboratórios que os conduzem, promover alta qualidade dos materiais de referência e dos métodos alternativos e as Boas Práticas de Laboratório, promover desenvolvimento de estudos de validação e adoção de novos métodos alternativos ao uso animal (CURREN; ESKES; CHENG, 2018).

2.2. Ensaios em monocamadas - 2D

Culturas celulares podem ser divididas em três tipos: culturas primárias, secundárias e linhagens contínuas. Células primárias e secundárias são usualmente diploides (com vida finita). Culturas primárias são derivadas diretamente de tecidos intactos como fígado ou rins, já culturas secundárias são derivadas das culturas primárias. Esses tipos usualmente envolvem células diploides, entretanto células de linhagens, geralmente derivadas de tecidos malignos, tendem a ser aneuploides (imortais) (HEINONEN; VERFAILLIE, 2018).

A primeiras culturas surgidas foram de explantes teciduais, mas após o conhecimento do processo de tripsinização, em 1916, as subculturas de células dissociadas promoveram um grande desenvolvimento passando a ser cultivadas em frascos de vidro e em placas para a formação de monocamadas. Outro pré-requisito para o sucesso das culturas foi o desenvolvimento de um meio definido. Ao exemplo do isolamento das células HeLa e dos fibroblastos WI-38 que foram marcos no desenvolvimento e uso de testes de monocamada *in vitro (HEINONEN; VERFAILLIE, 2018).*

Embora o potencial de crescimento ilimitado das linhagens celulares contínuas seja uma vantagem, a sua imortalização não o é, pois são cariotipicamente anormais e acumulam mutações que podem afetar o valor dos dados que fornecem. Por estas razões, estão a ser desenvolvidos novos sistemas de modelos, baseados em células que são expansíveis, mas que permanecem representativas dos seus tecidos de

origem. O estabelecimento de linhagens celulares permanentes através da indução da excessiva expressão da telomerase pode ser útil, mas não tem sido muito bem-sucedido até agora. Outra opção é estabelecer modelos baseados em células que têm naturalmente uma elevada atividade da telomerase, ou seja, células estaminais, que podem ser induzidas a diferenciar-se numa variedade de células fenotípicas e geneticamente "normais", representativas das condições *in vivo* (JENNINGS, 2015).

Os ensaios baseados em células têm sido um pilar importante do processo de descoberta de medicamentos, a fim de proporcionar uma ferramenta relativamente simples, rápida e rentável para evitar ensaios em animais em grande escala e dispendiosos. Até recentemente, a maioria das pesquisas para descoberta de medicamentos ou toxicologia *in vitro* era baseada em sistemas de cultura 2D ou testes em animais (HEINONEN; VERFAILLIE, 2018). No entanto, apenas cerca de 8% dos compostos passam para a fase de desenvolvimento clínico e muitos medicamentos falham em ensaios clínicos, em grande parte devido à eficácia clínica limitada ou à toxicidade imprevista e inaceitável (HEINONEN; VERFAILLIE, 2018).

As células cultivadas em placas não são capazes de aglomerar-se umas sobre as outras, mas sim crescer em monocamadas, o que não é natural para todos os tipos de células. Ainda, o estabelecimento de co-culturas em uma só placa pode aumentar o contato intercelular natural e a comunicação, mas a superfície 2D ainda inibe a capacidade das células formarem uma estrutura multidimensional (ANTONI et al., 2015). Como as culturas 2D não podem preservar a maioria das funções de diferenciação celular, acredita-se que os sistemas de cultura 3D *in vitro* ao permitirem uma melhor preservação dos fenótipos de diferenciação celular, têm o potencial de melhorar a predição do metabolismo e da toxicidade dos medicamentos (ANTONI et al., 2015).

2.3. Ensaios em modelos 3D

Células cultivadas em sistemas 3D conseguem manter suas diferenças comportamentais e perfis de expressão melhores que células cultivadas em sistemas 2D, pois refletem situações *in vivo* devido à disponibilidade de matriz extracelular e características mecânicas de microambiente *in vivo*.

Desde o início do século XIX, pesquisadores como Ross Harrison (1906) tentando recapitular a organogênese dos sistemas *in vivo*, desenvolveram o primeiro sistema de cultura 3D conhecido como *hanging-drop* (HEINONEN; VERFAILLIE,

2018). Esta técnica foi adotada por muitos cientistas e, nos anos 50, os tecidos de muitos órgãos foram cultivados utilizando técnicas semelhantes.

As matrizes 3D dividem-se em três grandes categorias: matrizes biológicas, sintéticas e híbridas de inspiração biológica (HEINONEN; VERFAILLIE, 2018). As matrizes 3D mais comumente usadas são derivadas da matriz extracelular de fontes biológicas. Elas têm a vantagem de que a própria matriz 3D inicia a sinalização celular em várias situações. Além disso, os componentes moleculares da matriz extracelular podem funcionar como moléculas bioativas e podem atuar como ligantes para uma série de receptores de superfície celular (adesão), ativando vias de sinalização desses receptores (HEINONEN; VERFAILLIE, 2018).

Sabendo-se que o colágeno é um componente universal dos tecidos conjuntivos, pesquisadores do início do século XX, observaram que as células passaram a crescer e sobreviver melhor em uma camada de colágeno seco do que em uma superfície de vidro ou em coágulos de plasma. Hoje em dia, o colágeno tipo I pode ser isolado de várias fontes biológicas, incluindo pele bovina, cauda de rato e placenta humana (HEINONEN; VERFAILLIE, 2018).

2.4. Modelo de pele reconstituída e modelo de fígado

A complexidade dos órgãos *in vivo* é difícil de emular, ao exemplo das localizações de células nos tecidos e junções que são difíceis de reproduzir usando sistemas de co-cultura em que diferentes tipos de células são misturadas e semeadas aleatoriamente (YOON NO et al., 2015).

Sendo assim, quando se fala de um organoide, não se trata de uma co-cultura simples. Ao exemplo da pele humana reconstituída e dos esferoides de fígado.

A pele, principal interface entre o corpo humano e o meio ambiente, é exposta a produtos químicos, cosméticos, detergentes, luz ultravioleta, patógenos, poluentes ambientais e microrganismos (WORTH et al., 2014; WUFUER et al., 2016). Sendo assim, sua principal função é proteger os órgãos, servindo como uma barreira fisiológica e, como tal, é necessário investigar a toxicidade e a eficácia dos materiais que podem gerar potenciais reações, tais como inflamação, irritação, alergias e câncer (WUFUER et al., 2016).

Experimentos em animais, principalmente em ratos, têm sido realizados em todo o mundo; no entanto, esses modelos têm duas limitações críticas. A primeira

compreende questões éticas e regulamentares, e a segunda é a considerável diferença entre a pele do rato e a pele humana, ou seja, na espessura, densidade e apêndices (WUFUER et al., 2016).

Desde o primeiro registro da construções de pele humana reconstituída no início da década de 1980, diversos modelos de pele *in vitro* têm sido desenvolvidos e comercializados (WUFUER et al., 2016), contudo, a maioria destes modelos publicados nos guias OECD que utilizam a pele como sistema teste, são de epiderme humana reconstituída (*Reconstructed Human Epidermis* - RhE). Estes modelos não propiciam interações entre queratinócitos e fibroblastos, que são os maiores constituintes da pele humana. Por essa razão, todos os estudos realizados com modelos de pele, na presente tese, foram realizados com modelos *in house* de pele inteira reconstituída (epiderme e derme).

Dentre os vários órgãos do corpo humano, o fígado é um dos mais adequados para aplicações microtecnológicas, devido à sua microarquitetura extremamente complexa. Além disso, o fígado é responsável pelo metabolismo de fármacos e toxinas, que é crucial para a sobrevivência e não pode ser comprometida. Devido à urgente necessidade do desenvolvimento de uma plataforma *in vitro* 3D utilizando células humanas para reproduzir este órgão, nas últimas décadas diversas microtecnologias foram empregadas, tais como cultura de pellets, cultura de spinner, *hanging drop*, superfície não adesiva, força externa, folhas de células e micromoldagem (YOON NO et al., 2015).

No presente trabalho, utilizamos células diferenciadas de HepaRG, conhecidas por sua capacidade de formar estruturas de canalículos biliares em cultura (MATERNE; MASCHMEYER; LORENZ; HORLAND *et al.*, 2015), e as combinamos com células primárias de HSteC (esteladas) para a produção de esferoides hepáticos, isto sem a utilização de polímeros de suporte.

2.5. Ensaio irritação e fotoirritação cutâneas

Ao contrário dos ensaios em monocamadas que são limitados a substâncias solúveis em água, nos modelo 3D como o de pele reconstituída pode-se testar qualquer tipo de substância, incluindo os produtos acabados (CANAVEZ et al., 2017). Sendo assim, os testes usando modelo de pele tornaram-se a melhor alternativa no

desenvolvimento de cosméticos, pois os efeitos adversos na pele são de grande preocupação para a segurança ocupacional e do consumidor (WORTH et al., 2014).

O guia de irritação cutânea (OECD nº 439) foi desenvolvido e adotado em 2010 em modelo de epiderme humana reconstituída (*Reconstructed Human Epidermis – RhE),* Sendo assim, quatro modelos comerciais preenchem os requisitos de qualidade e reprodutibilidade e foram validados pela OECD: EPISKIN™ SIT, validado pela performance padrão da ECVAM. EpiDerm™ EPI-200-SIT, SkinEthic™ RHE SIT42bis e Labcyte EPI-MODEL 24SIT, validados pela performance padrão da OECD (ESKES; HOFMANN, 2017); e em 2019 o guia foi atualizado para incluir mais dois modelos de pele, o epiCS® e o Skin+ ® que foram validados, mas ainda estão em vias de aprovação (OECD, 2019). No entanto, o guia de irritação preconiza a classificação do potencial irritante apenas se baseando na viabilidade dos tecidos pelo ensaio do MTT, mas vários outros biomarcadores podem ampliar a predição de toxicidade se realizados em paralelo, ao exemplo da avaliação da expressão de genes envolvidos na cascata da irritação, quantificação de interleucinas liberadas no meio cultura, imunolocalização de proteínas de proteção da pele, ou proliferação e apoptose dos tecidos tratados com as substâncias.

Ainda, para substâncias que absorvem na região do UV/VIS, o ICH de fototoxicidade recomenda que a avaliação da fotoirritação se dê por uma estratégia de ensaios em “fases”, ou seja, que primeiramente se utilize o guia validado OECD TG 432, 3T3NRU-PT, ensaio que utiliza fibroblastos 3T3 em monocamadas (2D) (ICH, 2013; OECD, 2019) e em caso de resultado positivo para fototoxicidade, o próximo teste seja avaliado em RhE, que é uma cultura de queratinócitos primários em 3D (CERIDONO et al., 2012; GASPAR; KAWAKAMI; BENEVENUTO, 2017; ICH, 2013; LELIÈVRE et al., 2007). Esta recomendação se dá pelo fato de que o primeiro ensaio não avalia a biodisponibilidade da substância teste frente ao estrato córneo da pele, o que pode gerar resultados falso positivos. Esta biodisponibilidade também é imprescindível quando a avaliação é em relação a atividade antioxidante, o teste em modelo de pele consegue provar a capacidade da substância em permear ou não até a epiderme viável, para exercer a atividade antioxidante, após a absorção pela pele.

No entanto, todos os ensaios mencionados são realizados em cultivo estático dos tecidos, os recentes avanços nos sistemas microfluídicos têm permitido a modelagem da fisiologia de vários órgãos. Estes chamados sistemas *organ-on-a-chip*, bem como os “*skin-on-a-chip”* têm o potencial de oferecer modelos fisiologicamente

relevantes tanto para estudo de doenças (WUFUER et al., 2016) quanto para avaliação da toxicidade e eficácia de medicamentos.

2.6. Ensaios de organoides em microfluídica

Os avanços nos métodos *in vitro* levaram ao desenvolvimento de modelos estáticos de cultura de células humanas de relevância fisiológica crescente. No entanto, as limitações na predição da verdadeira resposta humana a medicamentos e produtos químicos, tanto em termos de eficácia como de toxicidade, levaram ao desenvolvimento de modelos de cultura micro fluídica mais complexos, muitas vezes denominados sistemas microfisiológicos (DEHNE; HASENBERG; MARX, 2017). Estes sistemas são projetados para emular um ambiente semelhante ao *in vivo* (*vivo-like)* para culturas celulares *in vitro* e para mimetizar a biologia humana na menor escala aceitável, incluir fluxo de meio de cultura, realizar leituras funcionais e associar a um sistema multi-órgãos (DEHNE; HASENBERG; MARX, 2017).

Existem vários grupos desenvolvendo sistemas de chip para organoides únicos ou em associação. Dentre os maiores grupos para cultivo de organoide único a Mimetas, startup da Universidade de Leiden, desenvolveu o sistema em placa sem bomba. Já a Emulate Inc do Wyss Institute e a NORTIS da Universidade de Washington recentemente desenvolveram um chip de fígado associado a rim, em polidimetilsiloxano. A Philip Morris International desenvolveu um chip de dois órgãos de fígado conectado a organoide de pulmão em material não absorvente e biocompatível que contém uma microbomba acoplada e controlada por um aplicativo. A Insphero da ETH Zurique, produz organoides com modelos de doença, mas não o chip. A Cnbio innovations do MIT produz até cinco órgãos em placa microfluídica que é acoplada em uma unidade independente de incubacão e fluídica. Já a incubada Hesperos da Universidade Central Florida, possui o modelo de chip de vários órgãos associados em uma microfluídica controlada pela gravidade.

A principal vantagem dos chips da *spin-off* TissUse GmbH em relação aos chips dos outros grupos disponíveis, está na possibilidade de agregar a maioria dos fatores desejáveis da tecnologia microfluídica: Associação de organoides, com perfusão ativa, com vasculatura biológica, em arranjo de vários órgãos, com a bomba pulsátil em conformidade com farmacocinética e farmacodinâmica, apresenta designs fisiológicos, o que permite realizar estudos com aplicações únicas ou repetidas,

aplicações sistêmicas por vários dias e também modelos de doença (EWART et al., 2017).

A busca pelo ser humano em chip, ou seja, associação de mais de 10 órgãos em um único chip, não visa apenas a co-cultura de diferentes organoides relevantes em um único meio circulante, mas também obter uma homeostase auto suficientemente orgânica. Para tal, é certo que os sistemas circulatório, endócrino, gastrointestinal, imune, tegumentar, musculoesquelético, nervoso, reprodutivo, respiratório e urinário precisam estar presentes. Até o momento, chips contendo associação de dois órgãos; de fígado com pele; fígado com intestino; fígado com neurônio; fígado com pâncreas; fígado com pulmão, e com quatro órgãos (intestino, fígado, pele e rins ou intestino, fígado, neurônio e pele) já foram associados com sucesso. Além disso, músculo esquelético, tecido adiposo, modelo de folículo, medula óssea, linfonodo, vasculatura e modelo de tumor de pulmão, também já estão sendo produzidos (DEHNE; HASENBERG; MARX, 2017).

Devido ao alto potencial dos sistemas microfluídicos, tem sido observado um grande apoio financeiro por parte dos órgãos governamentais (US National Institutes of Health - NIH) e regulatórios (Food and Drug Administration - FDA) norte americanos e pelo Horizon 2020, da Comunidade Europeia, para o desenvolvimento desses sistemas. Além disso, as indústrias farmacêuticas têm feito parcerias para validação do modelo para diferentes propósitos. Especificamente a TissUse possui parceria com a Roche, Bayer, AstraZeneca, Boehringer Ingelheim, Beiersdorf, entre outras, para o desenvolvimento de diferentes modelos e abordagens para avaliação da toxicidade e risco baseados em mecanismos de ação. Grandes projetos apoiados pela Comissão Europeia possuem como proposta não somente a adoção desse modelo pelas indústrias, mas também como um caminho visando à aceitação regulatória em 2020 (EWART et al., 2017), uma vez que pesquisa regulatórias, com fármacos retirados do mercado, devido à sua alta toxicidade não prevista em ensaios pré-clínicos e clínicos fase 1 e 2, como é o caso do troglitazona (WAGNER et al., 2013), já tem produzido resultados satisfatórios.

Assim que um ensaio validado de segurança ou eficácia baseado em chip humano conseguir excluir um fármaco nos estudos pré-clínicos antes mesmo de serem testados em animais pela indústria farmacêutica os sistemas microfisiológicos terão contribuído para a redução de testes em animais de laboratório no desenvolvimento de medicamentos (MARX et al., 2020).

2.7. Seleção das substâncias avaliadas

Primeiramente, foi selecionada a xantolfila fucoxantina, que é um carotenoide marinho produzido por algas pardas. Têm sido descritas na literatura diversas atividades biológicas relacionadas a atividade antioxidante da fucoxantina. Tais atividades biológicas estão relacionadas a presença de uma ligação alênica conjugada a um grupo carbonila, e a um grupo acetila em sua estrutura molecular, estas são as responsáveis pelos benefícios associados a ela quando administrada oralmente (Riccione et al., 2011).

A fucoxantina tem absorção espectral na faixa de 320 a 500 nm (UVA I ao VIS, 448 nm max) e sua ação pode proteger a pele do fotoenvelhecimento causado pela luz UVA e VIS ao reduzir a produção de ERO (FREITAS et al., 2016; D'ORAZIO et al., 2012). Outros autores descreveram o potencial da fucoxantina para aplicação tópica na fotoproteção da pele, avaliados por métodos *in vitro* em culturas celulares. A fucoxantina a 0,001% quando aplicada topicamente em camundongos possui efeitos contra os danos induzidos por UVB (Urikura, Sugawara, Hirata, 2011). Entretando, o comportamento desse composto na pele humana ainda é desconhecido, bem como a concentração ideal de uso. Para tal, essa substância foi objeto de estudo quanto à fotoestabilidade, potencial fotoprotetor e sua fototoxicidade e fotoirritação avaliados na pele 3D, tanto após isolada da alga parda *Desmarestia anceps,* no primeiro capítulo (TAVARES et al., 2020a) quanto na versão comercial (95% pura) abordado no segundo capítulo (TAVARES et al., 2020b).

A segunda substância selecionada, foi o antifúgico terbinafina, um medicamento tópico (1% em creme) e oral (10 mg/g) disponível no mercado há mais de 15 anos. É um fármaco considerado seguro, mas que apresenta efeitos tóxicos apenas quando usado por longos períodos por via oral, devido ao seu potencial hepatotóxico por ser uma inibidora da enzima CYP2D6 (VICKERS et al., 1999), por essa razão este fármaco poderia ser útil como um controle hepatotóxico, uma vez que a terbinafina possui um baixo índice terapêutico (FDA, 2012). Na pele, a terbinafina possui alto poder de permeação, alta queratofilicidade e lipofilicidade (YEGANEH; MCLACHLAN, 2000). Avaliamos a terbinafina quanto a citotoxicidade, potencial de irritação cutânea em pele 3D e hepatotoxicidade quando avaliamos este fármaco no chip microfluídico de pele 3D associado a fígado 3D, no terceiro capítulo.

Além das substâncias mencionadas, foram sempre incluídos os controles positivos ou negativos recomendados para cada teste. Dentre os controles negativos e/ou positivos inerentes a cada ensaio, o lauril sulfato de sódio (LSS) foi o controle positivo de citotoxicidade em monocamadas (OECD *Guideline* nº 129) e de irritação cutânea (OECD *Test Guideline* nº 439) (OECD, 2010; 2019); a norfloxacina foi o controle positivo para a fototoxicidade em monocamadas (OECD, 2019) e o cetoprofeno para a fototoxicidade em modelo de pele reconstituída (ICH, 2013). O controle negativo foi o tampão fosfato-salino (*phosphate buffered saline* - PBS) ou os veículos selecionados para solubilizar a substância teste, como o alquil benzoato C12-15 ou etanol absoluto.

2.8. Coletânea de artigos

A presente tese foi subdividida na forma de capítulos, contendo uma coletânea de artigos relacionados a hipótese central da mesma. Nos dois primeiros capítulos, os artigos já foram publicados, enquanto que no terceiro capítulo, o artigo foi submetido e se encontra em processo de revisão.

Em todos os artigos o modelo de pele 3D foi utilizado para avaliar a toxicidade e a eficácia da fucoxantina ou a toxicidade da terbinafina. Seguindo uma linha evolutiva, o aumento da complexidade biológica do sistema teste está relacionado a uma superior predição de toxicidade em humanos por emular o microambiente nativo do órgão. Na Figura 1, o esquema representa a principal hipótese da tese que foi baseada na comparação entre ensaios *in vitro* de diferentes complexidades: ensaios em cultura celular em monocamadas, seguido de modelo de pele 3D inteira (derme e epiderme) e no topo dessa evolução, estaria o cultivo em microfluídica que contempla a circulação e a interação com outros órgãos.

Figura 1. Esquema sobre o desenvolvimento dos trabalhos da tese que avaliam a fucoxantina e a terbinafina versus o controle de cada ensaio. Observa-se a complexidade biológica crescente dos ensaios diretamente proporcional ao aumento da relevância para o desenvolvimento de novos fármacos. Adaptado de Mathes et al., 2014.

3. OBJETIVO

3.1. Objetivo

O objetivo deste trabalho foi desenvolver e comparar a capacidade de sistemas *in vitro* de diferentes complexidades: culturas 2D, pele 3D cultivada de modo estático ou em microfluídica associada ao modelo de fígado (HUMIMIC), em predizer a toxicidade e eficácia de substâncias teste seguindo protocolos estabelecidos e recomendados internacionalmente.

3.2. Objetivos específicos

1. Avaliar a fotoestabilidade, o potencial fototóxico e a atividade antioxidante da fucoxantina em ensaios em monocamadas e em modelo de pele 3D;
2. Miniaturizar o modelo de pele para aplicações em microfluídica e em outros ensaios;
3. Aplicar o modelo de pele desenvolvido, no ensaio de irritação cutânea da fucoxantina e propor a utilização de novos biomarcadores por expressão gênica (interleucinas, EGFR, HSPB1 e NAT1) para a identificação de agentes irritantes nos tecidos;
4. Aplicar o modelo de pele desenvolvido, no ensaio de irritação cutânea da terbinafina;
5. Adaptar o ensaio de irritação cutânea da terbinafina para o chip microfluídico associando ao modelo de pele o modelo de fígado (HUMIMIC), incluindo avaliação de outros biomarcadores (LDH, lactato, glicose, albumina, enzimas do CYP450), visando avaliar toxicidade sistêmica inerente a aplicação tópica.

4. TRABALHOS DESENVOLVIDOS

4.1. Capítulo 1 - Avaliação de fotoestabilidade, potencial fotoprotetor e fototóxico da fucoxantina por métodos *in vitro*

Article

Fucoxanthin for Topical Administration, a Phototoxic vs Photoprotective Potential in a Tiered Strategy Assessed by *in vitro* Methods

Renata Spagolla Napoleão Tavares [1], Camila Martins Kawakami [1], Karina de Castro Pereira [1], Gabriela Timotheo do Amaral [1], Carolina Gomes Benevenuto [1], Silvya Stuchi Maria-Engler [2], Pio Colepicolo [3], Hosana Maria Debonsi [1], and Lorena Rigo Gaspar [1,*]

[1] School of Pharmaceutical Sciences of Ribeirão Preto, University of São Paulo, SP 14040-903, Ribeirão Preto, São Paulo, Brazil; renatasnt@usp.br (R.S.N.T.); milakawakami@hotmail.com (C.M.K.); karina.pereira@usp.br (K.C.P.); gabriela.timotheo.amaral@usp.br (G.T.A.); carolgb@fcfrp.usp.br (C.G.B.); hosana@fcfrp.usp.br (H.M.D.)

[2] Clinical and Toxicological Analyses Department, School of Pharmaceutical Sciences, University of São Paulo, SP 05508-000, São Paulo, Brazil; silvya@usp.br

[3] Institute of Chemistry, University of São Paulo, SP 05508-000 São Paulo, Brazil; piocolep@iq.usp.br

***** Correspondence: lorena@fcfrp.usp.br; Tel.: +55 16 33154315

Received: 18 February 2020; Accepted: 13 March 2020; Published: 17 April 2020

Abstract: Fucoxanthin possesses a well-described antioxidant activity that might be useful for human skin photoprotection. However, there is a lack of scientific information regarding its properties when applied onto human skin. Thus, the objective of the present study was to assess the photoprotective and phototoxicity potential of fucoxanthin based on its ultraviolet (UVB 280–320 nm; UVA 320–400 nm) and visible (VIS 400–700 nm) absorption, photostability, phototoxicity in 3T3 mouse fibroblast culture vs. full-thickness reconstructed human skin (RHS), and its ability to inhibit reactive oxygen species formation that is induced by UVA on HaCaT keratinocytes. Later, we evaluated the antioxidant properties of the sunscreen formulation plus 0.5% fucoxanthin onto RHS to confirm its bioavailability and antioxidant potential through the skin layers. The compound was isolated from the alga *Desmarestia anceps*. Fucoxanthin, despite presenting chemical photo-instability (dose 6J/cm^2: 35% UVA and 21% VIS absorbance reduction), showed acceptable photodegradation (dose 27.5 J/cm^2: 5.8% UVB and 12.5% UVA absorbance reduction) when it was added to a sunscreen at 0.5% (*w*/*v*). In addition, it increased by 72% of the total sunscreen UV absorption spectra, presenting UV-booster properties. Fucoxanthin presented phototoxic potential in 3T3 fibroblasts (mean photo effect 0.917), but it was non-phototoxic in the RHS model due to barrier function that was provided by the stratum corneum. In addition, it showed a significant inhibition of ROS formation at 0.01% ($p < 0.001$), in HaCat, and in a sunscreen at 0.5% (*w*/*v*) ($p < 0.001$), in RHS. In conclusion, *in vitro* results showed fucoxanthin protective potential to the skin that might contribute to improving the photoprotective potential of sunscreens *in vivo*.

Keywords: antioxidant; fucoxanthin; phototoxicity; photostability; reconstructed human skin

---

1. Introduction

Concerning ultraviolet (UV) damage, at the beginning of this century, not many compounds were available for the protection against UVA (320-400 nm) radiation and, in response to the growing concern regarding the additional damage that is caused by this radiation, various UVA filters are now available for formulations worldwide. However, the number of UVA filters allowed in the USA is quite limited [1,2]. Another perspective is related to the fact that few compounds offer UVA I (340–400 nm) and

visible (VIS 400–700 nm) light protection, with increasing evidence of the harmful effects of VIS light on the skin. Liebel and co-workers [3] showed that VIS light induced the generation of high levels of free radicals in humans and of proinflammatory cytokines *in vitro*.

Even conventional sunscreens containing UVA and UVB filters, active ingredients that absorb or reflect UV, do not entirely block the UV radiation that reaches the skin [4]; additionally, they can undergo photodegradation and produce reactive oxygen species (ROS) with a phototoxic potential [5]. Besides that, some UV filters have controversial data regarding their skin permeation, estrogen-like effects, and induction of cutaneous sensitization and photosensitization [6,7]. They might have harmful impact not only on the human skin, but also on marine life and coral reefs, other aquatic ecosystems, like phytoplankton, marine diatom, and alga growth [8,9]. In 2018, the governor of Hawaii banned the in-state sale of sunscreens containing either oxybenzone or octinoxate, suspected to harm coral reefs [10]. After Hawaii, Florida and Key West followed this trend. This movement has stimulated the urgent research on alternatives and possibly eco-friendly photoprotective compounds [10].

Following this trend, natural and biocompatible UV filters have led to research on carotenoids that could be interesting in the development of new UV filters or UV boosters to increase the protection or performance of sunscreens [11]. Booster is a term that is currently used in the cosmetic field to define substances that, in small amounts, are capable of increasing the effectiveness of some other products [11] (i.e., increasing the effects of UV filters protecting the skin from sunlight-induced ROS production).

Fucoxanthin absorbs from 320 to 500 nm (UVA I to VIS, 448 nm max) and its action might avoid UVA-induced photoaging and protect from VIS- induced ROS production [2,12]. Since fucoxanthin contains an alene bond, a conjugated carbonyl group, one 5,6-monoepoxide, and an acetyl group, there is a biological potential that is associated with this structure of the molecule when orally administered [13]. It has been reported that this carotenoid shows intense antioxidant activity, as well as anti-inflammatory, anti-obesity, anti-diabetic, anti-tumor, antihypertensive, and anticancer properties [13,14]. Many authors have suggested the photoprotective effect of fucoxanthin on the skin, including protection against UVB-induced damage when 0.001% of fucoxanthin is applied to hairless mice [15]. However, its topical properties and safety for the human skin are still unknown.

Alternative *in vitro* methods validated for preclinical trials are being used to predict the safety and efficacy of unknown natural compounds instead of using animal models to evaluate the potential risk of a test chemical. The use of skin models is physiologically relevant in drug development, since it provides better prediction of human skin safety [16], besides ethical and economic concerns. Thus, for phototoxicity prediction, the recommended *in vitro* tiered strategy, including monolayer fibroblast 3T3 Neutral Red Uptake Phototoxicity (3T3 NRU PT) and reconstructed human epidermis (RHE), allows for the identification of phototoxic potential without animal testing [5,17,18]. Nevertheless, RHE does not present the dermal component, which is essential for many epidermal characteristics and proper skin functionalities, including the improvement of barrier function [19]. In our study, we replaced RHE with reconstructed human skin (RHS) to confirm the ability of the latter to detect the phototoxicity potential. Besides the evaluation of fucoxanthin photosafety, we evaluated the photoprotective potential of this molecule by its photostability under different irradiation exposure and when used in a sunscreen formulation. Additionally, we evaluated the maximal antioxidant potential of this molecule onto immortalized human keratinocytes (HaCat) cells, determining the ideal concentration range that is to be used for this effect. Later, we evaluated the antioxidant properties of the sunscreen formulation plus 0.5% fucoxanthin onto RHS to confirm its bioavailability and antioxidant potential through the skin layers.

Thus, the objective of the present study was to assess the photoprotective and phototoxicity potential of fucoxanthin based on its UV/VIS absorption, photostability, phototoxicity in 3T3 mouse fibroblast culture vs. full-thickness RHS, and its ability to inhibit reactive oxygen species formation that is induced by UVA on HaCaT keratinocytes.

2. Materials and Methods

2.1. Alga Material

During the expedition of 2011 (January 4th, managed by the project PROANTAR (*Programa Antártico Brasileiro*), the researchers collected 69.00 grams of *D. anceps* (wet) at the Punta Plaza location—Antarctic Continent (Admiralty Bay 62°04’14.5’’–62°10’03.5’’S and 58°20’15’’–58°27’60’’W). The material was frozen until the time for

transportation to our laboratories in Brazil, at the Laboratory of Organic Chemistry of the Marine Environment-Support Center for Research in Natural and Synthetic Products, School of Pharmaceutical Sciences of Ribeirão Preto (LQOAM-NPPNS, FCFRP-USP). The investigators preserved a sample of the material that was collected in a solution of formaldehyde with 4% seawater for morphological studies and the preparation of vouchers. They identified the macroalgae according to the standard taxonomic methodology in the Phycology Session and deposited exsiccates in the Phycological Herbarium of the Botanical Institute of São Paulo (SP), Brazil.

2.2. Extraction and Fractionation

We used a mass of 69.00 g (wet weight) to obtain the extract. The material was freshly thawed and washed with distilled water under a vacuum filter. Subsequently, it was fragmented and then extracted with the organic solvent dichloromethane (CH_2Cl_2): methanol (MeOH) (2:1) for 30 min. under stirring, in a thermal blanket with controlled temperature (not exceeding 30 °C). The material was filtered and extracted two more times while using ultrasound equipment for 15 minutes in the third procedure. We concentrated the organic *D. anceps* extract in a rotary evaporator under low pressure (Büchi R-300, Buchi Labotechnik, Flawil, Switzerland) and subjected it to a classical chromatographic column—30 cm with stationary phase Silica Gel 40–63 μm/ASTM Macherey-Nagel (Merck, Darmstadt, Germany), with a polarity gradient using n-hexane, ethyl acetate (EtOAc), and methanol (MeOH) (JT Baker, Port of Spain, Trinidad Y Tobago) to fractionate the extract.

2.3. Carotenoid Isolation

For the identification of fucoxanthin, the highest colored mass fractions were subjected to Electrospray Ionization Mass Spectrometry (ESI-MS) techniques (amaZon SL, Bruker, Bil-lerica, MA, USA). To isolate the carotenoid, we employed high-performance liquid chromatography (HPLC), analytical, and semi-preparative analyses while using two different types of equipment with three different columns. The first instrument and column used to yield the sub-purified fractions was a Shimadzu Chromatograph Model SCL-10AVP that was equipped with a Shimadzu diode array UV-VIS detector DAD (SPD-M10 AVP, Shimadzu, Kyoto, Japan), a computerized integration system Class-VP software 5.02 (Shimadzu, Kyoto, Japan) and the following chromatographic columns: analytical Supelco C-18 (25 cm × 4.4 mm, 5 μm) and semi-

preparative LC-18 Supelco (25 cm × 10 mm, 5 µm). The second analytical column was Polar RP column (100 mm × 3 mm, 5 µm) that was used to define a method to purify the carotenoid (from chlorophyll “a” as a contaminant). The second instrument was Shimadzu chromatograph (Shimadzu, Kyoto, Japan), Prominence model, CBM-20th controller, SPD-20th detector UV/VIS, with two pumps (LC-6AD), an FCR-10th automatic collector DGU-20A5 degasser and LC-Solution Single Software, a semi-preparative column Synergi Polar-RP (250 mm × 10 mm, 4 mm), and a semi-preparative Polar-RP guard column (10 × 10 mm, 4 mm), both being from Phenomenex® (Torrance, CA, USA).

2.4. Stability

2.4.1. UV Absorption

Solutions of 100 µg/mL of extract (the ideal concentration for maximal absorbance around 1 AU), fractions, and fucoxanthin alone in isopropanol were analyzed with a spectrophotometer in the 280 to 700 nm range for the determination of the UV absorption spectra.

2.4.2. Photostability Studies

For the determination of photostability, we studied the crude *D. anceps* extract, the fraction Fr15 containing fucoxanthin, and fucoxanthin that were isolated from this fraction in an isopropanol solution at 100 µg/mL or dissolved in a sunscreen formulation at 0.5% (*w*/*v*). For the photostability studies in an organic solution, 1 mL of each solution sample was added to glass beakers and then subjected to solvent evaporation until a dried film was obtained. The samples were then submitted or not to UV radiation of 7 mW/cm^2 emitted from a Philips UVA lamp Actinic BL/ 10 (Eindhoven, Netherlands) measured with a Dr. Hönle radiometer (Planegg, Germany) equipped with a UVA sensor [20–23]. For the *D. anceps* extract and Fr15, we applied a cumulative dose of 27.5 J/cm^2. That dose is recommended as being similar to 66 min. of exposure to sunlight at midday (6.94 mW/cm^2) on a typical September sunny day in the Ribeirão Preto, Brazil—latitude 21°10'39" south and longitude 47°48'37" west [4,23]. We applied a cumulative dose of 6 J/cm^2 to determine the photostability of fucoxanthin in isopropanol (the dose recommended for phototoxicity studies and similar to 14 min. of exposure to sunlight at midday in the Ribeirão Preto region). Each beaker subjected

to irradiation had a negative control that was sheltered from light. After irradiation, the dried film was resuspended in 1 mL of solvent, and the absorption spectrum of the solutions in the 280 to 700 nm range was analyzed. For the photostability study of fucoxanthin in a sunscreen formulation, we prepared the formulation base with a self-emulsifying wax (cetearyl alcohol, cetearyl glucosyde) and a liquid polymer (hydroxyethyl acrylate, sodium acryloyldimethyltaurate copolymer, squalane, and polysorbate 60), and, in the presence of the following UV filters: 4% avobenzone, 6% octocrylene, 8% octyl methoxycinnamate, and 3% octyl triazone, representing formulation “F3” in the Freitas [22] et al. (2015) study. We proceeded as indicated in the cited study to perform the photostability study using a sunscreen, spreading the preparation onto an area of 10 cm^2 (approximately 4 mg/cm^2) of a glass plate and then left to dry for 15 min. before exposure to a UVA dose of 27.5 J/cm^2. We used the area under the curve (AUC), which is the integral of the absorption spectrum of the samples in the UVB (280–320 nm), UVA (320–400 nm), and VIS (400–700 nm) ranges using the integration function of the MicroCal OriginPro Software (8 SRO, OriginLab Corporation, Northampton, MA, USA) to calculate the photostability [24]. We expressed the results as a percentage of the area of irradiated samples related to the area of non-irradiated samples.

2.5. Toxicity and Efficacy

2.5.1. Phototoxicity Test in 3T3 Mouse Fibroblast (3T3 NRU PT)

In this test, fibroblasts of the Balb 3T3 clone A31 that were provided by *Banco de Células do Rio de Janeiro,* BCRJ code 0047 (Rio de Janeiro, Brazil) cultured on two 96 well microtiter plates were pre-incubated with eight different concentrations of the test chemical (6.8–100 µg/mL) for one hour. We exposed one plate to a UVA irradiation dose of 9 J/cm^2 (SOL-500 sun simulator that was equipped with a metal halide lamp and H1 filter, Dr. Honle AG, Planegg, Germany), while another one was kept in the dark. The determination of cell viability comparing the plates determinates the substance cyto- and phototoxicity [5,25]. Based on the historical data that was produced in our laboratory, we defined this dose as a dose high enough to elicit a phototoxic response in positive controls and as a dose that did not produce interference higher than 20% in cell viability, as recommended by the Organisation for Economic Co-operation and Development (OECD) [26]. We measured UVA radiation with the

same radiometer mentioned before. For concentration-response analysis, we employed the Phototox Version 2.0 software, obtained from *Zentralstelle zur Erfassung und Bewertung von Ersatz- und Ergänzungsmethoden zum Tierversuch* (ZeBeT, Berlin, Germany) that calculates the photoirritation factor (PIF) and mean photo effect (MPE). According to the OECD Test Guideline 432, a substance is predicted to be phototoxic if MPE is higher than 0.15 or the PIF is higher than 5. A test substance with an MPE > 0.1 and < 0.15 (PIF > 1 and < 5) is predicted to be “probably phototoxic” [26]. The positive control was norfloxacin purchased from Sigma–Aldrich (St. Louis, MO, USA) [26].

2.5.2. Reconstructed Human Skin Model (RHS)

The ethics committees of Human Research Ethics Committee of Faculty of Pharmaceutical Sciences of Ribeirão Preto, São Paulo, Brazil approved the experimental procedures using primary human fibroblasts and keratinocytes from donated foreskins with informed consent from legal representatives and ethics approval conforming to the principles of the Declaration of Helsinki (CAAE n°: 55438216.0.0000.5403). We constructed the dermal equivalent with 3.6×10^5 fibroblasts, 5% fetal bovine serum (Gibco, Life Technologies, Carlsbad, CA, USA), and rat-tail type I collagen (Corning, Tewksbury, MA, USA) enough to 3 mL per insert six-well-plate-size (Corning, Tewksbury, MA, USA). After 2 h, we added 2.9×10^6 of the primary human keratinocytes on top of the dermis equivalent using 2 mL of keratinocyte medium. They were kept submerged for 24 h. Next, the culture was maintained at the air-liquid interface for 12 days to allow for keratinocytes differentiation [27].

2.5.3. Phototoxicity Test in RHS

On the 10th day of tissue cultivation, the skin models were exposed to fucoxanthin solubilized in c12-c15 alkyl benzoate (0.5%, *v*/*v*), which is a vehicle that is commonly used to solubilize lipophilic chemicals in cosmetics [5]. Sterile filter discs 16 mm in diameter were soaked in 50 µL test chemicals (c12–c15 alkyl benzoate) and directly applied to the stratum corneum of the skin models. Ketoprofen at 3% in alkyl benzoate is phototoxic and it was used as a positive control. Twenty hours after application of the test substances, the skin models were rinsed with phosphate-buffered saline

(PBS), dried with a sterile swab, and then transferred to fresh wells with the medium. The skin models were irradiated (sun simulator mentioned before) with 6 J/cm^2, the dose that was recommended by Kandarova and Liebsch [28], as necessary to produce a phototoxic response in the positive controls without damage to the tissue and the one used to pre-validate the test in 1999 by European Centre for the Validation of Alternative Methods (ECVAM*)* [29]. We measured UVA radiation with the same radiometer mentioned before, while we kept the non-irradiated plates in a dark box.

2.5.4. Viability Assay

RHS viability was measured by the end of the experiment of phototoxicity. It was determined by measuring the metabolic activity of the constructs after exposure and post-incubation while using a colorimetric test. The reduction of mitochondrial dehydrogenase activity was assessed via the decreased formazan production following incubation with MTT (3-(4,5-dimethylthiazol-2-yl)-2,5-diphenyltetrazolium bromide, Sigma-Aldrich, Cotia, Brazil). The formazan production was measured at 570 nm. We exposed other constructs in every batch to fucoxanthin, but not to MTT, to evaluate the ability of fucoxanthin to stain the constructs under test conditions. The formazan readings were corrected by the fucoxanthin-related optical densities (O.D.) and compared to those of negative control RHS [30]. The data are presented as relative viability according to equation 1, where "*O.D.a*" is from tissues treated and "*O.D.b*" is the mean of untreated tissues.

$$Relative\ viability\ (\%) = 100 \times {}^{O.D.a}/_{mean\ O.D.b} \quad (1)$$

2.5.5. HaCat Antioxidant Activity by Detection of Intracellular ROS using DCFH$_2$-DA

The keratinocytes HaCaT that were provided by *Banco de Células do Rio de Janeiro,* BCRJ code 0341 (Rio de Janeiro, Brazil) were seeded in two 96-well plates at a density of 1 × 10^5 cells/well and then incubated at 37 °C in a 5% CO_2 atmosphere for 24 h. Subsequently, cells were treated for one hour with fucoxanthin at 0.1, 1, 10, and 100 µg/mL (the same range of concentrations used for 3T3 NRU PT of 6.8–100 µg/mL). Next, we incubated the plates with the probe 2',7'-dichlorodihydrofluorescein diacetate (DCFH$_2$-DA) (10 µM) in the dark for 30 min. for permeation into the cell. After the period of incubation, we irradiated one plate with 4 J/cm^2 of UVA radiation (sun simulator), while the other one we kept in dark box. Immediately after irradiation,

fluorescence intensity was measured with a microplate reader (BioTek Synergy HT, Winooski, VT, USA) at an excitation wavelength of 485 nm and emission wavelength of 528 nm [31,32]. We expressed the results as percent fluorescence intensity when compared to the untreated control irradiated, which was considered to be 100%. Norfloxacin (100 µg/mL) and quercetin (10 µg/mL) were used as controls. All of the experiments were carried out in triplicate in three independent experiments. The experimental data was analyzed statistically by analysis of variance (ANOVA), a parametric test, followed by Tukey's test.

2.5.6. RHS Antioxidant Activity by Detection of Intracellular ROS using $DCFH_2$-DA

The RHS were incubated with the $DCFH_2$-DA probe in PBS (50 µM) in the dark for 45 min. After PBS washing, the tissues were treated with sunscreen with fucoxanthin at 0.5% (as described in 2.3.2 item) and the control was the sunscreen formulation without it, for 1 h. Subsequently, they were subjected to a dose of 10 J/cm^2 of UVA radiation, while control tissues were kept in the dark. Immediately after the irradiation period and PBS washing, the tissues were frozen in liquid nitrogen and 10 mm cryostat sections were made. The fluorescence intensity was measured while using a Ti-S inverted Microscope (Nikon Instruments Inc., Amsterdan Netherlands), 488 nm, at 100 ms exposition intensity. The images were quantified using Image J software [33,34]. The results were normalized to area/pixels and expressed in a percentage of fluorescence intensity in comparison to the irradiated and non-irradiated untreated controls.

3. Results

3.1. Extraction and Fractionation

We obtained the dry extract (1.29 g) from fresh wet alga material (69.00 g), with a yield of 2.31%. Next, 1.15 g of the extract was submitted to fractionation in a classical column, which resulted in 40 fractions. We selected fractions that yielded higher weight to have enough mass for all of the following tests; firstly, the selected fractions were screened in terms of their UV spectra.

3.2. UV Spectra

D. anceps extract presented absorption in the region of interest for photoprotection (280–400 nm), especially in the UVA and in the visible range (Figure 1a). Concerning brown algae, the typical absorptions in the regions of 400 nm and 660 nm (areas of blue and red, respectively) are due to the presence of carotenoids and chlorophylls, especially “chlorophyll a”, which is common to all photosynthetic organisms having a maximum absorption at 420 and 660 nm, respectively. Chlorophyll type “a” is predominant in algae due to its central role in the conversion of photochemical energy, while the chlorophyll “c” efficiently participates in photosynthesis as an accessory pigment (similar to the role of chlorophyll “b” in plants or green algae) [14].

The spectral composition of light is crucial for photoprotection mechanisms and photosynthetic efficiency and, thus, for the pigment content of macroalgae as well. According to Kuczynska et al. [35], different structures of chlorophyll “c” are responsible for its intense absorption in the region of 530 nm; also, a peak in the 680 nm region (Figure 1a) could be related to “chlorophyll a”. Carotenoids, on the other hand, exhibit intense absorption between 400 and 500 nm, after fractionation (Figure 1b), F15, F15a, F2, and F3a showed high UVA I/VIS absorbance.

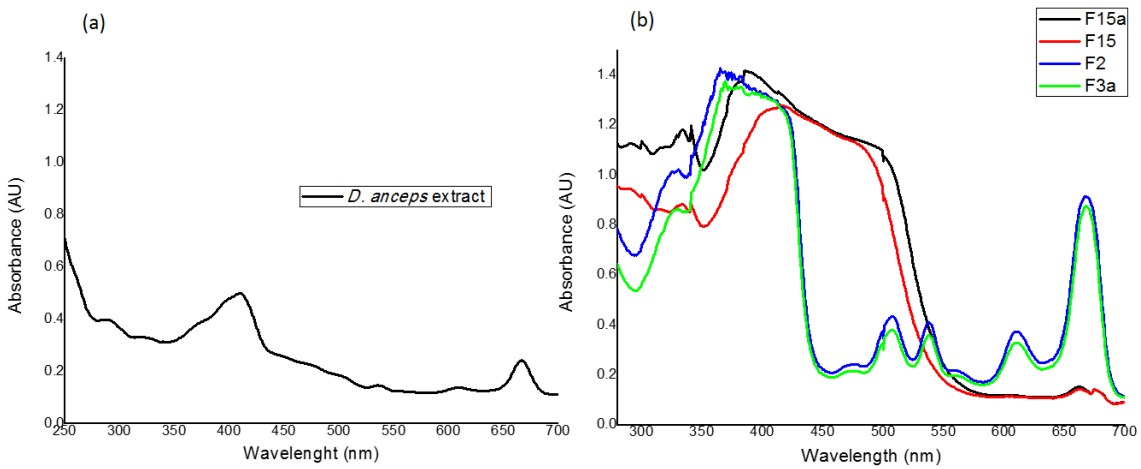

Figure 1. Absorption spectra of (**a**) The alga *D. anceps* crude extract; isopropanol solution, 100 µg/ mL; (**b**) The fractions obtained from this crude extract presented different spectrum profiles; F = fraction, numbers ordered by elution (nonpolar to polar “a” indicates the second day of the extraction. Representative curves from triplicates.

3.3. Identification and Isolation of Fucoxanthin

The high-resolution molecular mass spectrum (electrospray ionization, ESI) corresponding to the molecular weight of fucoxanthin, 658.90 g/mol, was identified based on the fragment pattern at *m/z* 659.4241 and 681.3878 corresponding to $[M + H]^+$ and $[M + Na]^+$ in the fractions F15 and F15a. We subjected the isolated fucoxanthin to NMR spectroscopy for its structural determination while comparing it with the literature (Table 1). The complete assignments of the ^1H and ^{13}C NMR spectra of fucoxanthin revealed signals that were assignable to polyene containing acetyl, conjugated ketone, olefinic methyl, two quaternary germinal oxygen methyls, two quaternaries geminal dimethyl, and allene groups. The NMR data are in line with the findings of Xia and coworkers [14] and Mori and coworkers [36], which suggested that fucoxanthin isolated from the alga *D. anceps* is mainly present in the all-*trans* form. By their coloring feature, other pigments, such as any xanthophyll common to brown algae, such as *cis*-fucoxanthin, diadinoxanthin, diatoxanthine, and β-carotene, could be present in the alga extract in addition to fucoxanthin [12]. These carotenoids also have a maximum absorption peak around 448 nm, as is the case for chlorophylls (b), (c), and (a), which are the main chlorophyll pigments in algae [14]. For the isolation of fucoxanthin from other carotenoids and chlorophylls, we performed an analytical chromatographic analysis with an exploratory method to verify the presence of compounds that absorb near 450 nm of fractions F15/F15a (higher yield and absorbance at 448 nm).

Table 1. Nuclear magnetic resonance of hydrogen and carbon (NMR ^{1}H and ^{13}C) of fucoxanthin (500 and 125 MHz, $CDCl_3$) in comparison with literature data (400 and 67.5 MHz, $CDCl_3$).

Position		^{1}H (δ; mult; *J*-Hz)		^{13}C (*δ*)	
		Literature *	Fucoxanthin	Literature *	Fucoxanthin
1				35.6	35.5
2	ax eq	1.36 dd (8.7; 14.2)	1.36 m	46.9	46.9
3		3.80 m	3.84 m	64.2	64.0
4	ax eq	1.77 dd (8.7; 14.2) 2.29 dd (2.9; 17.8)	1.77 dd (9.1; 13.9) 2.30 t (13.5)	41.5	41.3
5				66.0	67.0
6				66.9	66.8
7		3.64 d (20.4) 2.59 d (20.4)	3.65 d (18.4) 2.60 d (18.4)	40.6	40.0
8				197.7	197.7
9				134.3	134.4
10		7.14 d (12.8)	7.15 d (10.4)	139.0	139.0
11		6.58 m	6.57 m	123.2	
12		6.66 t (12.8)	6.66 t (11.3)	144.9	144.9
13				135.3	
14		6.40 d (11.6)	6.41 d (11.7)	136.6	136.4
15		6.67 m	6.66 m	129.3	
16	−Me	1.02 s	1.03 s	24.9	24.4
17	−Me	0.95 s	0.96 s	28.0	28.0
18		1.21 s	1.21 s	21.0	21.0
19		1.93 s	1.93 s	11.7	11.7
20		1.98 s	1.99 s	12.8	12.7
C-3'OAc	−Me	2.03 s	2.03 s	21.3	21.6
1'				35.0	35.5
2'	ax eq	1.41 dd (10.4; 14.9) 2.00 dd (2.9; 14.9)	1.42 d (11.9) 1.99 m	45.2	45.3
3'		5.37 tt (8.8; 12.0)	5.38 m	67.8	67.7
4'	ax eq	1.53 dd (10.4; 14.9) 2.29 dd (2.9; 17.8)	1,51 t (11.9) 2.30 m	45.1	45.1
5'				72.6	72.5
6'				117.3	117.3
7'				202.2	
8'		6.04 s	6.05 s	103.2	103.1
9'				132.4	132.3
10'		6.12 d (11.6)	6.13 d (11.1)	128.4	128.1
11'		6.71 t (12.0)	6.75 t (12.1)	125.5	
12'		6.34 d (11.6)	6.35 d (15.0)	137.0	136.4
13'				138.0	
14'		6.26 d (11.6)	6.27 d (11.5)	132.0	
15'		6.71 dd (12.0; 14.2)	6.75 t (13.7)	132.4	
16'	−Me	1.37	1.38 s	29.0	29.2
17'	−Me	1.065	1.07 s	31.9	32.0
18'		1.345	1.34 s	31.1	31.2
19'		1.805	1.81 s	13.9	13.9
20'		1.985	1.98 s	12.8	12.7
21				170.0	170.4

* Mori and coworkers, 2004 [36].

We established the method after optimization of analytical chromatographic elution: acetonitrile and water permitted sub-fractionation. The peak with the 47 min. retention time eluted the substance of interest that was monitored by absorption (λ max ~ 450 nm) (Supplementary Figure S1); chlorophyll, (a; c) together with fucoxanthin. Since these algal pigments are complexed, there is greater difficulty in separating them with superior purity [14]. However, after we modified the stationary phase, the mobile phase, and optimized the method employed in analytical chromatographic elution, we could separate them with a rough interval of 3 min (Supplementary Figure S2 or S3).

3.4. Photostability Studies

When irradiated with UVA at 27.5 J/cm^2, the crude extract was considered to be photo unstable in the UV/VIS range (more than 20% reduction), since there was a 28.5%, 43.2%, and 33.7% decrease in UVB, UVA, and VIS absorption, respectively (Figure 2a, Table 2). Fraction F15 (fucoxanthin rich fraction) with maximal absorbance around 450 nm was considered to be photostable in UVB, with only a 4% decrease of absorbance; however, it was photo unstable in the UVA/VIS regions with 44% and 49% absorbance depletion, respectively (Figure 2b, Table 2). We then evaluated fucoxanthin that was isolated in isopropanol solution using the same UVA dose used to induce phototoxicity to RHS (6 J/cm^2), in order to compare both of the experiments. With this lower dose, we observed no degradation in the UVB region, 35% in the UVA region, and 21% in the VIS region; the depletion of absorption of the isolated compound was not in the range considered to be photostable (Figure 2c) [2,4,37]. We repeated the photostability assay applying 0.5% (*w*/*v*) of pure fucoxanthin in a sunscreen formulation, formulation 3 (F3), based on the photostability studies of Freitas et al. [2]. The final sunscreen formulation was yellow-colored, but it was not able to stain the skin. When we added this marine carotenoid to a sunscreen formulation and irradiated with 27.5 J/cm^2, it was considered photostable (5.8% reduction in UVB and 16.5% reduction in UVA). However, since the sunscreen alone only provoked a reduction in the UVA absorption by 4%, the effect of fucoxanthin on UVA region was considered to be the difference of 12.5%. Additionally, the sunscreen with fucoxanthin increased the general UV absorbance by 72% compared with the sunscreen alone, proving to act as a UV-booster by light-absorbing effect, Figure 2d.

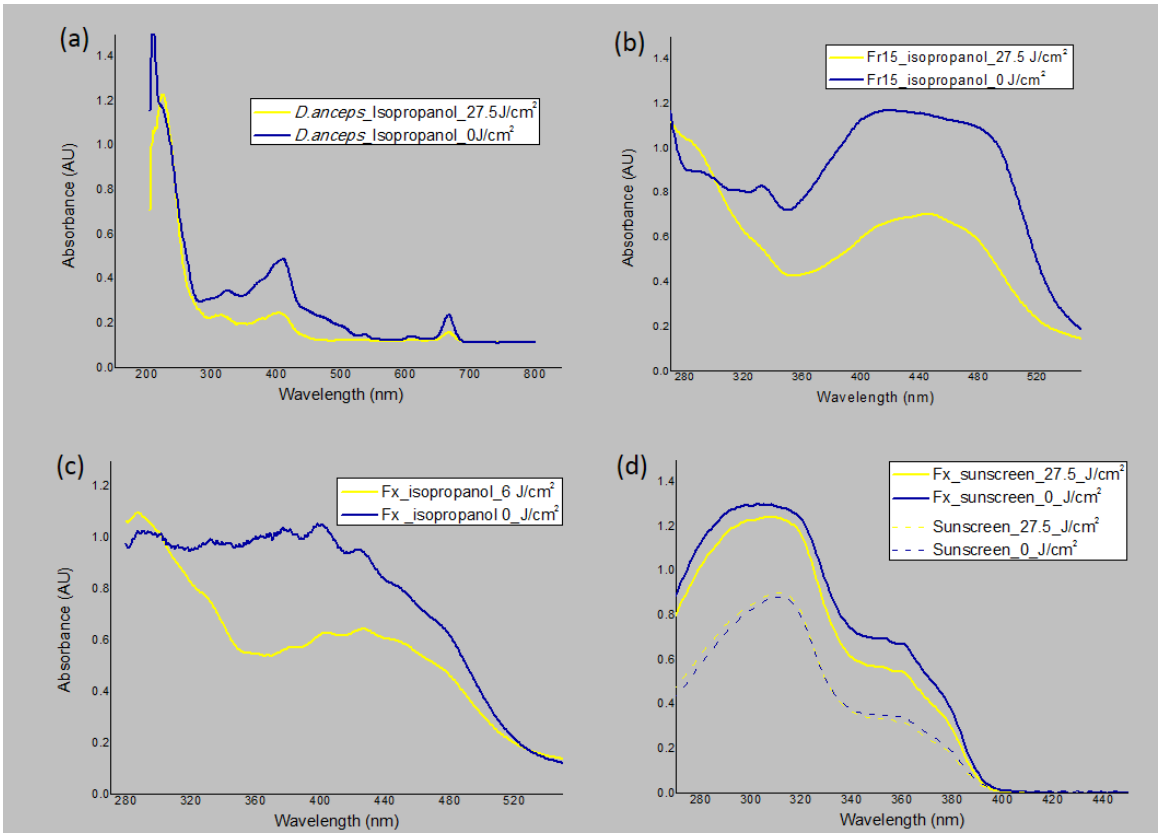

Figure 2. Photostability studies based on the electromagnetic spectrum of the samples irradiated (yellow line) or not (blue line). (**a**) *D. anceps* extract in solution irradiated or not with 27.5 J/cm^2. (**b**) Fr15 fraction containing fucoxanthin in solution irradiated or not with 27.5 J/cm^2. (**c**) Fucoxanthin (Fx) in solution irradiated or not with 6 J/cm^2. (**d**) Fx in a sunscreen formulation vs. sunscreen alone (dashed line) irradiated or not with 27.5 J/cm^2; n = 3, three independent experiments.

Table 2. Reduction of absorbance after irradiation with different doses of UVA light expressed in percentage. Calculation considering the Area Under the Curve (AUC) between samples irradiated or not in triplicates.

Sample	Irradiation Dose (J/cm^2)	Mean of the Reduction of Absorbance after Irradiation (%)		
		UVB	**UVA**	**VIS**
Crude Extract	27.5	28.5	43.2	33.7
Fraction F15 *	27.5	4.0	44.0	49.0
Fucoxanthin Isolated	6 **	0.0	35.0	21.0
Fucoxanthin in Sunscreen	27.5	5.8	16.5	NE

* fucoxanthin rich fraction, ** dose defined as enough to induce phototoxic responses, NE: Non-evaluated (sunscreen with absence of absorbance in the VIS range).

3.5. Phototoxicity in the Monolayer and RHS Assays

The prediction model classified the positive control (norfloxacin) as phototoxic and within the MPE range that was recommended by the OECD Test Guideline 432 (0.340 to 0.900) [26]. The crude extract was considered cytotoxic (IC50-UV 2.7 µg/mL), and its phototoxicity could not be assessed since it compromised all the cells when evaluated in the concentration range of 6.4 to 100 g/mL (Table 3). Fraction F15a containing fucoxanthin was considered less cytotoxic than the crude extract (IC_{50} − UV 26.12 and 25.22 µg/mL) but was deemed to be phototoxic (MPE: 0.343 and 0.478). Fucoxanthin only showed phototoxic potential (MPE: 0.920 and 0.915) and no cytotoxic potential (IC_{50} not determined in the range of 6.4 to 100 µg/mL) to fibroblasts 3T3 (Table 3).

Table 3. Data from the 3T3 fibroblasts phototoxicity assay of the promising alga fractions, pure fucoxanthin, and the positive control (norfloxacin).

Chemical	IC_{50} − UV	IC_{50} + UV	MPE	PIF	Result
Extract	2.76	3.05	−0.014	0.90	cytotoxic
Fraction F15a	26.12	4.45	0.343	7.08	photo/cytotoxic
	25.22	2.59	0.478	16.13	photo/cytotoxic
Fucoxanthin	-	2.77	0.920	48.21	phototoxic
	-	5.91	0.915	17.04	phototoxic
Positive Control (Norfloxacin)	-	2.487	0.615	43.75	phototoxic

n = 1 or 2 independent experiments, -: values not determined in the studied concentration range

Regarding the phototoxic potential of fucoxanthin, its molecular weight is high, 658.90 g/mol, which indicated that this substance would have a reduced bioavailability through the stratum corneum and stratified keratinocytes layers of the skin, which could lead to the absence of phototoxicity *in vivo* when topically applied. To confirm this hypothesis, we evaluated fucoxanthin for the phototoxicity potential in the RHS model,

at 0.5% (*w*/*v*), which is within the concentration range that is usually employed for antioxidants in a cosmetic formulation (0.01–1%).

RHE and RHS, due to the presence of a stratum corneum, appear to be capable of detecting known human dermal phototoxicants. Consequently, under adequate test conditions, a negative result in a 3D skin model indicates that the acute photoirritation potential of the formulation can be regarded as low. In this case, negative test results do not generally preclude further clinical photosafety assessment while using the to-be-marketed formulation [29].

The positive phototoxic control 3% ketoprofen was correctly classified, since it showed a reduction of approximately 41% in cell viability when compared to the non-irradiated tissue, which is higher than the cut off value of 30% reduction that was determined for the assay (Figure 3). In contrast, fucoxanthin reduced less than 30% in cell viability and showed 8.7% difference between the irradiated and non-irradiated RHS models, proving to be non-phototoxic at this concentration onto RHS.

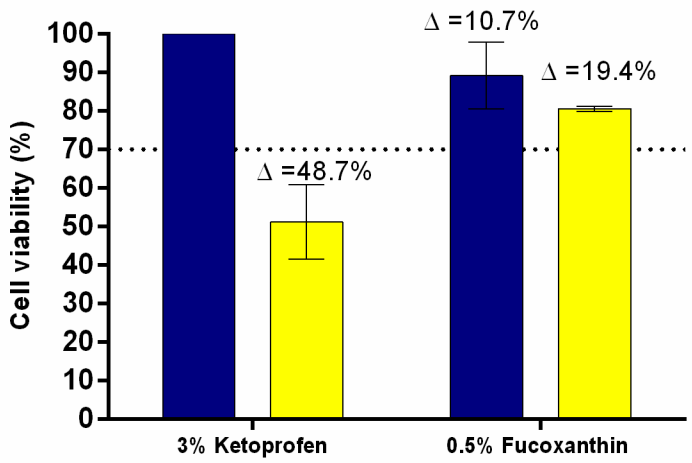

Figure 3. Phototoxicity assay using in-house Reconstructed human skin (RHS)—MTT assay, the positive control 3% ketoprofen was phototoxic (Δ > cut-off 30%) and 0.5% fucoxanthin was non-phototoxic (cell viability ~ 99%) when irradiated (yellow bar) or not (blue bar), mean ± SD, *n* = 2 in two independent experiments.

3.6. HaCat Antioxidant Activity by Detection of Intracellular ROS using DCFH$_2$-DA

After the non-phototoxic response that was observed in the RHS, the protective effect of fucoxanthin was evaluated by the detection of intracellular ROS immediately after UVA radiation using a probe 2',7'-DCFH$_2$-DA in keratinocytes HaCat. The dose

of 4 J/cm^2 used was defined by many authors, including Chignell and Sik [38], after no significant difference in viability was observed between control cells and cells exposed to this dose higher than 20%, while an increase in the DCF photochemical reactions (ROS formation) was observed [38]. Cellular esterases hydrolyze the probe that is cell-permeable to the non-fluorescent DCFH derivative [39]. In the presence of hydrogen peroxide, hydroxyl radicals, carbonate, and nitrite, DCFH is oxidized to the highly fluorescent DCF, which can be monitored by several fluorescence-based techniques derivative [39,40]. The results demonstrated that UVA radiation-induced ROS generation in the keratinocyte cell line (100%) when compared to the untreated control non-irradiated. The positive control norfloxacin (100 µg/mL) induced an increase of ROS production of around 25% in comparison to the untreated irradiated control (Figure 4). On the other hand, the antioxidant quercetin (10 µg/mL) induced a reduction of ROS generation of around 46% after UVA irradiation (Figure 4). The treatment with fucoxanthin at 1, 10, and 100 µg/mL induced a significant reduction of ROS production of about 17%, 15%, and 65%, respectively, when compared to the untreated irradiated control ($p < 0.001$) (Figure 4). However, this effect was not observed for fucoxanthin 0.1 µg/mL, a dose that provided a reduction of 12%, which was not considered statistically significant when compared to the control ($p > 0.05$). Furthermore, treatment with fucoxanthin at 100 µg/mL induced the maximal reduction of ROS production, which was statistically different from the other studied concentrations (0.1, 1, and 10 µg/mL) ($p < 0.001$).

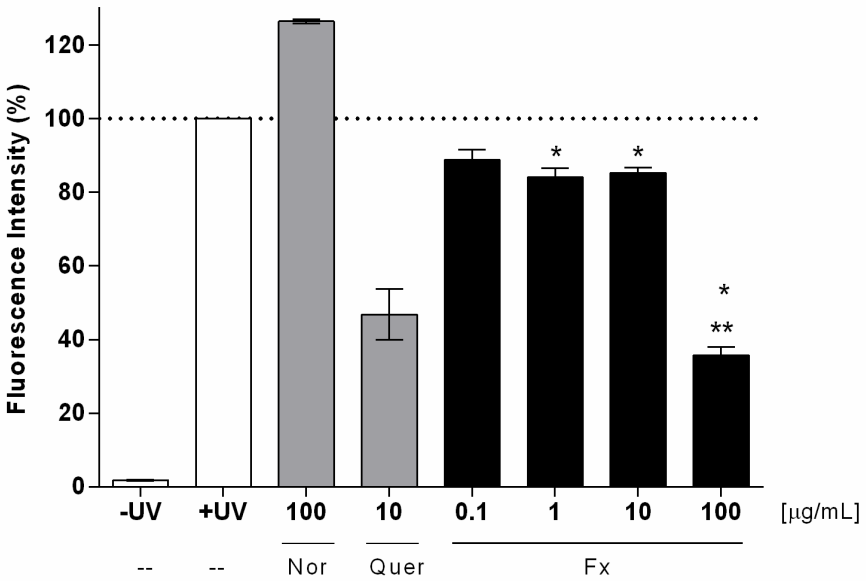

Figure 4. Intracellular Reactive Oxygen Species generation in HaCat after UVA irradiation (4 J/cm^2) using a fluorescent probe DCFH2-DA; untreated irradiated (+UV) and non-irradiated (−UV); norfloxacin—Nor (control); quercetin—Quer (control); fucoxanthin—Fx. Where "*" means significantly different from untreated control irradiated (+UV) (p < 0.001) and "**" significantly different from fucoxanthin at 0.1, 1, and 10 µg/mL (p < 0.001). Mean ± SD, n = 3 in three independent experiments.

3.7. RHS Antioxidant Activity by detection of intracellular ROS using DCFH$_2$-DA

Following the same mechanism of the probe DCFH$_2$-DA, but this time with a sunscreen containing or not 0.5% of fucoxanthin applied in RHS tissues [33,34], the results demonstrated that the UVA radiation increased ROS generation in the untreated RHS control irradiated when compared to the untreated and not irradiated control (p > 0.05), (Figure 5, 6a, and 6b). On the other hand, the sunscreen containing fucoxanthin 0.5% (*w*/*v*) induced a significant reduction of ROS generation after UVA irradiation when compared to the untreated control irradiated (+UV) and when compared to the sunscreen without fucoxanthin (Figure 5, 6a and 6d). RHS models only treated with sunscreen induced similar ROS production than untreated control irradiated (+UV) (p > 0.05) (Figure 5, 6c, and 6d).

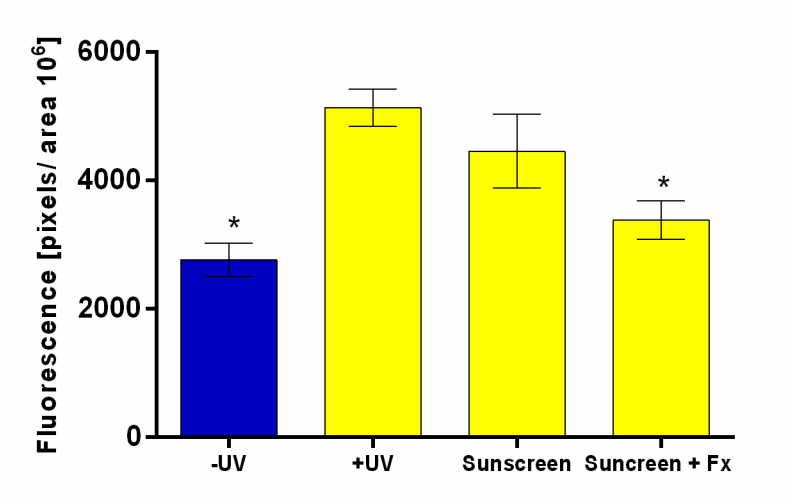

Figure 5. Reconstructed human skin after UVA irradiation (10 J/cm^2) using a fluorescent probe DCFH$_2$-DA. Reactive Oxygen Species generation quantified by the fluorescent intensity in pixels/area. Untreated (blue bar non-irradiated and yellow bars irradiated); sunscreen and sunscreen plus 0.5% fucoxanthin (Fx). Where "*" means significantly different from untreated irradiated (+UV) and from sunscreen treated models ($p < 0.001$). Mean ± SD, $n = 3$ in three independent experiments.

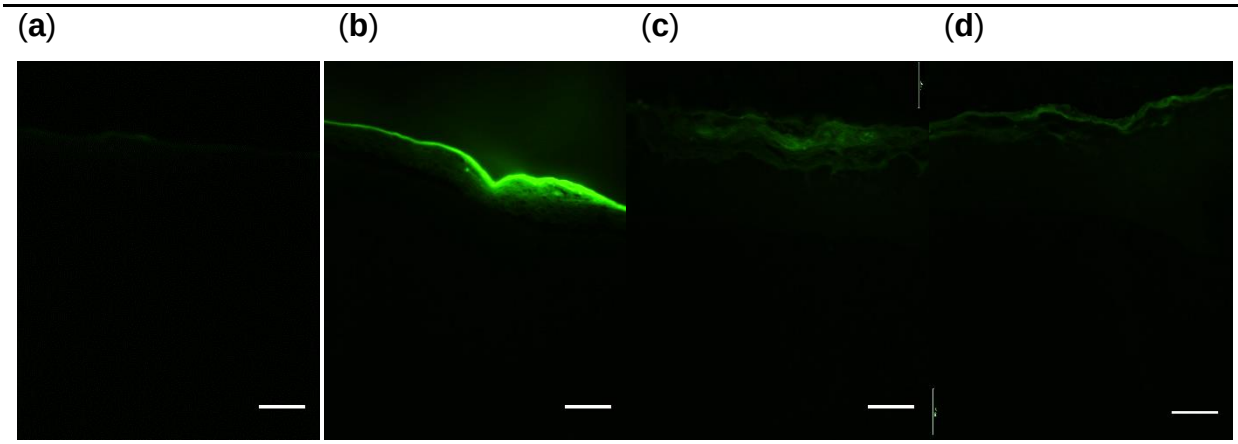

Figure 6. Representative reconstructed human skin (RHS) sessions (10 µm) exposed to a fluorescent probe DCFH$_2$-DA and submitted or not to UVA irradiation (10 J/cm^2)—(**a**) untreated non-irradiated; (**b**) untreated irradiated; (**c**) sunscreen irradiated; and, (**d**) sunscreen plus 0.5% fucoxanthin irradiated. Green fluorescent intensity represents the Reactive Oxygen Species (ROS) generation in the tissues. Scale bars = 100 µm, $n = 3$; three independent experiments.

4. Discussion

The marine carotenoid fucoxanthin that was isolated in this study from the alga *D. anceps* was the main carotenoid present in this brown alga [41]. It absorbs in the UV/VIS region, which is interesting for photoprotection and presents promising antioxidant properties that are observed in mice reported in the literature [12]. In the present study, fucoxanthin was, for the first time, evaluated *in vitro* by the toxicological and photoprotective perspective of its use in the human skin using 3D RHS.

Fucoxanthin showed photoinstability when being evaluated in an organic solvent. However, UV filters or boosters should be stable under UV exposure, since their exposure to sunlight might lead to photodegradation reactions that can compromise their physical properties and lead to the formation of undesirable photoproducts [42]. Zhang and Tang [43] discussed that the instability of carotenes is related to the poly chain conjugate and its susceptibility to oxidation, isomerization by heat, light, and chemical interactions. After analyzing the chemical UVA/VIS photoinstability of fucoxanthin, with degradation being over the acceptable range of 20% after a 6 J/cm^2 UVA dose, we added fucoxanthin at 0.5% to a sunscreen formulation to assess photostability at a 27.5 J/cm^2 UVA dose. In this study, the sunscreen formulation that contains a combination of two UV filters considered to be photo unstable (avobenzone and ethylhexyl methoxycinnamate) was studied in order to assess the fucoxanthin capabilities of alteration in the photostability of this photo unstable combination. However, the sunscreen plus fucoxanthin showed acceptable photodegradation (Figure 2d). Surprisingly, besides that, we observed that the sunscreen plus fucoxanthin enhanced UVA and UVB absorption by 72%, showing *in vitro* booster properties of fucoxanthin that should be further investigated.

According to ICH [44], the intrinsic photostability of a substance or product shall be demonstrated in such a way that exposure to light does not result in unacceptable changes [44].

Addressing the tiered strategy to assess acute phototoxicity according to ICH recommendations [18], 3T3 NRU-PT is the first step of the biological assays and it is considered to be a standalone test for negative results due to its high sensitivity (100%) for the identification of absence of phototoxic potential [45]. When a positive result is obtained, i.e. fucoxanthin showed a phototoxic potential (MPE: 0.917), a follow-up testing should be performed to obtain data with models that better reflect the human

situation, such as 3D skin models [45], since the 3T3 NRU-PT test is overestimated and it can produce false-positive results due to the lack of stratum corneum [28]. Firstly, our 3D full-thickness skin model proved to be able to detect the phototoxic potential of positive control, reducing the viability by more than 30% [28]. Secondly, fucoxanthin at 0.5% did not present phototoxicity (Figure 4). Therefore, the combined phototoxicity assays (monolayer and RHS) suggest that fucoxanthin would not be phototoxic to the human skin at 0.5% due to the reduced bioavailability through the stratum corneum and in the stratified epidermis. It is important to mention that skin models are more permeable than human skin [46], which means that they hardly produce false-negative results, which is very important when predicting the toxic potential of unknown substances. In addition, the viable epidermis is made of keratinocytes, which are less sensitive than fibroblasts to xenobiotics and UV radiation.

In the efficacy assay on monolayers, fucoxanthin not only did not harm the HaCat keratinocytes, but also protected the cells from UVA-induced ROS formation in a concentration-dependent manner (maximal effect at 0.01%) (Figure 4). The reduction in ROS production was probably due to its antioxidant properties under anoxic conditions, well described by other studies using in chemico (DPPH; ABTS) [14] and *in vitro* methods (HepG2, HaCat, PC12) [47]. While the other carotenoids have virtually no scavenging ability against ROS, fucoxanthin donates electrons as a part of its mechanism of capturing free radicals [12]. Furthermore, we also observed a significant reduction in the ROS production in RHS (complex 3D tissue) treated and irradiated with sunscreen plus fucoxanthin that we did not observe in the RHS that was treated with sunscreen alone (Figures 5 and 6). This suggests that fucoxanthin can also protect viable epidermis against UVA-induced ROS production, which is in agreement with the fucoxanthin protection observed in HaCat keratinocytes. These results could be considered to be very positive for the risk-benefit of its dermatological use, since fucoxanthin that reaches viable epidermis protects against UVA-induced ROS production (Figure 6d).

Our study corroborates those reported before [48], which employed the HaCat cell line and hairless mice to study the UVB protective effects of commercial all-trans-fucoxanthin (Sigma). They observed that fucoxanthin has anti-inflammatory activity by downregulating Cyclooxygenase-2 (COX-2) expression after UVB irradiation (mice) and a photoprotective effect against oxidative stress that is caused by UVB exposure via an increase of nuclear factor E2-related factor 2 (Nrf2) expression. Thus, although

Rodríguez-Luna et al. [48] obtained valuable information from hairless mice, it is well known that human adverse events cannot always be detected in animals, due to inherent genetic and physiological differences between species and that skin model constructed with human cells and physiologic relevant microarchitecture contributes to the better prediction of human effects. In the previous study of our group, commercial fucoxanthin at the same concentration, presented an absence of irritation, absence of morphological changes in the histology, and no significant dysregulation on homeostasis, metabolism, and in the inflammatory genes studied after following the OECD protocol for skin irritation [49].

Finally, it is important to mention that another well-known molecule, β-Carotene, a vitamin A precursor, is a popular "secondary" UV filter (characterized by a sun protection factor lower than 2), has a controversial use in the literature, regarding its antioxidant/prooxidant effect, depending on its concentration and O_2 tension [2,22,50–52]. However, β-Carotene is able to protect the collagen structure from infrared light in the skin [53] and it is used in cosmetic formulations for aged skin and actinic keratosis [51], which, for instance, could also suggest some skin benefits from the topical use of fucoxanthin when tested *in vivo,* due to the similarities of their molecular structures. In addition, fucoxanthin when orally administered in mice is reported to have low accumulation in the skin [54], which underscores the interest of topical use of fucoxanthin and such confirmation of its safety and effectiveness suggested by the present study.

5. Conclusions

In conclusion, we developed an effective extraction and purification of all-*trans*-fucoxanthin from the brown alga *D. anceps.* Although fucoxanthin presented chemical UV photo-instability, it increased by 72% of the total sunscreen UV absorption spectra (UVA and UVB) when added to sunscreen at 0.5%, presenting UV-booster properties with an acceptable photostability. The beneficial use of topical fucoxanthin should be further investigated *in vivo* in the concentration range of 0.01–0.5% (*w*/*v*). As, in this range, we observed an absence of phototoxicity in the RHS model and protective potential against UVA-induced ROS formation both in HaCat monolayers and on RHS models, which might contribute to improving the photoprotective potential of sunscreens.

Supplementary Materials: The following are available online at www.mdpi.com/xxx/s1, Figure S1: Chromatogram of the elution semi-preparative scale—carotenoid isolation, Figure S2: Chromatogram of the semi-preparative scale subfraction, analyzed in 450 nm—absorption region of fucoxanthin at a higher intensity (Au 450), Retention Time (RT) = 5.75 min black line, 650 nm—region of the band's absorption of chlorophyll “a” lower intensity. RT ~3 min, pink line, Figure S3: Chromatogram of the elution of the subfraction analytical scale, analyzed in (a) the 450 nm—absorption region of fucoxanthin at a higher intensity (3 Au), Retention time (RT) = 3.5 min; (b) 650 nm—the area of the chlorophyll absorption bands at a lower intensity (0.025 Au), RT ~6.5 min.

Author Contributions: Conceptualization, R.S.N.T., L.R.G., H.M.D.; investigation, R.S.N.T., C.M.K., K.C.P. and G.T.A.; methodology, R.S.N.T., C.M.K., C.G.B., S.S.M.-E, H.M.D.; writing—original draft preparation, R.S.N.T., and L.R.G.; writing—review and editing, R.S.N.T., P.C.; H.M.D. and L.R.G.; visualization, R.S.N.T. and L.R.G. supervision, L.R.G. and H.M.D.; project administration, L.R.G. and H.M.D.; funding acquisition, R.S.N.T., P.C., H.M.D., and L.R.G. All authors have read and agreed to the published version of the manuscript.

Funding: This research was funded by call Nº 64/2013, MCTI/CNPq/FNDCT-Ação Transversal-Programa Antártico Brasileiro-PROANTAR, from the Brazilian Government, R.S.N.T. gratefully acknowledges a doctoral scholarship from CNPq (grant number 132062/2014-3).

Acknowledgments: We are thankful to Ribeirão Preto State Hospital and to the Maria de Fátima Galli Sorita, Ana Laura Ferreira Marsico Dalto, and Alexandra Longo Camperoni for the partnership providing the foreskin. The authors are also grateful to Nair Sumie Yokoya and Aline Paternostro Martins for the identification, collection and depositing the voucher specimens in the herbarium of Botanical Institute of São Paulo. We thank Norberto Peporine Lopes for the MS-ESI analyses performed in the Department of Chemistry, Faculty of Philosophy, Sciences, and Languages of Ribeirão Preto and the Department of Physics and Chemistry, Faculty of Pharmaceutical Sciences of Ribeirão Preto - USP.

Conflicts of Interest: The authors declare no conflict of interest. The funders had no role in the design of the study; in the collection, analyses, or interpretation of data; in the writing of the manuscript, or in the decision to publish the results.

References

1. Fourtanier, A.; Moyal, D.; Seite, S. UVA filters in sun-protection products: Regulatory and biological aspects. *Photochem. Photobiol. Sci.* **2012**, *11*, 81–89, doi:10.1039/c1pp05152k.
2. Freitas, J.V.; Gaspar, L.R. *In vitro* photosafety and efficacy screening of apigenin, chrysin and beta-carotene for UVA and VIS protection. *Eur. J. Pharm. Sci.* **2016**, *89*, 146–153, doi:10.1016/j.ejps.2016.04.032.
3. Liebel, F.; Kaur, S.; Ruvolo, E.; Kollias, N.; Southall, M.D. Irradiation of skin with visible light induces reactive oxygen species and matrix-degrading enzymes. *J. Investig. Dermatol.* **2012**, *132*, 1901–1907, doi:10.1038/jid.2011.476.
4. Damiani, E.; Baschong, W.; Greci, L. UV-Filter combinations under UV-A exposure: Concomitant quantification of over-all spectral stability and molecular integrity. *J. Photochem. Photobiol. B* **2007**, *87*, 95–104, doi:10.1016/j.jphotobiol.2007.03.003.
5. Gaspar, L.R.; Tharmann, J.; Maia Campos, P.M.; Liebsch, M. Skin phototoxicity of cosmetic formulations containing photounstable and photostable UV-filters and vitamin A palmitate. *Toxicol. Vitr.* **2013**, *27*, 418–425, doi:10.1016/j.tiv.2012.08.006.
6. Matsumoto, H.; Adachi, S.; Suzuki, Y. [Estrogenic activity of ultraviolet absorbers and the related compounds]. *Yakugaku Zasshi* **2005**, *125*, 643–652, doi:10.1248/yakushi.125.643.
7. Ozáez, I.; Martínez-Guitarte, J.L.; Morcillo, G. Effects of *in vivo* exposure to UV filters (4-MBC, OMC, BP-3, 4-HB, OC, OD-PABA) on endocrine signaling genes in the insect Chironomus riparius. *Sci. Total. Environ.* **2013**, *456–457*, 120–126, doi:10.1016/j.scitotenv.2013.03.081.
8. Tovar-Sánchez, A.; Sánchez-Quiles, D.; Basterretxea, G.; Benedé, J.L.; Chisvert, A.; Salvador, A.; Moreno-Garrido, I.; Blasco, J. Sunscreen products as emerging pollutants to coastal waters. *PLoS ONE* **2013**, *8*, e65451, doi:10.1371/journal.pone.0065451.
9. Downs, C.A.; Kramarsky-Winter, E.; Segal, R.; Fauth, J.; Knutson, S.; Bronstein, O.; Ciner, F.R.; Jeger, R.; Lichtenfeld, Y.; Woodley, C.M.; et al. Toxicopathological Effects of the Sunscreen UV Filter, Oxybenzone (Benzophenone-3), on Coral Planulae and Cultured Primary Cells and Its Environmental Contamination in Hawaii and the U.S. Virgin Islands. *Arch. Environ. Contam. Toxicol.* **2016**, *70*, 265–288, doi:10.1007/s00244-015-0227-7.
10. Pandika, M. Looking to Nature for New Sunscreens. *ACS Cent. Sci.* **2018**, *4*, 788–790, doi:10.1021/acscentsci.8b00433.

11. Sohn, M. UV Booster and Photoprotection. In *Principles and Practice of Photoprotection*; Wang, S.Q., Lim, H.W., Eds.; Springer International Publishing: Cham, Switzerland, 2016; pp. 227–245.
12. D'Orazio, N.; Gemello, E.; Gammone, M.A.; de Girolamo, M.; Ficoneri, C.; Riccioni, G. Fucoxantin: A treasure from the sea. *Mar. Drugs* **2012**, *10*, 604–616, doi:10.3390/md10030604.
13. Riccioni, G.; D'Orazio, N.; Franceschelli, S.; Speranza, L. Marine carotenoids and cardiovascular risk markers. *Mar. Drugs* **2011**, *9*, 1166–1175, doi:10.3390/md9071166.
14. Xia, S.; Wang, K.; Wan, L.; Li, A.; Hu, Q.; Zhang, C. Production, characterization, and antioxidant activity of fucoxanthin from the marine diatom Odontella aurita. *Mar. Drugs* **2013**, *11*, 2667–2681, doi:10.3390/md11072667.
15. Urikura, I.; Sugawara, T.; Hirata, T. Protective effect of Fucoxanthin against UVB-induced skin photoaging in hairless mice. *Biosci. Biotechnol. Biochem.* **2011**, *75*, 757–760, doi:10.1271/bbb.110040.
16. Mathes, S.H.; Ruffner, H.; Graf-Hausner, U. The use of skin models in drug development. *Adv. Drug Deliv. Rev.* **2014**, *69–70*, 81–102, doi:10.1016/j.addr.2013.12.006.
17. Ceridono, M.; Tellner, P.; Bauer, D.; Barroso, J.; Alépée, N.; Corvi, R.; De Smedt, A.; Fellows, M.D.; Gibbs, N.K.; Heisler, E.; et al. The 3T3 neutral red uptake phototoxicity test: Practical experience and implications for phototoxicity testing--the report of an ECVAM-EFPIA workshop. *Regul. Toxicol. Pharmacol.* **2012**, *63*, 480–488, doi:10.1016/j.yrtph.2012.06.001.
18. ICH. Photosafety Evaluation of Pharmaceuticals. In *S10 Guideline*, ICH: Geneva, Switzerland, 2013.
19. Catarino, C.M.; do Nascimento Pedrosa, T.; Pennacchi, P.C.; de Assis, S.R.; Gimenes, F.; Consolaro, M.E.L.; de Moraes Barros, S.B.; Maria-Engler, S.S. Skin corrosion test: A comparison between reconstructed human epidermis and full thickness skin models. *Eur. J. Pharm. Biopharm.* **2018**, *125*, 51–57, doi:10.1016/j.ejpb.2018.01.002.
20. Cambon, M.; Issachar, N.; Castelli, D.; Robert, C. An *in vivo* method to assess the photostability of UV filters in a sunscreen. *J. Cosmet. Sci.* **2001**, *52*, 1–11.
21. Whitehead, K.; Hedges, J.I. Photodegradation and photosensitization of mycosporine-like amino acids. *J. Photochem. Photobiol. B* **2005**, *80*, 115–121, doi:10.1016/j.jphotobiol.2005.03.008.
22. Freitas, J.V.; Lopes, N.P.; Gaspar, L.R. Photostability evaluation of five UV-filters, trans-resveratrol and beta-carotene in sunscreens. *Eur. J. Pharm. Sci.* **2015**, *78*, 79–89, doi:10.1016/j.ejps.2015.07.004.
23. Maia-Campos, P.M.B.G.; Benevenuto, C.G.; Calixto, L.S.; Melo, M.O.; Pereira, K.C.; Gaspar, L.R. Palmariapalmata, Cichorium intybus, and Medicago sativa extracts in cosmetic formulations: An integrated approach of *in vitro* toxicity and *in vivo* acceptability studies. *Cutan. Ocul. Toxicol.* **2019**, *38*, 322–329, doi:10.1080/15569527.2019.1579224.

24. Diffey, B.L. Optimizing the spectral absorption profile of sunscreens. *Int. J. Cosmet. Sci.* **2017**, *39*, 90–92, doi:10.1111/ics.12353.
25. Liebsch, M.; Spielmann, H.; Pape, W.; Krul, C.; Deguercy, A.; Eskes, C. UV-induced effects. *Altern. Lab. Anim.* **2005**, *33* (Suppl. S1), 131–146, doi:10.1177/026119290503301s14.
26. OECD. *Test No. 432: In vitro 3T3 NRU Phototoxicity Test, OECD Guidelines for the Testing of Chemicals*; OECD Publishing: Paris, France, 2019.
27. Pennacchi, P.C.; de Almeida, M.E.; Gomes, O.L.; Faião-Flores, F.; de Araújo Crepaldi, M.C.; Dos Santos, M.F.; de Moraes Barros, S.B.; Maria-Engler, S.S. Glycated Reconstructed Human Skin as a Platform to Study the Pathogenesis of Skin Aging. *Tissue Eng. Part A* **2015**, *21*, 2417–2425, doi:10.1089/ten.TEA.2015.0009.
28. Kandarova, H.; Liebsch, M. The EpiDerm™ Phototoxicity Test (EpiDerm™ H3D-PT) In *Alternatives for Dermal Toxicity Testing*; Springer International Publishing: Cham, Switzerland, 2017.
29. Liebsch, M.; Traue, D.; Barrabas, C.; Spielmann, H.; Gerberick, G.F.; Cruse, L.; Diembeck, W.; Pfannenbecker, U.; Spieker, J.; Holzhutter, H.-G.; et al. Prevalidation of the epiderm™ phototoxicity test. In *Proceedings of International Scientific Conference*, Alternatives to animal testing, 2nd ed.; CPL Press: Brussels, Belgium, 1999; pp. 160–166.
30. OECD. *Test No. 439: In vitro Skin Irritation: Reconstructed Human Epidermis Test Method*; OECD Publishing: Paris, France, 2019.
31. Pygmalion, M.J.; Ruiz, L.; Popovic, E.; Gizard, J.; Portes, P.; Marat, X.; Lucet-Levannier, K.; Muller, B.; Galey, J.B. Skin cell protection against UVA by Sideroxyl, a new antioxidant complementary to sunscreens. *Free Radic. Biol. Med.* **2010**, *49*, 1629–1637, doi:10.1016/j.freeradbiomed.2010.08.009.
32. Alves, G.A.D.; Oliveira de Souza, R.; Ghislain Rogez, H.L.; Masaki, H.; Fonseca, M.J.V. Cecropia obtusa extract and chlorogenic acid exhibit anti aging effect in human fibroblasts and keratinocytes cells exposed to UV radiation. *PLoS ONE* **2019**, *14*, e0216501, doi:10.1371/journal.pone.0216501.
33. Marionnet, C.; Pierrard, C.; Golebiewski, C.; Bernerd, F. Diversity of biological effects induced by longwave UVA rays (UVA1) in reconstructed skin. *PLoS ONE* **2014**, *9*, e105263, doi:10.1371/journal.pone.0105263.
34. Rasmussen, C.; Gratz, K.; Liebel, F.; Southall, M.; Garay, M.; Bhattacharyya, S.; Simon, N.; Vander Zanden, M.; Van Winkle, K.; Pirnstill, J.; et al. The StrataTest® human skin model, a consistent *in vitro* alternative for toxicological testing. *Toxicol. Vitr.* **2010**, *24*, 2021–2029, doi:10.1016/j.tiv.2010.07.027.
35. Kuczynska, P.; Jemiola-Rzeminska, M.; Strzalka, K. Photosynthetic Pigments in Diatoms. *Mar. Drugs* **2015**, *13*, 5847–5881, doi:10.3390/md13095847.
36. Mori, K.; Ooi, T.; Hiraoka, M.; Oka, N.; Hamada, H.; Tamura, M.; Kusumi, T. Fucoxanthin and Its Metabolites in Edible Brown Algae Cultivated in Deep Seawater. *Mar. Drugs* **2004**, *2*, 63–72, doi:10.3390/md202063.
37. Hojerová, J.; Medovcíková, A.; Mikula, M. Photoprotective efficacy and photostability of fifteen sunscreen products having the same label SPF subjected

to natural sunlight. *Int. J. Pharm.* **2011**, *408*, 27–38, doi:10.1016/j.ijpharm.2011.01.040.

38. Chignell, C.F.; Sik, R.H. A photochemical study of cells loaded with 2′,7′-dichlorofluorescin: Implications for the detection of reactive oxygen species generated during UVA irradiation. *Free Radic. Biol. Med.* **2003**, *34*, 1029–1034, doi:10.1016/s0891-5849(03)00022-4.
39. Kalyanaraman, B.; Darley-Usmar, V.; Davies, K.J.; Dennery, P.A.; Forman, H.J.; Grisham, M.B.; Mann, G.E.; Moore, K.; Roberts, L.J.; Ischiropoulos, H. Measuring reactive oxygen and nitrogen species with fluorescent probes: Challenges and limitations. *Free Radic. Biol. Med.* **2012**, *52*, 1–6, doi:10.1016/j.freeradbiomed.2011.09.030.
40. Wardman, P. Fluorescent and luminescent probes for measurement of oxidative and nitrosative species in cells and tissues: Progress, pitfalls, and prospects. *Free Radic. Biol. Med.* **2007**, *43*, 995–1022, doi:10.1016/j.freeradbiomed.2007.06.026.
41. Rautenberger, R.W.C.; Bischof, K. Acclimation to UV radiation and antioxidative defence in the endemic Antarctic brown macroalga *Desmarestia anceps* along a depth gradient. *Polar Biol.* **2013**, *36*, 1779–1789, doi:10.1007/s00300-013-1397-2.
42. Santos, A.J.; Miranda, M.S.; Esteves da Silva, J.C. The degradation products of UV filters in aqueous and chlorinated aqueous solutions. *Water Res.* **2012**, *46*, 3167–3176, doi:10.1016/j.watres.2012.03.057.
43. Zhang, H.; Tang, Y.; Zhang, Y.; Zhang, S.; Qu, J.; Wang, X.; Kong, R.; Han, C.; Liu, Z. Fucoxanthin: A Promising Medicinal and Nutritional Ingredient. *Evid. Based Complement. Altern. Med.* **2015**, *2015*, 723515, doi:10.1155/2015/723515.
44. ICH. Photostability Testing of New Drug Substances and Products. In *Q1B Guideline*; ICH: Geneva, Switzerland, 1996.
45. Gaspar, L.R.; Kawakami, C.M.; Benevenuto, C.G. Overview on the Current Status of Available Test Methods and Additional Promising Methods for Assessing UV-Induced Effects. In *Alternatives for Dermal Toxicity Testing*; ©Springer International Publishing AG: Cham, *Switzerland*, 2017; p. 463.
46. Kejlová, K.; Jírová, D.; Bendová, H.; Kandárová, H.; Weidenhoffer, Z.; Kolárová, H.; Liebsch, M. Phototoxicity of bergamot oil assessed by *in vitro* techniques in combination with human patch tests. *Toxicol. Vitr.* **2007**, *21*, 1298–1303, doi:10.1016/j.tiv.2007.05.016.
47. Zeng, J.; Zhang, Y.; Ruan, J.; Yang, Z.; Wang, C.; Hong, Z.; Zuo, Z. Protective effects of fucoxanthin and fucoxanthinol against tributyltin-induced oxidative stress in HepG2 cells. *Environ. Sci. Pollut. Res. Int.* **2018**, *25*, 5582–5589, doi:10.1007/s11356-017-0661-3.
48. Rodríguez-Luna, A.; Ávila-Román, J.; González-Rodríguez, M.L.; Cózar, M.J.; Rabasco, A.M.; Motilva, V.; Talero, E. Fucoxanthin-Containing Cream Prevents Epidermal Hyperplasia and UVB-Induced Skin Erythema in Mice. *Mar. Drugs* **2018**, *16*, doi:10.3390/md16100378.
49. Tavares, R.S.N.; Maria-Engler, S.S.; Colepicolo, P.; Debonsi, H.M.; Schäfer-Korting, M.; Marx, U.; Gaspar, L.R.; Zoschke, C. Skin Irritation Testing beyond

Tissue Viability: Fucoxanthin Effects on Inflammation, Homeostasis, and Metabolism *Pharmaceutics* **2020**, *136*, 1–12, doi:10.3390/pharmaceutics12020136.

50. Biesalski, H.K.; Obermueller-Jevic, U.C. UV light, beta-carotene and human skin--beneficial and potentially harmful effects. *Arch. Biochem. Biophys.* **2001**, *389*, 1–6, doi:10.1006/abbi.2001.2313.
51. Bayerl, C. Beta-carotene in dermatology: Does it help? *Acta Dermatovenerol. APA* **2008**, *17*, 160–162.
52. Zhang, P.; Omaye, S.T. Antioxidant and prooxidant roles for beta-carotene, alpha-tocopherol and ascorbic acid in human lung cells. *Toxicol. Vitr.* **2001**, *15*, 13–24, doi:10.1016/s0887-2333(00)00054-0.
53. Fernández, E.; Fajarí, L.; Rodríguez, G.; Cócera, M.; Moner, V.; Barbosa-Barros, L.; Kamma-Lorger, C.S.; de la Maza, A.; López, O. Reducing the Harmful Effects of Infrared Radiation on the Skin Using Bicosomes Incorporating β-Carotene. *Skin Pharmacol. Physiol.* **2016**, *29*, 169–177, doi:10.1159/000447015.
54. Hashimoto, T.; Ozaki, Y.; Taminato, M.; Das, S.K.; Mizuno, M.; Yoshimura, K.; Maoka, T.; Kanazawa, K. The distribution and accumulation of fucoxanthin and its metabolites after oral administration in mice. *Br. J. Nutr.* **2009**, *102*, 242–248, doi:10.1017/S0007114508199007.

4.2. Capítulo 2 - Potencial de irritação cutânea da fucoxantina e sua influência na inflamação, homeostase e metabolismo da pele 3D

Article

Skin Irritation Testing beyond Tissue Viability: Fucoxanthin Effects on Inflammation, Homeostasis, and Metabolism

Renata Spagolla Napoleão Tavares [1], Silvya Stuchi Maria-Engler [2], Pio Colepicolo[3], Hosana Maria Debonsi [1], Monika Schäfer-Korting [4], Uwe Marx [5], Lorena Rigo Gaspar [1] and Christian Zoschke [4,*]

[1] School of Pharmaceutical Sciences of Ribeirão Preto, University of São Paulo, Av. do Café s/n, Monte Alegre, Ribeirão Preto, SP 14040-903, Brazil; renatasnt@usp.br

[2] Clinical and Toxicological Analyses Department, School of Pharmaceutical Sciences, , University of São Paulo, Av. Prof. Lineu Prestes, 748, Cidade Universitária, São Paulo, SP 05508-000, Brazil; silvya@usp.br

[3] Institute of Chemistry, University of São Paulo, Av. Prof. Lineu Prestes, 748, Cidade Universitária, São Paulo, SP 05508-000, Brazil; piocolep@iq.usp.br

[4] Institute of Pharmacy (Pharmacology & Toxicology), Freie Universität Berlin, Königin Luise Str 2+4, Berlin, 14195, Germany; christian.zoschke@fu-berlin.de

[5] TissUse GmbH, Oudenarder Str. 16, Berlin, 13347, Germany; uwe.marx@tissuse.com

***** Correspondence: christian.zoschke@fu-berlin.de; Tel.: +49-30-838-56189

Received: 20 November 2019; Accepted: 31 January 2020; Published: 5 February

Abstract: UV light catalyzes the ozone formation from air pollutants, like nitrogen oxides. Since ozone reacts with cutaneous sebum lipids to peroxides and, thus, promotes inflammation, tumorigenesis, and aging, even broad-spectrum sunscreens cannot properly protect skin. Meanwhile, xanthophylls, like fucoxanthin, proved their antioxidant and cytoprotective functions, but the safety of their topical application in human cell-based models remains unknown. Aiming for a more detailed insight into the cutaneous fucoxanthin toxicity, we assessed the tissue viability according to OECD test guideline no. 439 as well as changes in inflammation (IL-1α, IL-6, IL-8), homeostasis (EGFR, HSPB1) and metabolism (NAT1). First, we proved the suitability of our 24-well-based reconstructed human skin for irritation testing. Next, we dissolved 0.5% fucoxanthin either in alkyl benzoate or in ethanol and applied both solutions onto the tissue surface. None of the solutions decreased RHS viability below 50%. In contrast, fucoxanthin ameliorated the detrimental effects of ethanol and reduced the gene expression of pro-inflammatory interleukins 6 and 8, while increasing NAT1 gene expression. In conclusion, we developed an organ-on-a-chip compatible RHS, being suitable for skin irritation testing beyond tissue viability assessment. Fucoxanthin proved to be non-irritant in RHS and already showed first skin protective effects following topical application.

Keywords: antioxidants; epidermal growth factor receptor; interleukins; irritation; metabolism response; N-acetyltransferase; small heat and shock protein beta 1

---

1. Introduction

Epidemiological data and clinical presentation provide conclusive evidence for UV radiation as the major cause of skin aging, cancer, and inflammation (Flament et al. 2013, Xu et al. 2011). UVB radiation promote the dimerization of pyrimidine DNA bases to cyclobutane dimers and subsequently C to T base transitions. Abundant C to T base transitions and CC to TT tandem mutations are referred to as a UVB signature or fingerprint. UVA radiation increases numbers of reactive oxygen species, which oxidize DNA bases to 8-hydroxyguanine, and cause G-to-T base transversion (Nishisgori 2015). Thereby, the production of reactive oxygen species has two major causes. First, UV radiation directly oxidizes the major sebum component squalene and, thus, drives the expression of pro-inflammatory cytokines (Awad et al. 2018). Second, UVA reacts

with nitrogen oxides and volatile organic compounds, both abundant air pollutants in urban areas, to ozone . Ozone itself does not penetrate the skin, but the ozone-mediated peroxidation of unsaturated lipids on the skin's surface induces oxidative stress and inflammatory responses in deeper skin layers (Valacchi et al. 2016).

Prevention is considered as the prime strategy to reduce the number of skin cancer patients because treatment remains insufficiently effective in terms of cure rates and recurrence (Ulrich et al. 2009). Yet, the widely recommended sunscreen application also provides insufficient protection against direct or indirect sunlight effects. Frequent underdosage (Heerfordt et al. 2018) and abuse of sunscreens for intentional prolonged sun exposure (Autier 2009) contribute to their low efficacy. Moreover, current sunscreens currently do not absorb VIS and IR light. This filter gap allows VIS and IR radiation penetrating deep skin layers and to produce 50% of the total amount of reactive oxygen species in skin (Lohan et al. 2016). Due to minor amounts of endogenous antioxidants in deeper skin layers, reactive oxygen species are hardly eliminated in the dermis (Thiele et al. 2001) as well as in aged skin (Rhie et al. 2001). Taken together, even optimal application of currently existing sunscreen will not provide full protection from the effects of sunlight and air pollution, emphasizing the need for effective antioxidants in skin care.

Antioxidants address this issue by lowering the amount of reactive oxygen species. Administered either orally in nutraceuticals or topically in cosmetic products, antioxidants comprise carotenoids, squalene, and vitamins, to name but a few. Although nutraceuticals received considerable interest, studies on bioavailability, efficacy, and mechanism of action are scarce (Perez-Sanchez et al. 2018). Furthermore, their uncontrolled use might cause secondary effects and interactions with medicinal products. Focusing on carotenoids, β-carotene and fucoxanthin are known for their antioxidant and cytoprotective functions and exemplarily represent the two carotenoid classes, carotenes and xanthophylls. Fucoxanthin was first isolated from the marine brown seaweeds and differs from other carotenoids due to an unusual allenic carbon (C-7′),5,6-monoepoxide, two hydroxyl groups, a carbonyl group, and an acetyl group in the terminal ring of fucoxanthin (Peng et al. 2011). This particular chemical structure causes similar or higher antioxidant activities in comparison to those of α-tocopherol as well as suppressive effects on superoxide anion and nitric oxide generation (Sachindra et al. 2007, Murakami et al. 2000). Despite of the high antioxidant activity, oral fucoxanthin application does not result in efficient cutaneous

concentrations. Fucoxanthin and its metabolites were primarily found in adipose tissue, liver, lungs, kidney, heart, and the spleen of mice (Hashimoto et al. 2009). Thus, a topical application of the lipophilic compound should achieve higher fucoxanthin doses at the target site.

The poor water solubility of fucoxanthin (log*P* 7.8) poses a challenge for the formulation of topically-used fucoxanthin products. Alkyl benzoate and ethanol are frequently used as solubilizers for highly lipophilic substances (Gaspar et al. 2013), and especially ethanol enhances the skin penetration (Lane 2013).

Herein, we investigated the toxicological effects of fucoxanthin, dissolved either in alkyl benzoate or ethanol, on inflammation (interleukin-1α, 6, 8), homeostasis (epidermal growth factor receptor, small heat and shock protein beta 1), and metabolism (N-acetyltransferase 1) as well as on tissue viability in reconstructed human skin from primary human cells. To evaluate fucoxanthin effects, we selected pro-inflammatory cytokines IL-1α, IL-6, and IL-8, as well as EGFR, to study the beginning of re-epithelialization and HSPB1 to monitor the protective functions under stress conditions as well as NAT1, since fucoxanthin is totally deacetylated in the intestinal lumen.

2. Materials and Methods

2.1. Reconstructed Human Skin

The experimental procedures conformed to the principles of the Declaration of Helsinki and were approved by the ethics committees of Charité—Universitätsmedizin Berlin (EA1/081/13). Informed written consent was obtained from all the donors or their parent or legal guardian. The reconstructed human skin (RHS) was cultured in 24-well plates with primary human keratinocytes and fibroblasts (passage 3, pooled from three donors) from foreskin with ethical committee approval (EA1/081/13), and after parents had signed the written informed consent. We made the dermal compartment on day 01 by pouring 0.5 mL collagen I (Biochrom; Berlin, Germany) with 1.14×10^5 normal human dermal fibroblasts into the insert (0.4 µm pore size; Millicell, Merck, Darmstadt, Germany). We seeded 3.7×10^5 normal human keratinocytes onto the dermal compartment on day 2 and raised the constructs to the air-liquid interface on day 3. The culture medium was changed three times a week for seven days.

2.2. Test Substance Application

After the RHS were fully differentiated on day 10, we placed them into new 24-well plates containing 0.5 mL of fresh medium and performed the test according to OECD test guideline no. 439 [40]. In brief, 10 µL of the following test substances were applied for 15 min: phosphate-buffered saline (PBS, Sigma-Aldrich, München, Germany), 5% (*w*/*v*) sodium dodecyl sulfate (SDS, CAS-no: 151-21-3; Carl Roth, Berlin, Germany), 0.5% (*w*/*v*) all-*trans*-fucoxanthin (≥95% pure, CAS-no: 3351-86-8; Sigma-Aldrich), C12-15 alkyl benzoate (Crodamol™ AB, CAS- no 68411-27-8; Croda, Brazil), and ethanol (99.5%, CAS-no: 64-17-5; Merck, Germany). Subsequently, the constructs were washed 12 times with 0.5 mL PBS, dried with a sterile cotton swab, and placed into new 24-well plates with fresh medium for 42 h at 37 °C, 5% CO_2.

2.3. Viability Assay

Constructs were incubated with the test substances for 15 min followed by a 42 h post-incubation period. RHS viability was determined by measuring the metabolic activity of the constructs after exposure and post-incubation using a colorimetric test according to OECD test guideline no. 439 (OECD 439 2019). The reduction of mitochondrial dehydrogenase activity was assessed via the decreased formazan production following incubation with MTT (3-(4,5-dimethylthiazol-2-yl) -2,5-diphenyltetrazolium bromide, Sigma-Aldrich). The formazan production was measured at 570 nm (FLUOstar OPTIMA, BMG Labtech; Ortenberg, Germany). We performed tests for interference of chemicals with MTT endpoint and correction in accordance to MatTek's "*In vitro* EpiDerm™ Skin Irritation Test" ((Kandárová et al. 2009), steps 1–4). The formazan readings were corrected by the fucoxanthin-related optical densities as well as by the optical densities due to direct MTT reduction and compared to those of negative control RHS (OECD 439 2019). Data are presented as the relative viability according to Equation (1):

$$\begin{aligned} &Relative\ viability\ (\%) \\ &= 100 * [OD\ (test\ substance)/mean\ OD\ (negative\ control)] \end{aligned} \quad (1)$$

2.4. Morphology and Immunofluorescence

Each RHS was snap frozen, sectioned into 8 µm slices (Leica CM 1510S; Wetzlar, Germany), and analyzed by hematoxylin-eosin or immunofluorescence staining.

Antibodies against the following proteins were purchased from abcam (Cambridge, UK): filaggrin (1:1000; ab81468), involucrin (1: 500; ab111781), and from Dianova (Hamburg, Germany): keratin-10 (1:200, cat-no. AF0197-01). Pictures were taken with a fluorescence microscope (BZ-8000, Keyence, Neu-Isenburg, Germany) and analyzed by ImageJ software 1.52a (Rueden et al. 2017).

2.5. Gene Expression

Real-time qPCR endpoint analysis was performed according to established procedures [46]. Briefly, the epidermal and dermal compartments of the RHS were mechanically separated. RNA from the epidermis was isolated using the NucleoSpin RNA II Kit (Macherey-Nagel, Düren, Germany). The TaqMan® Reverse Transcription Kit (Thermo Fisher Scientific Inc., Waltham, MA, USA) synthesized cDNA by reverse transcription of 100 ng total RNA. Quantitative PCR was performed using the QuantStudio 5 Real-Time PCR System (Thermo Fisher Scientific) and the SensiFAST SYBR Lo-ROX Kit (Bioline, Luckenwalde, Germany) according to the manufacturer's instructions. The primers were designed with UCSC Genome Browser (Kent et al. 2002) as described in Table 1 and were synthesized by EuroPrime (Invitrogen, Berlin, Germany). Gene expressions were normalized to the housekeeping gene ACTB.

Table 1. Primer sequences for PCR studies.

Gene Name	Used Primer Sequence	
	Forward	**Reverse**
ACTB	CCACCATGTACCCTGGCATT	GCTTGCTGATCCACATCTGCT
EGFR	GCCGACAGCTATGAGATGGAG	TGGAGGTGCAGTTTTTGAAGTG
HSPB1	GACCCCACCCAAGTTTCCTC	TCGGATTTTGCAGCTTCTGG
IL-1α	GTGACTGCCCAAGATGAAGACC	TGCCAAGCACACCCAGTAGTC
IL-6	CTGGATCAGGACTTTTGTACTCATCT	CCAATCTGGATTCAATGAGGAGACT
IL-8	GTGGAGAAGTTTTTGAAGAGGGC	TCTGGCAACCCTACAACAGAC
NAT1	ATCCGAGCTGTTCCCTTTGAG	AACATACCCTCCCAACATCGTG

2.6. Statistical Analysis

Data are presented as the mean + SD obtained from three independent experiments. Due to the explorative data analysis, a level of $p \leq 0.05$ was considered to indicate a statistically significant difference. One-way ANOVA and subsequent Tukey post hoc tests were performed with GraphPad Prism 5.0 (La Jolla, CA, USA).

3. Results

3.1. Fucoxanthin Effects on RHS Morphology

The 10-day culture of reconstructed human skin (RHS) resulted in a stratified epidermis with well-expressed *stratum basale, spinosum, granulosum, and corneum* (Figure 1a). Keratinocyte differentiation induced cell flattening and the expression of keratin-10 in suprabasal layers (Figure 1b). Keratin-10 and 14 was expressed throughout all epidermal layers (Figure 1b). Moreover, involucrin found in the *stratum corneum* showed the formation of a cornified envelope (Figure 1c). Although we observed also parakeratosis—an almost regular feature of skin models—and only small amounts of filaggrin, the RHS morphology suggested a sufficient skin barrier formation.

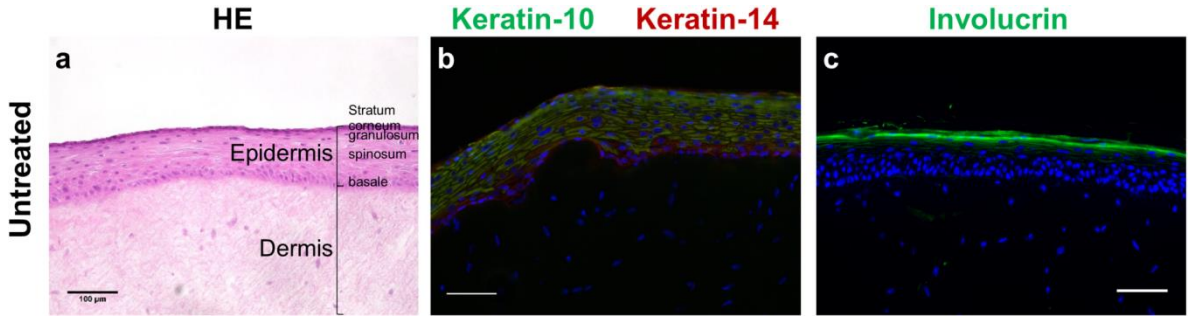

Figure 1. Morphology and protein expression in reconstructed human skin. (**a**) Hematoxylin-eosin staining showing all layers of human skin. (**b**) Immunolocalization of keratin-10 (green) in suprabasal epidermal layers and keratin-14 (red) in all epidermal layers. (**c**) Immunolocalization of involucrin (green), indicating terminal keratinocyte differentiation. Images are representative of three batches; nuclei in blue (DAPI); scale bars = 100 µm.

Neither fucoxanthin nor the vehicle alkyl benzoate disturbed tissue morphology (Figure 2a,b). Ethanol caused a detachment of the stratum corneum from the viable epidermis as well as slight damages in the coherence of the viable epidermis (Figure 2c). The filaggrin expression in RHS was slightly increased following exposure to fucoxanthin and ethanol (Figure 2d,f). Involucrin was homogenously distributed in the stratum corneum following all substance exposures (Figure 2g–i).

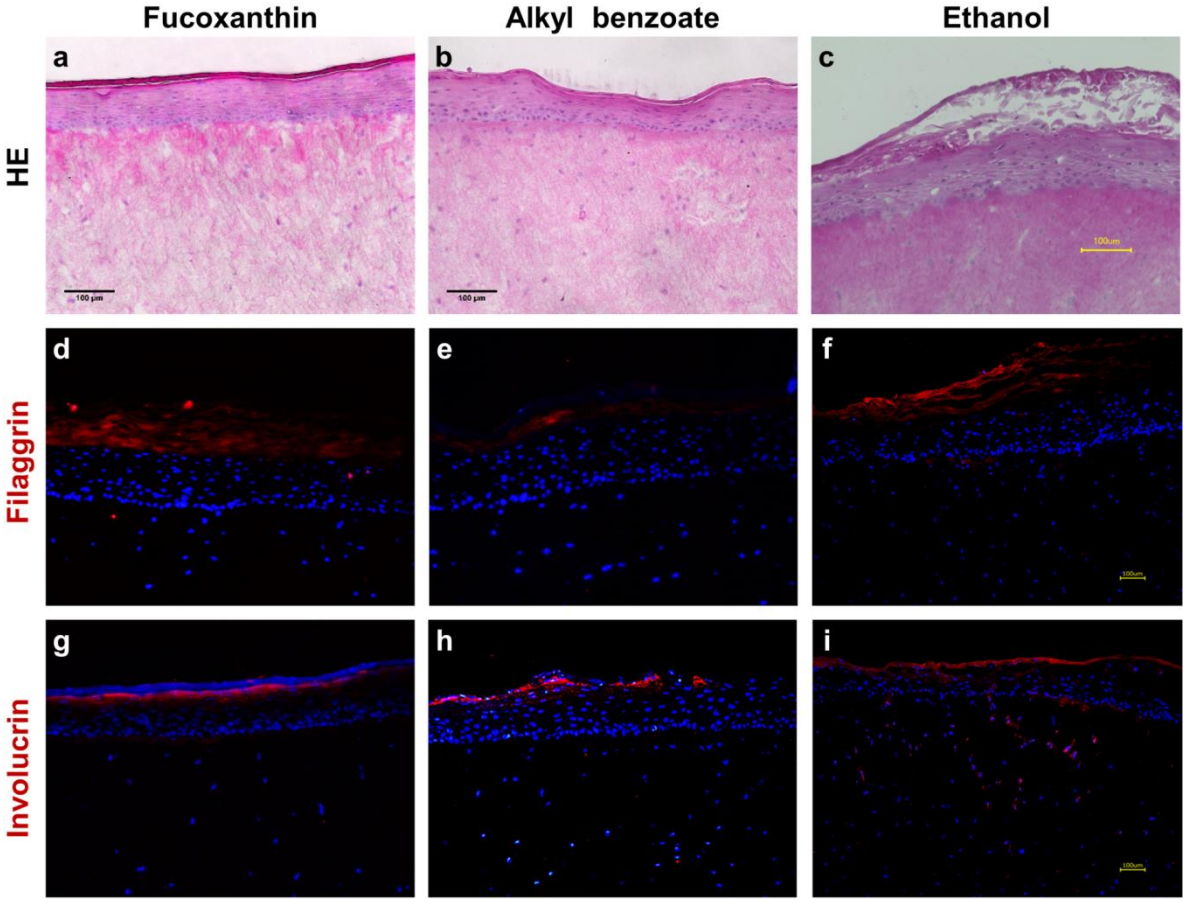

Figure 2. Morphology and protein expression in reconstructed human skin following fucoxanthin exposure versus the vehicles alone. (**a**–**c**) Hematoxylin-eosin staining with slightly disturbed morphology in c. (**d**–**f**) Immunolocalization of filaggrin with enhanced expression in d and f. (**g**–**i**) Similar immunolocalization of involucrin in all samples. Images are representative of at least three batches; nuclei in blue (DAPI); scale bars = 100 µm.

3.2. Fucoxanthin Effects on RHS Viability

Before assessing the RHS viability following substance exposure, we evaluated the interference of fucoxanthin with an MTT test. Fucoxanthin solutions as well as RHS treated with fucoxanthin were stained red, resulting in absorbance at 450 nm after isopropanol extraction although no MTT was added to these control tissues. Next, we investigated the direct reduction of MTT by fucoxanthin in solution as well as in freeze-killed tissues. Although we observed only a minor effect, we subtracted the absorbance due to fucoxanthin's color and due to a direct interaction with MTT from all absorbance values of fucoxanthin-treated RHS in the viability tests. Phosphate-buffered saline

(PBS) and sodium dodecyl sulfate (SDS) served as negative and positive controls, respectively, as recommended by the OECD.

The viability of RHS following SDS exposure and 42 h post-treatment incubation period decreased to 2.6 ± 2.4%, correctly identifying SDS as skin irritant (Figure 3). Moreover, the standard deviation between tissue replicates fell far below 18%, and, thus, met the acceptability criteria of OECD test guideline no. 439.

Fucoxanthin showed a significantly higher viability than the positive control (Figure 3). Since the values exceeded also the threshold of 50%, fucoxanthin was not irritant to RHS. When testing the solvent controls, we observed a marked decrease in viability to 52.8 ± 9.0%. This tissue damage was ameliorated in the ethanolic test solution of fucoxanthin, as seen by a relative viability of 75.7%.

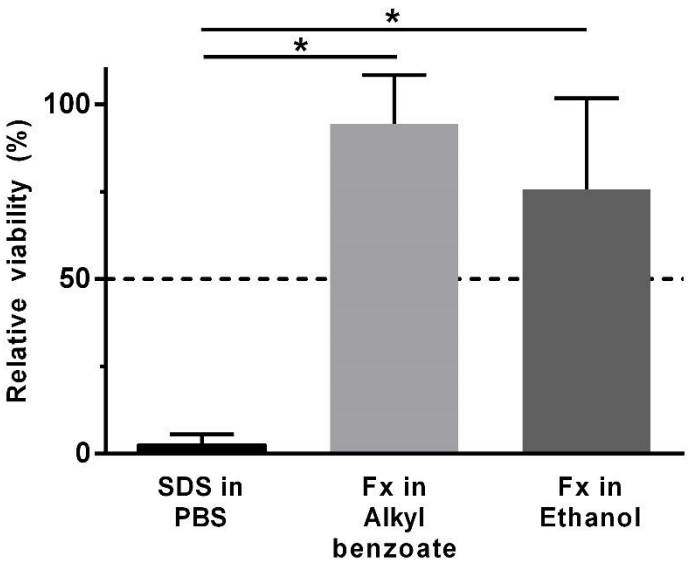

Figure 3. Fucoxanthin effects on the viability of reconstructed human skin. Test substances below the 50% threshold (dashed line) are predicted to be skin irritant. PBS—phosphate buffered saline (negative control); SDS—sodium dodecyl sulfate (positive control); Fx—fucoxanthin. Alkyl benzoate and ethanol were exposed for 15 min to the RHS and subsequently washed off. Mean + SD, $n \geq 3$, $^*p \leq 0.05$ compared to SDS.

3.3. Fucoxanthin Effects on RHS Gene Expression

Next, we evaluated the gene expression following substance exposure and 42 h post-treatment incubation period to get a more detailed insight into the toxicity of fucoxanthin (Figure 4). SDS markedly increased the gene expression of N-

acetyltransferase 1 (NAT1) as well as of pro-inflammatory genes, like interleukin (IL)-1α, 6, and 8, compared to the levels in PBS-treated RHS. Moreover, the gene expression of epidermal growth factor receptor (EGFR) and small heat and shock protein beta 1 (HSPB1) were slightly elevated.

Fucoxanthin exposure increased none of these gene expressions. When applied in alkyl benzoate solutions, we detected almost no change in gene expression. The ethanolic solution of fucoxanthin decreased the gene expression of IL-6 and 8 compared to the gene expression in ethanol-treated RHS to 33% or 15% compared to the solvent control samples. NAT1 gene expression was doubled compared to ethanol-treated RHS.

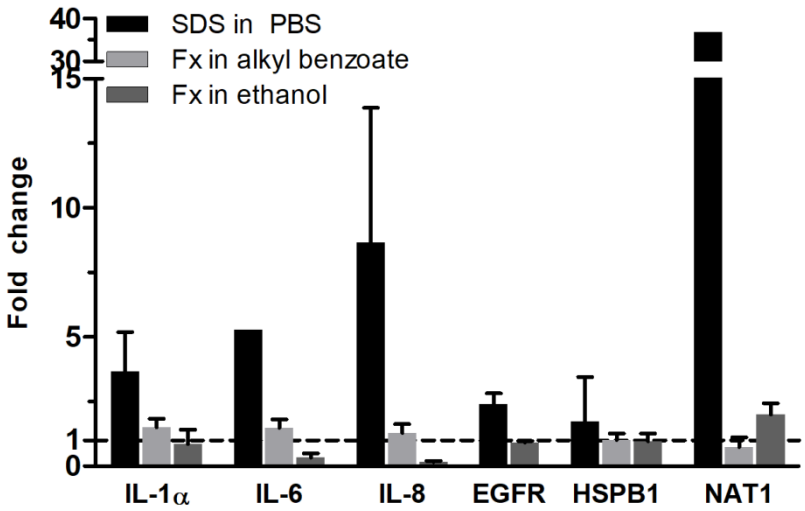

Figure 4. Fucoxanthin effects on the gene expression of reconstructed human skin. Fold change in gene expression was calculated in relation to the gene expression in reconstructed human skin exposed to the respective solvent (dashed line), SDS to PBS and Fx to alkyl benzoate or to ethanol. SDS—sodium dodecyl sulfate; PBS—phosphate-buffered saline; Fx—fucoxanthin; IL—interleukin; EGFR—epidermal growth factor receptor; HSPB1—small heat and shock protein beta 1; NAT1—N-acetyltransferase 1. Mean + SD, *n* = 3.

4. Discussion

Intrigued by the marked antioxidant efficacy of fucoxanthin (Sachindra et al. 2007, Murakami et al. 2000), we investigated the potential toxicity of fucoxanthin in two different solvents, which are frequently used in dermatological products. Our results proved fucoxanthin to be non-irritant and suggested using alkyl benzoate as a solvent

for the fucoxanthin (Figure 3). Absolute ethanol reduced the viability of RHS, but was necessary to dissolve the lipophilic fucoxanthin. Both viability testing and gene expression analysis revealed the ameliorating effects of fucoxanthin on the ethanol-induced inflammation in RHS (Figures 3 and 4). Moreover, we proved the applicability of our novel 24-well-sized RHS, being fully compatible with organ-on-a-chip applications (Figures 1 and 2). Using RHS extends the approach of OECD test guideline no. 439 and becomes mandatory when investigating biochemical pathways due to the known epidermal-dermal cross-talk in normal and diseased skin models (Maas-Szabowski, Stark, and Fusenig 2000, Berroth et al. 2013).

The strong clinical need for skin protection is emphasized by the extraordinary increase of skin cancer patients. In Brazil, non-melanoma skin cancer accounts for 30% of diagnosed cancers (The Brazilian National Cancer Institute 2008), while in Australia, more people have been diagnosed with skin cancer than all other cancers combined (International Agency for Research on Cancer 2014). The underlying biochemical mechanisms clearly provided the correlation between the cumulative exposure to UV radiation and skin cancer (Nishisgori 2015) and the contribution of VIS and IR radiation and air pollutants to cutaneous carcinogenesis has been described (Valacchi et al. 2016, Lohan et al. 2016) as well. Aging accelerates a vicious circle of cumulative damage to the skin, reduced amounts of antioxidants among other age-associated conditions, like xerosis, impaired skin barrier, and wound healing, promoting the penetration of more pollutants into the skin (Parrado et al. 2019). The correlation of an additional 10 $\mu g/m^3$ NO_2 in the air with 25% more pigment spots on female cheeks (Hüls et al. 2016) shows the cosmetic, and may indicate a medical, need for the prevention from extrinsic factors. However, protection from UV, or even from the entire spectrum of solar radiation cannot prevent from its detrimental effects, since nitric oxide, volatile organic compounds, and particulate matter also contributes to skin aging, inflammation, and cancer (Burke 2018). Thus, the strategy against skin aging must include a multitude of different approaches, including cleansing products to reduce the particle load on skin, agents that strengthen the skin barrier function, products that protect from sunlight, anti-inflammatory agents, and antioxidants (Mistry 2017).

Antioxidants from natural sources, like fucoxanthin, address these clinical and cosmetic needs due to the antioxidant properties. Herein, we exclusively investigated the effects of the commercially available fucoxanthin and not multi-compound algae

extracts. Nevertheless, fucoxanthin needs to accumulate in sufficient amounts at the target site. The lipophilicity (log*P* 7.8) of fucoxanthin, as well as the accumulation of fucoxanthin and its degradation products in murine adipose tissue, liver, lungs, kidney, heart, and spleen (Hashimoto et al. 2009), questions the efficacy of orally-administered fucoxanthin in skin. Thus, we applied the fucoxanthin solution topically to RHS and selected 0.5% as concentration, being in the range used for antioxidants in cosmetic formulations (0.01–1%). We dissolved the highly lipophilic fucoxanthin in alkyl benzoate, being devoid of genotoxic properties and frequently used in cosmetics as a solvent, emollient, preservative, and plasticizer (Becker et al. 2012). Moreover, alkyl benzoate is already used to solubilize UV filters in sunscreens (Gaspar et al. 2013). For comparison, we also included an ethanolic solution based on the recommendations for poorly water-soluble substances in skin irritation testing (Kandárová et al. 2018). Moreover, the high ethanol concentration was required to dissolve fucoxanthin and allowed us to investigate the potentially ameliorating effects of this antioxidant.

Even the small amount of 10 µL ethanol solution per tissue, equal to 17 µL/cm^2, disturbed the RHS morphology (Figure 2c), viability (Figure 3), and altered the gene expression (Figure 4). This is well in accordance with previous observations, where high concentrations were necessary for drug dissolution, as well (Wanjiku et al. 2019); more than 80% of cell death occurred even following the exposure to 50% ethanol in skin models (Li, Margolis, and Hoffman 1991). The mechanism of tissue damage by ethanol is related to oxidative stress and well-known from the oral cavity (Zukowski, Maciejczyk, and Waszkiel 2018). Ethanol directly reacts to hydroxyethyl radicals and subsequently contributes to the formation of other ROS species. Chronic ethanol exposure causes CYP induction, mitochondrial damage, reduced antioxidant defense mechanisms, and thereby amplifies ROS-related tissue damage. Meanwhile, ethanol is also most effective in increasing the skin absorption of lipophilic drugs, like butenafine (log*P* 6.6) (Zhang et al. 2017). Assuming that ethanol also effectively increased the penetration of fucoxanthin (log*P* 7.8), fucoxanthin can counteract the pro-oxidative effects of ethanol. Thus, both ethanol and fucoxanthin toxicity data in our study are in accordance with previously-published results on polyphenols in grapes and red wine, which are suggested to protect from ethanol damage (Sun et al. 2001). However, the efficacy of fucoxanthin will depend on the fucoxanthin concentrations within the tissue, as observed for other antioxidants.

The change in IL-6 and 8 gene expressions following test substance exposure correlates to the expression of IL-1α, HSPB1, and EGFR. IL-1α activates the p38 MAPK pathway to increase the expression of HSPB1, which causes anti-apoptotic effects, possesses chaperone-like activity and refolds denatured proteins, and is cytoprotective against heat shock [34]. EGFR also increases the expression of IL-8 (Frankart et al. 2012) and plays an essential role in re-epithelialization by increasing keratinocyte proliferation and cell migration in wounded skin (Barrientos et al. 2008). The constant gene expressions of EGFR and HSPB1 substantiate the absence of damage from fucoxanthin, but does not explain the reduction in IL-6 and IL-8 gene expression.

HSPB1 gene expression remained stable, even following the exposure to SDS. Although HSPB1 exerts protective functions under stress conditions (Verschuure et al. 2003), previous results with increased HSPB1 expressions were obtained 24 h after SDS treatment by Western blotting. Thus, the 42 h period of incubation was recommended for skin irritation testing (OECD 439 2019), yet probably too long to detect maximum increase in HSPB1 gene expression.

Finally, we investigated the expression of NAT1 in RHS, since fucoxanthin is totally deacetylated in the intestinal lumen (for review see (Peng et al. 2011)). We observed an upregulation of NAT1 following the application of fucoxanthin in ethanol (Figure 4), indicating an activation of cutaneous metabolism, being relevant when applying drugs or cosmetic actives to the skin.

Instead of using murine models (Rodríguez-Luna et al. 2018b), we developed a full-thickness RHS to assess the potential toxic effects of fucoxanthin. Accumulating insights into the predictive power of animal-based tests in toxicology (Bailey, Thew, and Balls 2014) emphasize the need for human cell-based models. Nevertheless, the skin model in this study consisted of primary juvenile cells and did not consider age-related changes in skin function. Future studies should investigate the efficacy of fucoxanthin in aged RHS (Hausmann et al. 2020), thereby taking age-related differences between young, middle-aged, and senior patients into account. Moreover, emerging markets for cosmetics demand the use of human cell-based test systems. For example, Brazil banned cosmetic products from being tested in animal models in 2019, but the Brazilian legislation gap in the use of biological material of human origin, which until recently impeded access to commercially-available skin models (De Vecchi et al. 2018). Thus, in-house or open-source protocols are urgently needed, but also

need to be validated for their intended use. In the present study, we presented a fast (10-day culture) RHS protocol at reasonable price (3.7×10^5 keratinocytes per construct), which is fully compatible to organ-on-a-chip applications. Multi-organ-chips provide the opportunity to study substance effects in an interconnected and perfused *in vitro* model, aiming to include the influence of liver function into substance evaluation (Maschmeyer, Hasenberg, et al. 2015).

5. Conclusions

Taken together, our study clearly demonstrated the non-irritancy of fucoxanthin. Fucoxanthin ameliorated detrimental effects of ethanol on tissue viability and inflammatory response. We observed metabolism activation by NAT1 upregulation, but no change in HSPB1 regulation. Finally, we proved the applicability of our novel, organ-on-a-chip compatible RHS for the evaluation of substance effects.

Author Contributions: Conceptualization: R.S.N.T., H.M.D., L.R.G., and C.Z.; investigation: R.S.N.T., S.S.M.-E., U.M., and C.Z.; writing—original draft preparation: R.S.N.T., M.S.-K., L.R.G., and C.Z.; writing—review and editing: R.S.N.T., L.R.G., and C.Z.; visualization: R.S.N.T. and C.Z.; supervision: L.R.G. and C.Z.; project administration: L.R.G. and C.Z.; funding acquisition: R.S.N.T., P.C.N., H.M.D., M.S.K., and L.R.G.

Funding: This research was funded by The São Paulo Research Foundation, FAPESP (grant numbers 2014/50928-2 and 2016/06931-4), by CNPq (grant number 465687/2014-8), and by the Bundesministerium für Bildung und Forschung (Berlin-Brandenburg Research Platform BB3R, grant number 031A262A). R.S.N.T. gratefully acknowledges a doctoral scholarship of DAAD/CAPES/CNPq 15° 2017 (grant number 290281/2017-2). The publication of this article was funded by Freie Universität Berlin.

Acknowledgments: The authors highly appreciated the excellent technical assistance of Carola Kapfer.

Conflicts of Interest: The authors declare no conflict of interest. The funders had no role in the design of the study; in the collection, analyses, or interpretation of data; in the writing of the manuscript; or in the decision to publish the results.

References

1. Flament, F.; Bazin, R.; Laquieze, S.; Rubert, V.; Simonpietri, E.; Piot, B. Effect of the sun on visible clinical signs of aging in caucasian skin. *Clin Cosmet Investig Dermatol* **2013**, *6*, 221-232, doi:10.2147/CCID.S44686.
2. Xu, F.; Yan, S.; Wu, M.; Li, F.; Xu, X.; Song, W.; Zhao, J.; Xu, J.; Kan, H. Ambient ozone pollution as a risk factor for skin disorders. *Br J Dermatol* **2011**, *165*, 224-225, doi:10.1111/j.1365-2133.2011.10349.x.
3. Nishisgori, C. Current concept of photocarcinogenesis. *Photochemical & photobiological sciences : Official journal of the European Photochemistry Association and the European Society for Photobiology* **2015**, *14*, 1713-1721, doi:10.1039/c5pp00185d.
4. Awad, F.; Assrawi, E.; Louvrier, C.; Jumeau, C.; Giurgea, I.; Amselem, S.; Karabina, S.A. Photoaging and skin cancer: Is the inflammasome the missing link? *Mech Ageing Dev* **2018**, *172*, 131-137, doi:10.1016/j.mad.2018.03.003.
5. Burke, K.E. Mechanisms of aging and development—a new understanding of environmental damage to the skin and prevention with topical antioxidants. *Mech Ageing Dev* **2018**, *172*, 123-130, doi:https://doi.org/10.1016/j.mad.2017.12.003.
6. Valacchi, G.; Muresan, X.M.; Sticozzi, C.; Belmonte, G.; Pecorelli, A.; Cervellati, F.; Demaude, J.; Krol, Y.; Oresajo, C. Ozone-induced damage in 3d-skin model is prevented by topical vitamin c and vitamin e compound mixtures application. *J Dermatol Sci* **2016**, *82*, 209-212, doi:10.1016/j.jdermsci.2016.02.007.
7. Ulrich, C.; Jürgensen, J.S.; Degen, A.; Hackethal, M.; Ulrich, M.; Patel, M.J.; Eberle, J.; Terhorst, D.; Sterry, W.; Stockfleth, E. Prevention of non-melanoma skin cancer in organ transplant patients by regular use of a sunscreen: A 24 months, prospective, case–control study. *Br J Dermatol* **2009**, *161*, 78-84, doi:10.1111/j.1365-2133.2009.09453.x.
8. Heerfordt, I.M.; Torsnes, L.R.; Philipsen, P.A.; Wulf, H.C. Sunscreen use optimized by two consecutive applications. *PLOS ONE* **2018**, *13*, e0193916, doi:10.1371/journal.pone.0193916.
9. Autier, P. Sunscreen abuse for intentional sun exposure. *Br J Dermatol* **2009**, *161 Suppl 3*, 40-45, doi:10.1111/j.1365-2133.2009.09448.x.
10. Lohan, S.B.; Muller, R.; Albrecht, S.; Mink, K.; Tscherch, K.; Ismaeel, F.; Lademann, J.; Rohn, S.; Meinke, M.C. Free radicals induced by sunlight in different spectral regions - *in vivo* versus ex vivo study. *Exp Dermatol* **2016**, *25*, 380-385, doi:10.1111/exd.12987.
11. Thiele, J.J.; Schroeter, C.; Hsieh, S.N.; Podda, M.; Packer, L. The antioxidant network of the stratum corneum. *Curr Probl Dermatol* **2001**, *29*, 26-42, doi:10.1159/000060651.
12. Rhie, G.; Shin, M.H.; Seo, J.Y.; Choi, W.W.; Cho, K.H.; Kim, K.H.; Park, K.C.; Eun, H.C.; Chung, J.H. Aging- and photoaging-dependent changes of enzymic and nonenzymic antioxidants in the epidermis and dermis of human skin *in vivo*. *J Invest Dermatol* **2001**, *117*, 1212-1217, doi:10.1046/j.0022-202x.2001.01469.x.
13. Perez-Sanchez, A.; Barrajon-Catalan, E.; Herranz-Lopez, M.; Micol, V. Nutraceuticals for skin care: A comprehensive review of human clinical studies. *Nutrients* **2018**, *10*, doi:10.3390/nu10040403.
14. Peng, J.; Yuan, J.-P.; Wu, C.-F.; Wang, J.-H. Fucoxanthin, a marine carotenoid present in brown seaweeds and diatoms: Metabolism and bioactivities relevant to human health. *Marine drugs* **2011**, *9*, 1806-1828, doi:10.3390/md9101806.

15. Sachindra, N.M.; Sato, E.; Maeda, H.; Hosokawa, M.; Niwano, Y.; Kohno, M.; Miyashita, K. Radical scavenging and singlet oxygen quenching activity of marine carotenoid fucoxanthin and its metabolites. *J Agric Food Chem* **2007**, *55*, 8516-8522, doi:10.1021/jf071848a.
16. Murakami, A.; Nakashima, M.; Koshiba, T.; Maoka, T.; Nishino, H.; Yano, M.; Sumida, T.; Kim, O.K.; Koshimizu, K.; Ohigashi, H. Modifying effects of carotenoids on superoxide and nitric oxide generation from stimulated leukocytes. *Cancer letters* **2000**, *149*, 115-123, doi:10.1016/s0304-3835(99)00351-1.
17. Hashimoto, T.; Ozaki, Y.; Taminato, M.; Das, S.K.; Mizuno, M.; Yoshimura, K.; Maoka, T.; Kanazawa, K. The distribution and accumulation of fucoxanthin and its metabolites after oral administration in mice. *The British journal of nutrition* **2009**, *102*, 242-248, doi:10.1017/s0007114508199007.
18. Gaspar, L.R.; Tharmann, J.; Maia Campos, P.M.; Liebsch, M. Skin phototoxicity of cosmetic formulations containing photounstable and photostable uv-filters and vitamin a palmitate. *Toxicol In vitro* **2013**, *27*, 418-425, doi:10.1016/j.tiv.2012.08.006.
19. Lane, M.E. Skin penetration enhancers. *International journal of pharmaceutics* **2013**, *447*, 12-21, doi:10.1016/j.ijpharm.2013.02.040.
20. OECD 439. Test no. 439: *In vitro* skin irritation: Reconstructed human epidermis test method. In *Oecd guidelines for the testing of chemicals, section 4: Health effects [cited 2020/01/12]*, Available from: doi:https://doi.org/10.1787/9789264242845-en, 2019.
21. Kandárová, H.; Hayden, P.; Klausner, M.; Kubilus, J.; Sheasgreen, J. An *in vitro* skin irritation test (sit) using the epiderm reconstructed human epidermal (rhe) model. *JoVE* **2009**, doi:10.3791/1366, e1366, doi:doi:10.3791/1366.
22. Rueden, C.T.; Schindelin, J.; Hiner, M.C.; DeZonia, B.E.; Walter, A.E.; Arena, E.T.; Eliceiri, K.W. Imagej2: Imagej for the next generation of scientific image data. *BMC Bioinformatics* **2017**, *18*, 529, doi:10.1186/s12859-017-1934-z.
23. Kent, W.J.; Sugnet, C.W.; Furey, T.S.; Roskin, K.M.; Pringle, T.H.; Zahler, A.M.; Haussler, D. The human genome browser at ucsc. *Genome Res* **2002**, *12*, 996-1006, doi:10.1101/gr.229102.
24. Maas-Szabowski, N.; Stark, H.J.; Fusenig, N.E. Keratinocyte growth regulation in defined organotypic cultures through il-1-induced keratinocyte growth factor expression in resting fibroblasts. *J Invest Dermatol* **2000**, *114*, 1075-1084, doi:10.1046/j.1523-1747.2000.00987.x.
25. Berroth, A.; Kühnl, J.; Kurschat, N.; Schwarz, A.; Stäb, F.; Schwarz, T.; Wenck, H.; Fölster-Holst, R.; Neufang, G. Role of fibroblasts in the pathogenesis of atopic dermatitis. *J Allerg Clin Immun* **2013**, *131*, 1547-1554.e1546, doi:https://doi.org/10.1016/j.jaci.2013.02.029.
26. The Brazilian National Cancer Institute. Non-melanoma skin cancer. In *Cancer types [cited 2020/01/12]*, Available from: https://www.inca.gov.br/tipos-de-cancer/cancer-de-pele-nao-melanoma, 2008.
27. International Agency for Research on Cancer. World cancer report 2014. Available from: http://apps.who.int/bookorders/anglais/detart1.jsp?codlan=1&codcol=80&codcch=275 [cited 2020/01/12], 2014; Vol. World Health Organization.
28. Parrado, C.; Mercado-Saenz, S.; Perez-Davo, A.; Gilaberte, Y.; Gonzalez, S.; Juarranz, A. Environmental stressors on skin aging. Mechanistic insights. *Frontiers in pharmacology* **2019**, *10*, 759, doi:10.3389/fphar.2019.00759.

29. Hüls, A.; Vierkotter, A.; Gao, W.; Kramer, U.; Yang, Y.; Ding, A.; Stolz, S.; Matsui, M.; Kan, H.; Wang, S., et al. Traffic-related air pollution contributes to development of facial lentigines: Further epidemiological evidence from caucasians and asians. *J Invest Dermatol* **2016**, *136*, 1053-1056, doi:10.1016/j.jid.2015.12.045.
30. Mistry, N. Guidelines for formulating anti-pollution products. *Cosmetics* **2017**, *4*, 57.
31. Becker, L.C.; Bergfeld, W.F.; Belsito, D.V.; Hill, R.A.; Klaassen, C.D.; Liebler, D.; Marks, J.G., Jr.; Shank, R.C.; Slaga, T.J.; Snyder, P.W., et al. Safety assessment of alkyl benzoates as used in cosmetics. *Int J Toxicol* **2012**, *31*, 342s-372s, doi:10.1177/1091581812467379.
32. Kandárová, H.; Bendova, H.; Letasiova, S.; Coleman, K.P.; De Jong, W.H.; Jirova, D. Evaluation of the medical devices benchmark materials in the controlled human patch testing and in the rhe *in vitro* skin irritation protocol. *Toxicol In vitro* **2018**, *50*, 433-438, doi:10.1016/j.tiv.2018.02.009.
33. Wanjiku, B.; Yamamoto, K.; Klossek, A.; Schumacher, F.; Pischon, H.; Mundhenk, L.; Rancan, F.; Judd, M.M.; Ahmed, M.; Zoschke, C., et al. Qualifying x-ray and stimulated raman spectromicroscopy for mapping cutaneous drug penetration. *Anal Chem* **2019**, *91*, 7208-7214, doi:10.1021/acs.analchem.9b00519.
34. Li, L.N.; Margolis, L.B.; Hoffman, R.M. Skin toxicity determined *in vitro* by three-dimensional, native-state histoculture. **1991**, *88*, 1908-1912, doi:10.1073/pnas.88.5.1908 %J Proceedings of the National Academy of Sciences.
35. Zukowski, P.; Maciejczyk, M.; Waszkiel, D. Sources of free radicals and oxidative stress in the oral cavity. *Archives of oral biology* **2018**, *92*, 8-17, doi:10.1016/j.archoralbio.2018.04.018.
36. Zhang, A.; Jung, E.C.; Zhu, H.; Zou, Y.; Hui, X.; Maibach, H. Vehicle effects on human stratum corneum absorption and skin penetration. *Toxicology and industrial health* **2017**, *33*, 416-425, doi:10.1177/0748233716656119.
37. Sun, A.Y.; Ingelman-Sundberg, M.; Neve, E.; Matsumoto, H.; Nishitani, Y.; Minowa, Y.; Fukui, Y.; Bailey, S.M.; Patel, V.B.; Cunningham, C.C., et al. Ethanol and oxidative stress. *Alcoholism, clinical and experimental research* **2001**, *25*, 237s-243s, doi:10.1097/00000374-200105051-00038.
38. Frankart, A.; Coquette, A.; Schroeder, K.R.; Poumay, Y. Studies of cell signaling in a reconstructed human epidermis exposed to sensitizers: Il-8 synthesis and release depend on egfr activation. *Arch Dermatol Res* **2012**, *304*, 289-303, doi:10.1007/s00403-012-1209-5.
39. Barrientos, S.; Stojadinovic, O.; Golinko, M.S.; Brem, H.; Tomic-Canic, M. Perspective article: Growth factors and cytokines in wound healing. *Wound Rep Reg* **2008**, *16*, 585-601, doi:10.1111/j.1524-475X.2008.00410.x.
40. Verschuure, P.; Tatard, C.; Boelens, W.C.; Grongnet, J.F.; David, J.C. Expression of small heat shock proteins hspb2, hspb8, hsp20 and cvhsp in different tissues of the perinatal developing pig. *European journal of cell biology* **2003**, *82*, 523-530, doi:10.1078/0171-9335-00337.
41. Rodríguez-Luna, A.; Ávila-Román, J.; González-Rodríguez, M.L.; Cózar, M.J.; Rabasco, A.M.; Motilva, V.; Talero, E. Fucoxanthin-containing cream prevents epidermal hyperplasia and uvb-induced skin erythema in mice. *Marine Drugs* **2018**, *16*, 378.
42. Bailey, J.; Thew, M.; Balls, M. An analysis of the use of animal models in predicting human toxicology and drug safety. *Alternatives to laboratory animals : ATLA* **2014**, *42*, 181-199.

43. Hausmann, C.; Vogt, A.; Kerscher, M.; Ghoreschi, K.; Schäfer-Korting, M.; Zoschke, C. Optimizing skin pharmacotherapy for older patients: The future is at hand but are we ready for it? *Drug Discov Today* **2020**, 10.1016/j.drudis.2020.01.011, doi:10.1016/j.drudis.2020.01.011.
44. De Vecchi, R.; Dakic, V.; Mattos, G.; Rigaudeau, A.-S.; Oliveira, V.; Garcia, C.; Alépée, N.; Bouez, C. Implementation, availability and regulatory status of an OECD accepted reconstructed human epidermis model in brazil. *Vigilância Sanitária em Debate* **2018**, *6*, 64, doi:10.22239/2317-269x.01055.
45. Maschmeyer, I.; Hasenberg, T.; Jaenicke, A.; Lindner, M.; Lorenz, A.K.; Zech, J.; Garbe, L.A.; Sonntag, F.; Hayden, P.; Ayehunie, S., et al. Chip-based human liver-intestine and liver-skin co-cultures--a first step toward systemic repeated dose substance testing *in vitro*. *Eur J Pharm Biopharm* **2015**, *95*, 77-87, doi:10.1016/j.ejpb.2015.03.002.

4.3. Capítulo 3 - Avaliação de toxicidade da terbinafina por via tópica e sistêmica em condição estática versus dinâmica (organ-on-a-chip)

Artigo submetido a publicação na revista *International Journal of Pharmaceutics* em 28 de abril de 2020 (vide anexo), devolvido em 30 de maio para revisões e submetido novamente em 24 de julho, 2020.

Toxicity of Topically Applied Drugs beyond Skin Irritation: Static Skin Model vs. Two Organs-on-a-Chip

Tavares, R. S. N.[1]; Phuong-Tao, T. [2]; Maschmeyer, I.[2]; Maria-Engler, S. S.[3]; Schäfer-Korting, M.[4]; Winter, A.[2]; Zoschke, C.[4]; Lauster, R.; Marx, U.[2]; Gaspar, L. R.[1*]

[1] *School of Pharmaceutical Sciences of Ribeirão Preto, University of São Paulo, Av. do Café s/n, Bairro Monte Alegre, Ribeirão Preto, SP, Brazil.*

[2] *TissUse GmbH, Oudenarder Str. 16, 13347, Berlin, Germany.*

[3] *Clinical and Toxicological Analyses Department, School of Pharmaceutical Sciences, University of São Paulo, Av. Prof. Lineu Prestes, 748, Cidade Universitária, São Paulo, SP 05508-000, Brazil.*

[4] *Institute of Pharmacy (Pharmacology & Toxicology), Freie Universität, Königin-Luise-Str. 2+4, 14195 Berlin, Germany.*

*Corresponding author:
Prof. Lorena Rigo Gaspar
University of São Paulo, School of Pharmaceutical Sciences of Ribeirão Preto, Av. do Café s/n, Bairro Monte Alegre, Ribeirão Preto, SP, Brazil. 14040-903, Brazil
Email: lorena@fcfrp.usp.br

Abstract

Skin model cultivation under static conditions limits the observation of the toxicity to this single organ. Biology-inspired microphysiological systems associating skin with a liver in the same circulating medium provide a more comprehensive insight into systemic substance toxicity; however, its advantages or limitations for topical substance toxicity remain unknown. Herein, we performed topical (OECD test guideline no. 439) and systemic administration of terbinafine in reconstructed human skin (RHS) vs. a RHS plus liver model cultured in TissUse' HUMIMIC Chip2 (Chip2). Aiming for a more detailed insight into the cutaneous substance irritancy/toxicity, we assessed more than the MTT cell viability: lactate dehydrogenase (LDH), lactate and glucose levels, as well as inherent gene expressions. Sodium dodecyl sulfate (SDS) was the topical irritant positive control. We confirmed SDS irritancy in both static RHS and Chip2 culture by the damage in the morphology, reduction in the lactate production and lower glucose consumption. In the static RHS, the SDS-treated tissues also released significantly high LDH (82 %; $p < 0.05$), corroborating with the other metabolic levels. In both static RHS and Chip2 conditions, we confirmed absence of irritancy or systemic toxicity by LDH, glucose or lactate levels for topical 1 % and 5 % terbinafine and systemic 0.1% terbinafine treatment. However, topical 5% terbinafine treatment in the Chip2 upregulated IL-1α in the RHS, unbalanced apoptotic and proliferative cell ratios in the liver and significantly increased its expression of CYP1A2 and 3A4 enzymes ($p < 0.05$), proving that it has passed the RHS barrier promoting a liver impact. Systemic 0.1 % terbinafine treatment in the Chip2 increased skin expression of EGFR, increased apoptotic cells in the liver, downregulated liver albumin expression and upregulated CYP2C9 significantly ($p < 0.05$), acting as an effective hepatotoxic terbinafine control. The combination of the skin and liver model in the Chip2 allowed a more sensitive assessment of skin and hepatic effects caused by chemicals able to pass the skin (5% terbinafine and SDS) and after systemic 0.1% terbinafine application. The present study opens up a more complex approach based on the microphysiological system to assess more than a skin irritation process.

Keywords: Liver model**,** microphysiology, organ-on-a-chip, skin irritancy, terbinafine, toxicity

1. Introduction

Skin model cultivation under static conditions limits the observation of the toxicity to this single organ. However, irritant agents are able to disrupt the skin barrier function and increase the penetration of water, since a complex chain of biological events, such as erythema, induration and edema, precedes the physiological signs of irritation (Gibbs et al., 2002). It also promotes a toxic response to other organs associated after crossing the skin. Consequently, the readout of the skin irritation prediction model, initiating with the tissue damage, is a cell viability assessment of the skin model (OECD, 2019). Thus, an *in vitro* skin irritation assay cannot evaluate the secondary effects of the irritation process.

The human skin, in addition to acting as a passive physical barrier with its stratum corneum, which protects the body from the deleterious effects of noxious chemicals, also protects the body through enzymes that are present inside the skin. These enzymes detoxify compounds penetrating the skin or bioactivate them to reactive metabolites (Bacqueville et al., 2017; van Eijl et al., 2012), which is a fundamental process in the toxicity evaluation.

Microfluidic microenvironments present improved cell-matrix interactions, crosstalk between co-cultured cells and organoids, and shear stress, which are advantages compared to static cultures (Dehne et al., 2017; Sriram et al., 2018; Wufuer et al., 2016,).

This type of microfluidic device, called HUMIMIC Chip2, are, thus, envisioned to be superior tools to other models with a continuous (Ramadan and Ting, 2016) or gravity-driven flow (Bal-Öztürk et al., 2018; Wufuer et al., 2016). Since it is pulsatile (Ataç et al., 2013) and the pump is in accordance with pharmacokinetic and pharmacodynamic physiological designs, it allows one to carry out many studies. Like with single or repeated applications, systemic applications for several days, association of organoids, permeation studies, models disease (Materne et al., 2015, Schimek et al., 2018; Wagner et al., 2013,), and especially, for toxicity testing, developing substances such as drugs, cosmetics, and chemicals (Dehne et al., 2017; Wufuer et al., 2016).

Numerous researchers contributed in constructing biology-inspired microphysiological systems. Especially single skin-on-a-chip models to analyze barrier function by Transepithelial Electrical Resistance, inflammation and edema induced

with TNF-α, irritation, assessing angiogenesis mechanisms induced by irritant contact dermatitis pathophysiology (Lee et al., 2017; Wufuer et al. 2016; Alexander, Eggert, Wiest, 2018; Jusoh, Ko, Jeon, 2019) or benefits of the pumpless skin-on-a-chip microfluidic platform (Abaci et al., 2015). Besides skin in co-culture: associated to hair follicle, to vasculature, and to liver in two or four organs-on-a-chip for systemic repeated dose safety assessment (Ataç et al., 2013; Schimek et al., 2015; Wagner et al., 2013; Maschmeyer et al., 2015a; Maschmeyer et al., 2015b). Toxicity is often based on complex interactions among tissues; to provide a more comprehensive insight into topical substance toxicity, we combined for the first-time skin and liver models in the in the same circulating medium (two organs-on-a-chip), to assess more than skin irritation. Co-culture of this interaction may provide additional topical toxicity background to avoid false-negative results (Dehne et al., 2017).

The drug terbinafine, which is an antifungal, topical and systemic safe commercially available medicine, was selected (Yeganeh and McLachlan, 2000) as our test chemical. It presents high permeation power on the skin due to its high lipophilicity. However, it also presents potential hepatotoxic effects when used for prolonged oral therapy (Yeganeh and McLachlan, 2000). We selected a non-irritant concentration commercially available (1 %) and a fivefold higher concentration as a possible irritant. We also assessed a systemic treatment at 0.1 % (tenfold higher than the recommended plasma concentration) as a possible hepatotoxic control.

Concerning the biomarkers involved in the skin irritation, we aimed to assess the key event related to tissue trauma, studying the morphology of the tissues and the gene expression of the epidermal growth factor receptor (EGFR), and the key event of skin or liver inflammation gene mediators: interleukins (IL) 1α, 6 and 8 analyses, following our previous study (Tavares et al., 2020). We selected four of the main cytochrome P450 enzymes related to liver xenobiotic phase I metabolism plus an albumin gene also linked to the healthy liver functions (Wagner et al., 2013), for the study of gene expression involved in the liver metabolism of terbinafine and the irritant positive control, sodium dodecyl sulfate (SDS).

Therefore, we combined the in-house reconstructed human skin (RHS) with a liver model to assess xenobiotics metabolite toxicity data in comparison with single RHS cultured in a static condition. The aim was to provide more information regarding the secondary toxicity involved in the skin irritation process through a microphysiological co-culture system.

2. Materials and methods

2.1. Reconstructed human skin

Normal human dermal fibroblasts and normal human keratinocytes were isolated from foreskin of boys younger than 10 years after medically indicated circumcision. The experimental procedures conformed to the principles of the Declaration of Helsinki and were approved by the ethics committees of Charité - Universitätsmedizin Berlin (EA1/081/13). Informed written consent was obtained from all donor parents or legal guardians. The isolation of fibroblasts and keratinocytes were performed as previously described (Zoschke et al., 2016; Zoschke et al., 2017). In brief, foreskin was washed, cut into pieces, and incubated with dispase solution overnight at 4°C. Next, the epidermis was mechanically separated from the dermis and the dermal pieces placed upside down in a cell culture plate. The fibroblasts grew out of the tissue within four weeks. The epidermal pieces were incubated with trypsin-EDTA solution for 20 min at 37°C to isolate single keratinocytes, which were subsequently seeded into cell culture flasks and grown for one week. The medium for maintaining the pool of primary fibroblasts (passage number between 3 and 7 of three donors) was Dulbecco's Modified Eagle Medium plus supplements penicillin/streptomycin (1 %), L-glutamine (1 %) provided by Sigma-Aldrich (München, Germany). The fetal calf serum from Biochrom (Berlin, Germany) was added at a concentration of 10 % (v/v). We maintained the pool of primary human keratinocytes (passage number between 3 and 5 of three donors) in Epilife® medium supplemented with a human keratinocyte growth supplement kit provided by Life Technologies (Berlin, Germany). The full-thickness (epidermis and dermis) RHS was developed in-house with in a 24-well plate size insert (Millicell-PCF, Merck, Darmstadt, Germany) to fit in the chip device, fully differentiated after ten days and it was described previously (Tavares et al., 2020).

2.2. Human liver spheroid

Differentiated human hepatoma cell line (HepaRGs) (Lot HPR116080) were obtained from Biopredic International (Rennes, France). We purchased the primary human hepatic stellate cells (HSCs) from ScienCell (Carlsbad, CA, USA). We thawed the differentiated HepaRGs and seeded them confluently four days before the spheroid formation. We used a standard HepaRG culture medium described earlier (Bauer et al., 2017), it consisted of William's Medium E (PAN-Biotech, Aidenbach, Germany)

supplemented with 10% foetal calf serum (Corning, Lowell, MA, USA), 5 µg/ml human insulin (PAN-Biotech), 2 mM L-glutamine (Corning), 5 × 10−5 M hydrocortisone hemisuccinate (Sigma–Aldrich, St. Louis, MO, USA), 50 µg/ml Gentamycin Sulfate (Corning) and 0.25 µg/ml Amphotericin B (Corning) or was purchased directly from Biopredict. On the following day, we added 2 % dimethyl sulfoxide to the standard HepaRG medium and maintained it for three days until the spheroid formation. We expanded human hepatic stellate cells in the Stellate Cell medium (maximal passage number of 5), provided by ScienCell (Carlsbad, CA, USA) (Lot PFP). Human liver spheroids were formed, according to a protocol described by Bauer and co-workers (2017).

2.3. HUMIMIC Chip2 design and fabrication

The microphysiological HUMIMIC Chip2 24-well (TissUse GmbH, Berlin, Germany) described earlier (Hübner et al., 2018) consists of two connected compartments in which we cultivate skin and liver organ equivalents. A microfluidic channel interconnects these compartments. The pulsatile flow obtained with an on-chip micropump allows a cross talk between the organ equivalents. Wagner et al. (2013) described the fabrication of the polydimethylsiloxane chip with a 2-mm high layer containing the respective microfluidic channel (height of 100 µm.), micropump and lid for the reservoirs. The micropump is capable of providing a pulsatile flow of medium through 500 mm wide 100 mm high channels with a pumping volume range of 7–70 ml min^{-1} and a frequency of 0.2–2.5 Hz (Ataç et al., 2013). We used a frequency of 0.3 Hz in our experiments, which leads to a flow-rate of approximately 30 ml min^{-1}. The circuit is sealed onto a glass microscope slide using low-pressure plasma oxidation at the bottom (Femto; Diener, Ebhausen, Germany). The Chip2 micropump is activated by pressured air or vacuum (coming from the chip starter), resulting in a progressive lowering and raising of the 500 µm thick elastic membranes (**Figure 1**). A commercially produced batch of the Chip2 24-well was used for the experiments after passing quality control. We applied total volume of 1 mL composed of 50% RHS medium (described in the item 2.1) and 50% liver medium (described in the item 2.2.) to attend both “organs” demand. Afterwards, we loaded the Chip2 with one RHS and 40 liver spheroids. All the analyses presented in the results and discussion section called “Chip2” data were based on the association of RHS plus liver model on-a-chip, while the called “RHS” data were based on the static single skin model culture.

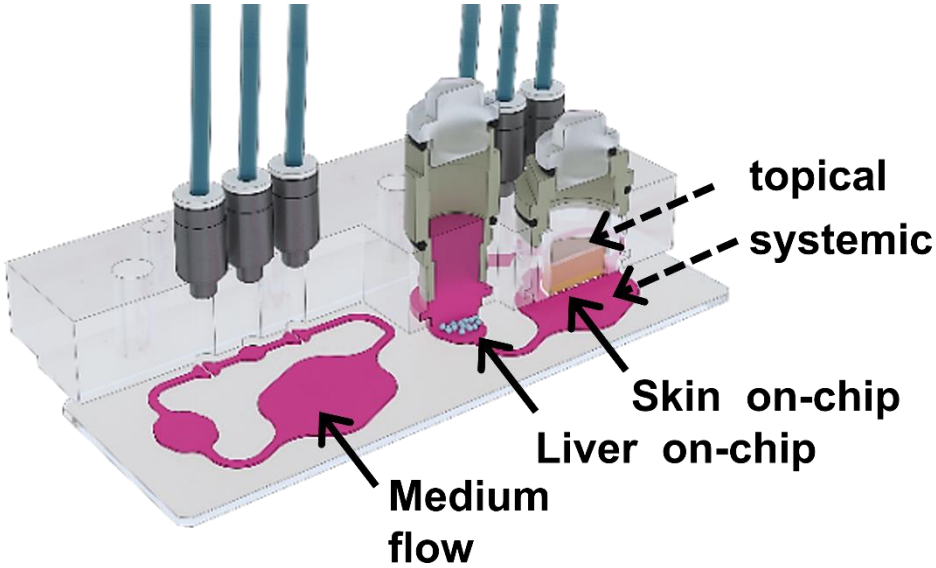

Figure 1. Cross-section of the HUMIMIC Chip2. The liver (cyan, left) and RHS (brown, right) are connected by a microfluidic tube system filled with medium (magenta). The peristaltic three-valve micropump (black, rear) ensures the medium exchange between liver and RHS on-chip. The test compounds were either applied topically to the RHS or systemically into the microfluidic tube system. Reprinted and modified, with permission, from Hübner et al. (2018).

2.4. Skin irritation assay in the static RHS

We exchanged the medium underneath the RHS inserts (0.5 mL) one day before the experiment. We performed the skin irritation assay onto RHS in accordance with the standard operating procedure (SOP) “In vitro Skin Irritation Test: Human Epidermis Model Episkin™” from the Organisation for Economic Co-operation and Development, OECD test guideline no. 439 (OECD, 2019). Briefly, we applied 10 µL of terbinafine (terbinafine HCl, Fragon of Brazil Pharmaceuticals, Brazil) 1 % or 5 % (w/v) dissolved in ethanol (99.5% pure, CAS-no: 64-17-5, Merck, Germany) on top of each RHS. We placed the plate in the incubator at 37 °C for 15 min. We exposed the RHS to controls: Ethanol (solvent control), Dulbecco’s Phosphate-Buffered Saline (DPBS, Corning®, Kaiserslautern , Germany) as negative control and 5 % SDS (w/v) (≥99 % pure, CAS-no: 151-21-3; Carl Roth, Berlin, Germany) as positive control (OECD, 2019). After the 15 min of exposure, we washed the RHS with DPBS and dried with sterile cotton swabs. We placed the inserts into new well-plates with fresh medium incubating for 42 hours (OECD, 2019). After 42 hours, we collected the medium underneath each RHS in the static 24-well plate. The medium collected was used for

interleukin 6 (IL-6) release and metabolism analyses of lactate dehydrogenase (LDH) activity, glucose consumption, lactate production, described in 2.8 and 2.9 items. Tissue samples were either harvested, frozen for histological and biomarker studies, or used for the MTT tissue viability assay.

2.5. Skin irritation assay in the HUMIMIC Chip2

We loaded the chip with 1 mL of circulating medium (mentioned in 2.3. item) one day before the experiment, later we loaded the chips with one insert of skin model in the 24-well size chip compartment, and 40 liver spheroids in the 96-well size chip compartment for the dynamic condition.

We adapted the skin irritation assay for the skin side of the chip following the same SOP, mentioned in the 2.4. item of the OECD test guideline no. 439 (OECD, 2019). However, there was a pulsatile flow during the 15 min of chemical exposition in the incubator at 37 °C. After the 15 min of exposure, we washed the skin model with DPBS, dried with sterile cotton swabs, closed the lid of the skin side and renewed the medium from the liver side of the chip. We collected the medium after 42 hours, for the same analyses mentioned for static RHS, besides albumin to assess liver metabolism.

2.6. Systemic treatment in the static RHS and Chip2

For systemic treatment, in the first day of the experiment, we replaced the medium for fresh one containing ethanol (control) or 0.1% terbinafine in ethanol. Both mediums had a final volume of ethanol smaller than 1% of the total volume. We prepared and homogenized the medium solutions before we transferred it to the 24-well plate (static) or to the Chip2. To reproduce the time that the chemical would interact systemically with both “organs” after the drug is released from the skin model in the topical application (skin irritation mentioned in the 2.4. item), we followed the same post-incubation time of 42 hours. All the analyses mentioned in the 2.4 item were also done for the systemic treated tissues and its medium samples.

2.7. MTT tissue viability assay

The MTT (3-(4,5-dimethylthiazol-2-yl)-2,5-diphenyltetrazolium bromide, 98% pure, Sigma-Aldrich) assay was performed following the manufacturer’s instructions only for the skin models in the static conditions. Briefly, in the third day of the experiment (after exposure/post-incubation time of 42 hours), RHS tissue samples

were placed in a fresh 24-well plate containing 500 µL/well of MTT (1 mg/mL) in medium (Dulbecco's Modified Eagle Medium, 1 % antibiotics, 1 % l-glutamine) for 3 h at 37 °C. Each RHS was placed carefully in 2-mL tubes with 0.5 mL acidic isopropanol solution (also used as a blank) for MTT extraction for 2 h on a shaker (300 rpm). We transferred each MTT solution in triplicate (100 µL) into 96-well assay plates for the optical density (OD) reading at 570 nm (CLARIOstar, BMG Labtech, Ortenberg, Germany). Background readings for all the samples were determined and subtracted to obtain the correct optical density. Data were from three biologically independent experiments with RHS, each with three technical replicates. The percentage of viability was determined for each tissue using the equation:

$$\%\ \text{viability} = 100 \text{ x } [\text{OD (sample)} / \text{OD (solvent control)}] \quad (1)$$

The test chemical is considered irritant if the RHS viability after exposure/post-incubation is less than or equal to 50 %. It is non-irritant if the viability is higher than 50 % following OECD test guideline no. 439 (OECD, 2019).

2.8. Histological studies

Aiming to assess changes in the morphology of the tissues, in the third day of the experiment after test chemical exposition/post-incubation time, we embedded the RHS and liver spheroids in Tissue-Tek® O.C.T. compound (Sakura Finetek, Torrance, CA, USA) for hematoxylin and eosin staining (usual procedures). Regarding immunofluorescence staining, the tissue sections of 8 µm were fixed in acetone at -20 °C for 10 min, washed with DPBS and blocked with goat serum 10 % (v/v) in DPBS for 20 min at room temperature. Mouse anti-human cytokeratin 10 (Santa Cruz, Heidelberg, Germany), rabbit anti-human cytokeratin 14 (Santa Cruz, Heidelberg, Germany), and mouse anti-human Ki67 (eBioscience) were used as primary antibodies and goat anti-mouse Alexa-488 (Life Technologies, Carlsbad, Ca, USA) and goat anti-rabbit CF594 as secondary antibodies including DAPI for nuclei staining. The Apo-Direct Apoptosis Detection Kit (Thermo Fisher Scientific Inc.) was used for terminal deoxynucleotidyl transferase dUTP, nick end labeling (TUNEL) staining, according to the manufacturer's instructions. We examined the stained slides under a

Keyence fluorescence microscope (Osaka, Japan) and assessed for histopathological changes associated with chemical exposure.

2.9. Enzyme immunoassay of inflammatory biomarker IL-6

The culture media was quantitatively analyzed using enzyme-linked Immunosorbent Assay kits for IL-6, according to manufacturer's protocol. We measured the IL-6 release level regarding skin irritation in a culture medium (only topical treatments). We collected 300µL of the medium after post-incubation period of 42 hours to a frozen resistant plastic tubes, and the medium were kept under minus 20 ºC until the day of the assay with total medium samples collected during the experiments. Data were from three biologically independent experiments with RHS/Chip2, each with three technical replicates. Regarding the calculation of a comparable value between RHS and Chip2 conditions, the amount of IL-6 was calculated as follows:

$$Amount\ of\ IL6 = IL6\ conc\ \left[\frac{ng}{mL}\right] * \frac{volume[mL]}{cell[10^5]} * 10^5 \qquad (2)$$

2.10. Metabolic levels

We collected approximately 200µL of each medium sample in the day one (before medium exchange and previous the treatment) and in the day three (42 hours post-incubation time). The same medium sample was used for glucose, lactate, LDH and albumin (only samples from Chip2) analysis. We used the Indiko Plus system (Thermo Fisher Scientific, Germany) in combination with the following kits: Glucose (HK) 981779 kit (Thermo Fisher Diagnostics GmbH, Germany), Lactate Fluitest LA 3011 kit (Analyticon Biotechnologies AG, Germany), LDH IFCC 981782 kit (Thermo Fisher Diagnostics GmbH, Germany), and Albumin CSF FS 65558 Kit (DiaSys, Holzheim, Germany) according to the manufacturer's instructions in each case. Regarding the calculation of a comparable value between RHS and Chip2 conditions, the amount of each metabolite was calculated as followed:

$$Amount\ of\ gluc\ or\ lac\ or\ LDH = conc\ * \frac{volume[mL]}{cell[10^5]} * 10^5 \qquad (3)$$

Regarding the calculation of LDH release, 1 % Triton X 100 was used to quantify maximal LDH released from tissues; it was set to 100%; the other values were calculated using the following equation:

$$LDH\ release = amount\ of\ LDH * \frac{100}{amount\ of\ LDH \max release} \quad (4)$$

2.11. Gene expression analysis

The skin models in the air-liquid interface were collected with a tweezer and dried with a cotton swab, the epidermis was detached from the dermis and the first were digested with a RNA buffer. We transferred the liver spheroids from the medium to the RNA buffer using wide bore tip. Total RNA from the epidermis and liver spheroids were isolated using the NucleoSpin RNA kit (Macherey-Nagel, Düren, Germany). We determined the RNA purity by A260/A280 and A260/A230 ratios and calculated the total RNA concentrations using the DS-11 spectrophotometer (CLARIOstar, BMG Labtech, Ortenberg, Germany). The cDNA was synthesized by reverse transcription of 100 ng total RNA using the TaqMan® Reverse Transcription Kit (Thermo Fisher Scientific Inc). The QuantStudio 5 Real-Time PCR System (Thermo Fisher Scientific Inc.) and the SensiFAST SYBR Lo-ROX Kit (Bioline, Luckenwalde, Germany) were used for real-time quantitative PCR, according to the manufacturer's instructions. Data analysis was performed using an excel datasheet. We designed the genes using the Genome Browser database (https://genome-euro.ucsc.edu/, see Table 1). Finally, we normalized the expression levels of genes of interest to the housekeeping gene beta actin (ACTB) and calculated the fold change to solvent control effect in relative gene expressions of treated tissues compared to ethanol-treated control tissues, determined following 42 hours of treatment.

Table 1. Genes and respective sequences. Genes with asterisks were used as housekeeping genes.

GENE	SEQUENCE 3' – 5' UP	SEQUENCE 3' – 5' DOWN
***ACTB**	CCACCATGTACCCTGGCATT	GCTTGCTGATCCACATCTGCT
ALBUMIN	TCAGCTCTGGAAGTCGATGAAAC	AGTTGCTCTTTTGTTGCCTTGG
CYP1A2	ATCCCCCACAGCACAACAAG	CCATGCCAAACAGCATCATC
CYP2C19	AGCTGGGACAGAGACAACAAGC	CGTCACAGGTCACTGCATGG
CYP2C9	GGTGGGGAGAAGGTCAATGTATC	GACAGAGACGACAAGCACAACC
CYP3A4	GGAAGTGGACCCAGAAACTGC	TTACGGTGCCATCCCTTGAC
EGFR	GCCGACAGCTATGAGATGGAG	TGGAGGTGCAGTTTTTGAAGTG
IL-1A	GTGACTGCCCAAGATGAAGACC	TGCCAAGCACACCCAGTAGTC
IL-6	CTGGATCAGGACTTTTGTACTCATCT	CCAATCTGGATTCAATGAGGAGACT
IL-8	GTGGAGAAGTTTTTGAAGAGGGC	TCTGGCAACCCTACAACAGAC

2.11. Statistical analysis

We analyzed the normal distribution between samples (Anderson-Darling) and afterwards tested for differences among groups using one-way ANOVA, followed by Tukey and Dunnett post-test as appropriate. A p-value < 0.05 was considered statistically significant.

3. Results

3.1. Histological studies

In the pretest, the untreated skin models after full differentiation were cultured on-chip for three days with a mixed medium consisting of 50 % skin medium and 50 % of the liver medium without the liver model. The epidermis showed multiple well-differentiated layers (*basal, spinous, granulosum and stratum corneum*) (**Figure 2b**) like the original human skin. It showed compatible histomorphology without meaningful changes when compared to the untreated static skin models, cultured with 100 % skin medium (**Figure 2a**). Both skin models presented well distributed fibroblasts in the dermis, which, for instance, was fully adhered to the epidermis.

Cytokeratin 10 is present in the upper layers and cytokeratin 14 in the basal layer in the human stratified epidermis (Maschmeyer et al., 2015). We observed that the immunolocalization of cytokeratins (10 and 14) in the RHSs treated with ethanol were also well distributed (**Figure 2c, d**).

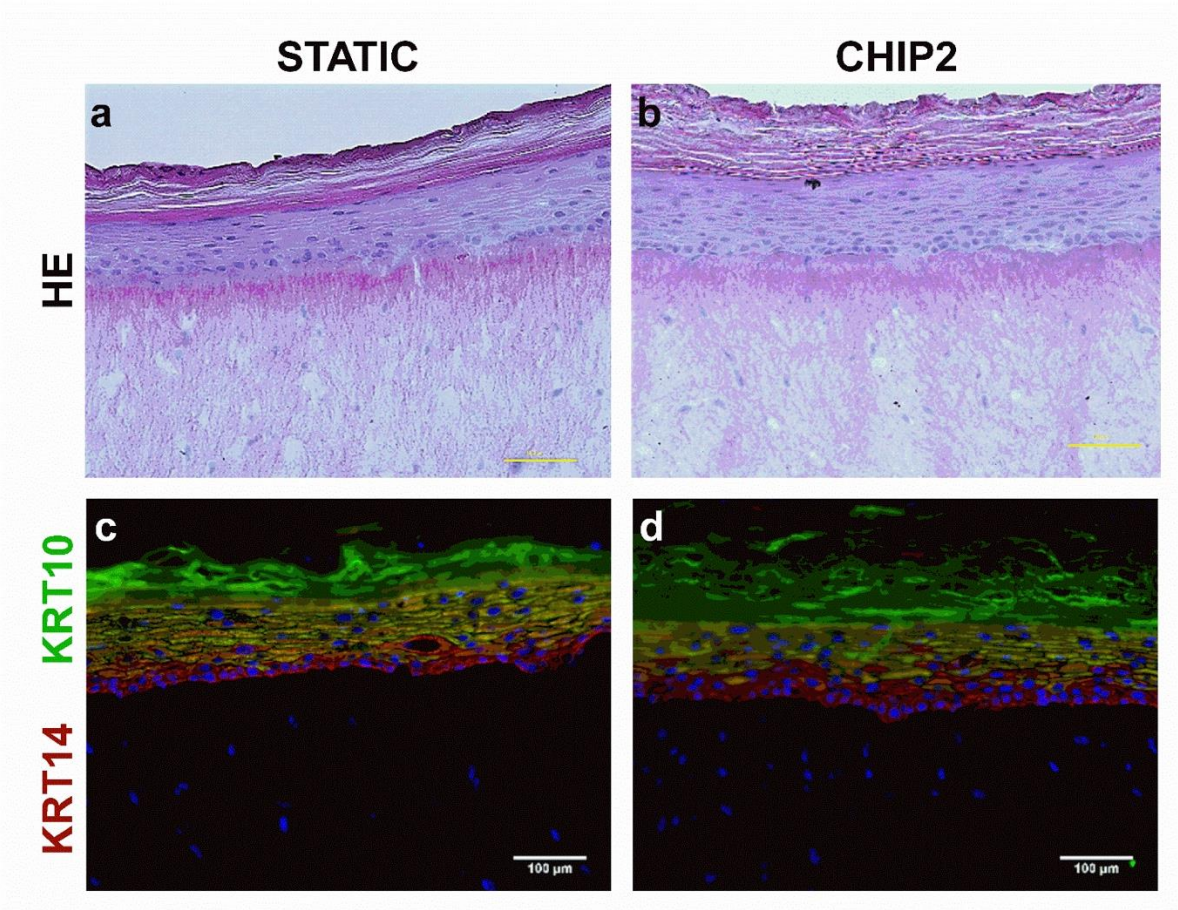

Figure 2. Skin morphology. Hematoxylin and eosin staining of **(a)** RHS in static culture and **(b)** Chip2 RHS. Immunolocalization of keratin-14 (KRT14, red) and keratin-10 (KRT10, green) **(c)** RHS in static culture and **(d)** Chip2 RHS. Images were representative of three batches. Scale bar = 100 µm.

The Chip2 skin models treated with the positive control 5 % SDS (**Figure 3a**) presented no sign of living cells (blue nucleus) at the edges of the RHS and detected apoptotic cells in the basal layers of the epidermis and the dermis, showing the penetration of the irritant SDS through the layers. The models treated with the solvent ethanol and terbinafine (**Figure 3b, c, d, e, f, g**) presented apoptotic cells only closer to the stratum corneum, indicating an adequate supply of nutrients and no sign of damage (blue nucleus).

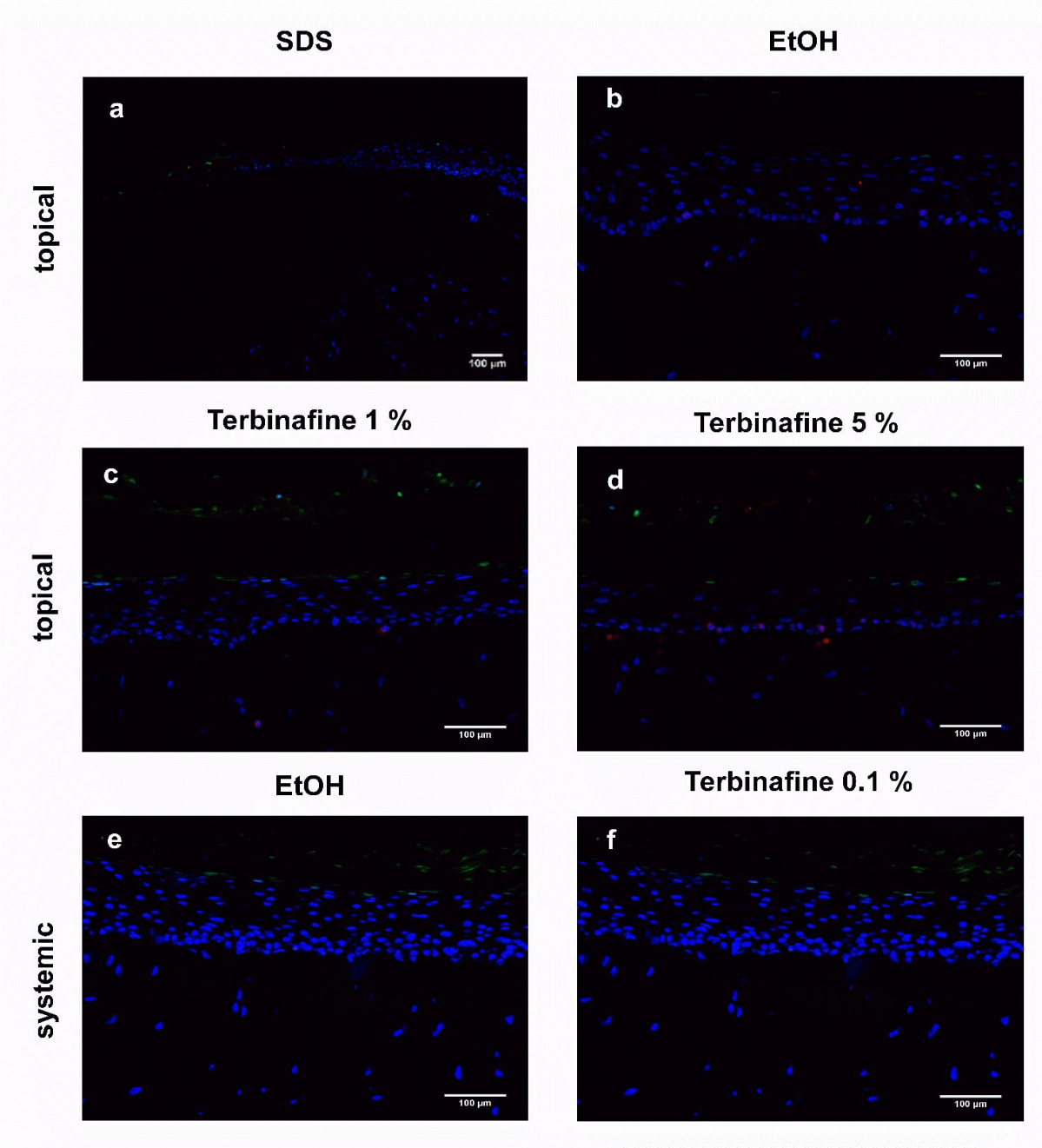

Figure 3. Effects on skin cell proliferation and apoptosis on Chip2. Immunolocalization of proliferative (Ki-67, red) and apoptotic (TUNEL, green) following the topical application on RHS of SDS 5 %, EtOH, terbinafine 1 %, terbinafine 5 % and following the systemic application of EtOH and terbinafine 0.1 %. Cell nuclei were stained with DAPI (blue). Images were representative of three batches. Scale bar = 100 µm.

This liver spheroid is reported to be cultured up to 28 days (Maschmeyer et al., 2015a), we observed a reduction in the proliferative and apoptotic cells in the untreated

liver models from day 0 to day 3, which means stability in the grow phase of the 3D culture. After this stabilization we evaluated the number of positive cells for Ki67 (proliferation) and TUNEL (apoptosis) qualitatively for each exposition condition in the immunofluorescence slides in comparison to the untreated liver spheroids **(Figure 4)**. We observed the effect was dependent on the application route and concentration of terbinafine or SDS used. In the SDS topical treatment, the blue nuclei were less rounded indicating lysis by necrosis; accordingly, we observed no increase in the proliferation/apoptosis ratio (no signals of repair or controlled death) **(Figure 4a).** Possibly, the SDS destroyed and passed through the RHS barrier reaching the circulation to promote the liver damage. We observed an increase in the apoptotic and proliferative cells followed skin topical application of ethanol **(Figure 4b)** and 1% terbinafine (**Figure 4c**). However, 5% terbinafine topical treatment showed to reduce liver proliferation in comparison to untreated liver ones, which demonstrates the effective permeation through the RHS to the “bloodstream” that was transferred by active flow to the liver compartment (**Figure 4d**). The systemic solvent control (EtOH) (**Figure 4g**) did not change the proliferation/apoptosis profile substantially in comparison to the untreated tissue (**Figure 4f**). In the systemic terbinafine treatment, the proliferation was similar to untreated liver at day O (**Figure 4e**); however, the apoptosis was increased, suggesting a hepatic effect (**Figure 4h**).

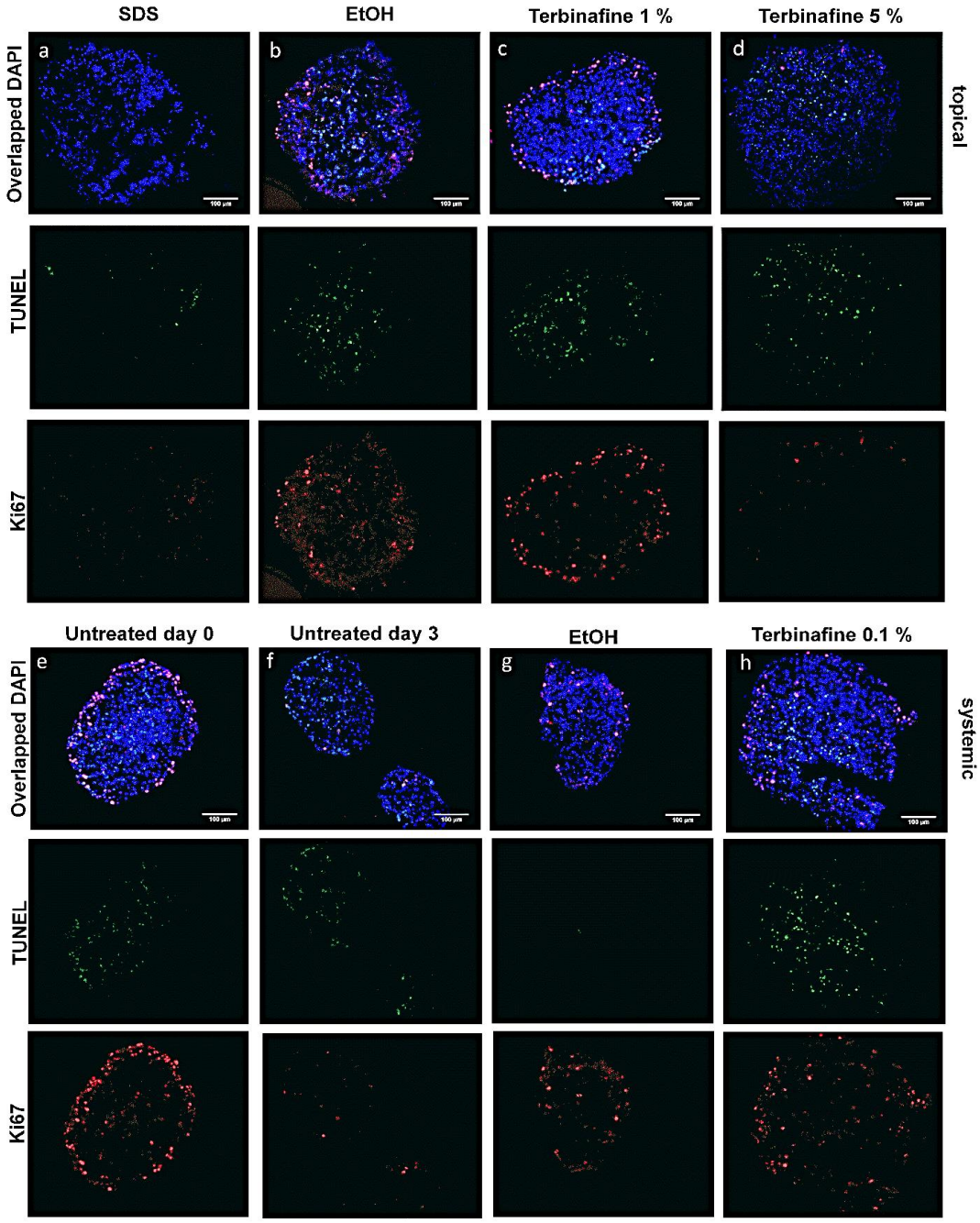

Figure 4. Effects on liver cell proliferation and apoptosis on Chip2. Qualitative immunolocalization of proliferative (Ki-67, red) and apoptotic (TUNEL, green) at day 3 following the topical application on RHS of (a) SDS 5 %, (b) EtOH, (c) terbinafine 1 %, (d) terbinafine 5 % and the following systemic application of (g) EtOH, (h) terbinafine 0.1 %. For comparison, untreated liver spheroids at day 0 (e) and at day 3 (f). Cell nuclei were stained with DAPI (blue) are overlapped with red and green channels in the first row of each condition, followed by green channel in the second row and by red channel in the third row. Images were representative of triplicates in three independent experiments. Scale bar = 100 µm.

3.2. RHS Viability

The RHS models were exposed in a static condition to the irritant chemical 5 % SDS as a positive control. The SDS was correctly classified as an irritant, decreasing the viability to 2 % by using the MTT tissue viability assay. According to the prediction model, the viability was higher than 50 % for topical 1 and 5 % terbinafine, which classifies both concentrations as non-irritants (OECD, 2019). However, 5% terbinafine was statistically more toxic to the RHS than 1% terbinafine application ($p < 0.05$). Terbinafine was also considered non-irritant by using the MTT skin viability assay after systemic application (0.1 % terbinafine in the medium, **Figure 5**).

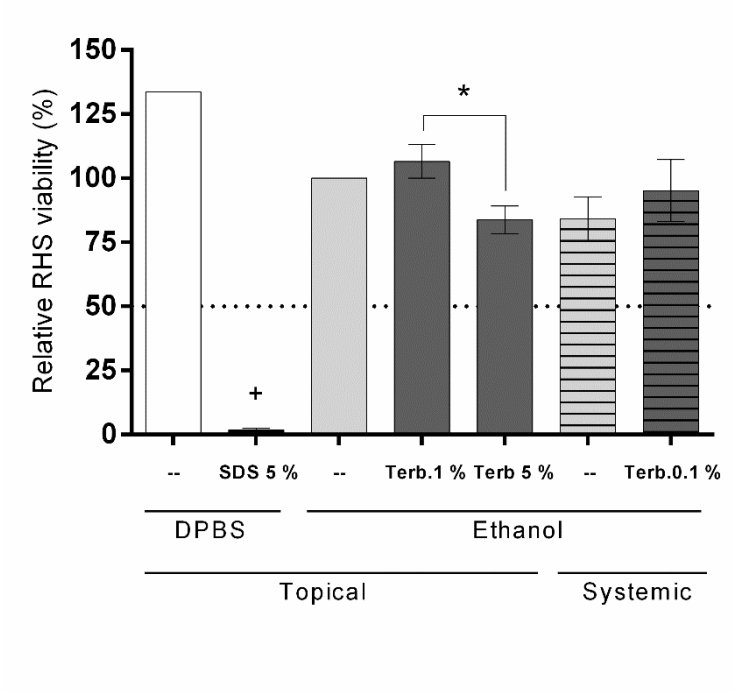

Figure 5. Substance effects on the viability of static RHS. Test substances below the 50 % threshold (dotted line) are predicted to be a skin irritant. DPBS –Dulbecco's Phosphate-Buffered Saline (negative control); SDS – sodium dodecyl sulfate (positive control); Terb – terbinafine. We exposed for 15 min the RHS to a test chemical, and subsequently washed. Where only the solvent was applied, DPBS or ethanol, the symbol was stated as "--". Mean ± SD, triplicates from three independent experiments resulting in n = 9 samples per group, $^{*}p < 0.05$ compared to Terb 5 %, $^{+}p < 0.05$ compared to all other treatments.

Since terbinafine was not soluble in hydrophilic solvents or sesame oil, ethanol is recommended and was chosen as the solvent control (Kandarova and Liebsch, 2017). Topical ethanol produced a reduction in the skin viability when compared to the negative control DPBS; however, this decrease was reproducible and had a small standard deviation (± 0.038). Therefore, we calculated the test chemical's irritant potential by reducing the solvent effect.

A second endpoint for the assessment of the viability of the exposed tissues was through the quantification of the cytosolic enzyme LDH. The latter's presence in the medium is often used as an indicator of cellular toxicity by leakage (Li et al., 2011) and leakage is related to necrosis cell death. The 1 % (v/v) Triton X 100 in DPBS destroyed the whole tissue (100 %) in 1 h and was, thus, used as the LDH positive control, representing the maximal activity in the medium.

The skin models exposed to 5 % SDS reached the highest concentrations of LDH in the static condition (79.57 %), corroborating with the data observed in the MTT test (1.81 % skin viability) (**Figures 6 and 5, respectively)**. The viability of Chip2 conditions was measured by LDH release in the culture medium after this post-treatment period (**Figure 6**). In Chip2 conditions, tissues presented an LDH release similar to static conditions with no significant differences between the terbinafine and solvent control groups. The exception was the on-chip SDS positive control that showed statistically different lower release compared to the static condition ($p < 0.05$). In this case, the positive control would be considered non-irritant in the Chip2.

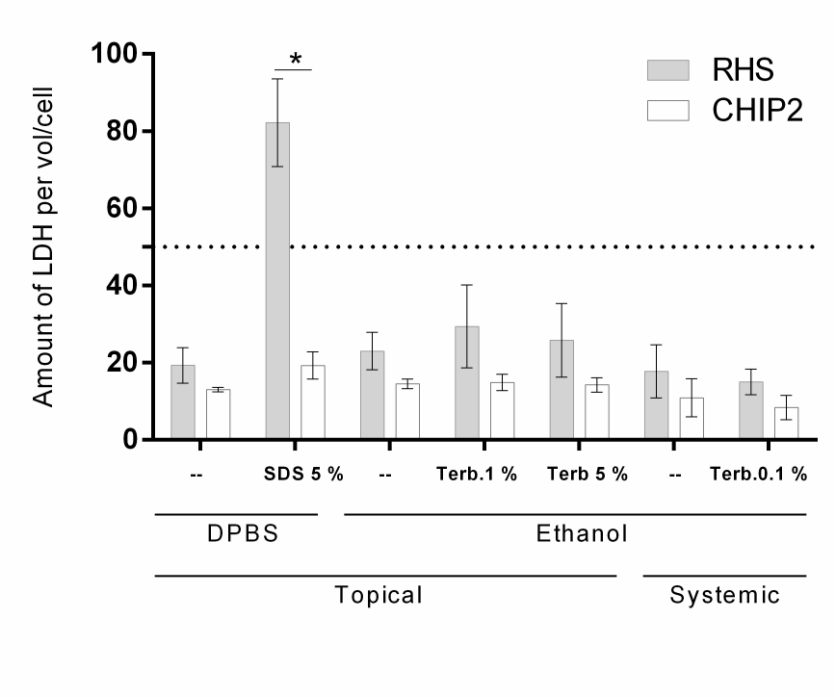

Figure 6. Substance effects on the release of LDH. Amount of LDH released from RHS (grey bar) or Chip2 (RHS+liver, white bar) to the culture medium 42 h post-treatment. Where only the solvent was applied, DPBS or ethanol, the symbol was stated as "--." Values were normalized per volume culture medium and cell number per model. Triton was used as a positive control and LDH release set to 100 %; LDH release at 50 % (dotted line). Mean ± SD, triplicates from three independent experiments resulting in n = 9 samples per group, *$p < 0.05$.

The static topical treatment of RHS with 1%, 5 % terbinafine, and the systemic treatment with 0.1 % terbinafine and ethanol resulted in statistically higher consumption of glucose (Figure 7a) in the medium compared to the Chip2 condition ($p < 0.05$). Consequently, they also showed statistically higher concentrations of lactate production ($p < 0.05$)., except for topical 1% terbinafine (Figure 7b). These data suggested superior metabolic activity in the static single RHS culture. However, when we compare terbinafine and ethanol treatments to its DPBS control, they were not different, not presenting toxicity neither to static RHS, nor to Chip2 conditions. Regarding RHS treatment with SDS (irritant positive control), it presented statistically higher toxicity than the negative control DPBS, observed by the lower consumption of glucose and lower lactate production, in both static or Chip2 conditions (**Figure 7a, b**).

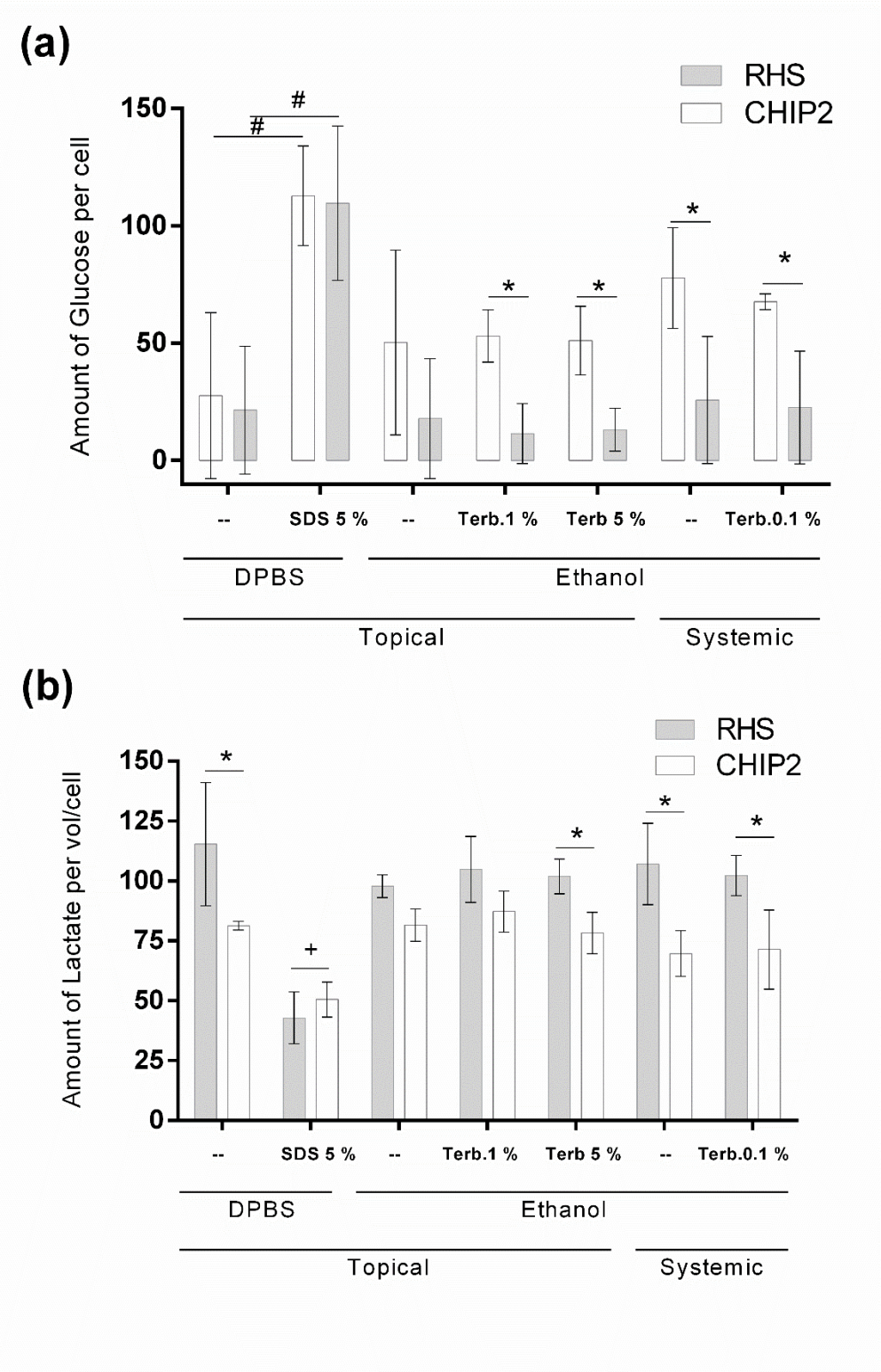

Figure 7. Substance effects on the glucose consumption and lactate production. The amount of glucose (a) or lactate (b) in the medium collected from RHS (grey bar) or Chip2 (RHS + liver, white bar) to the culture medium 42 h post-treatment. Where only the solvent was applied, DPBS or ethanol, the symbol was stated as "--." Values were normalized per volume culture medium and cell number

per model. Mean ± SD, triplicates from three independent experiments resulting in n = 9 samples per group; where "*" means differences between the static and Chip2 and "#" means differences compared to negative control (DPBS), and "+" differences compared to all other treatments ($p < 0.05$).

Liver models are expected to produce albumin and this biomarker is useful to monitor liver-like activity in the dynamic co-cultures (Wagner et al., 2013). After the RHS topical treatment with DPBS, ethanol, 1 % and 5 % terbinafine, and systemic ethanol and 0.1% terbinafine we observed maintenance of albumin content produced by liver spheroids, which means they were not toxic to the liver (Wagner et al., 2013). On the other hand, we observed that the RHS topical treatment with 5 % SDS presented a slight decrease the albumin concentration in the medium between day 01 and 03, however, it was not significant (**Figure 8)**.

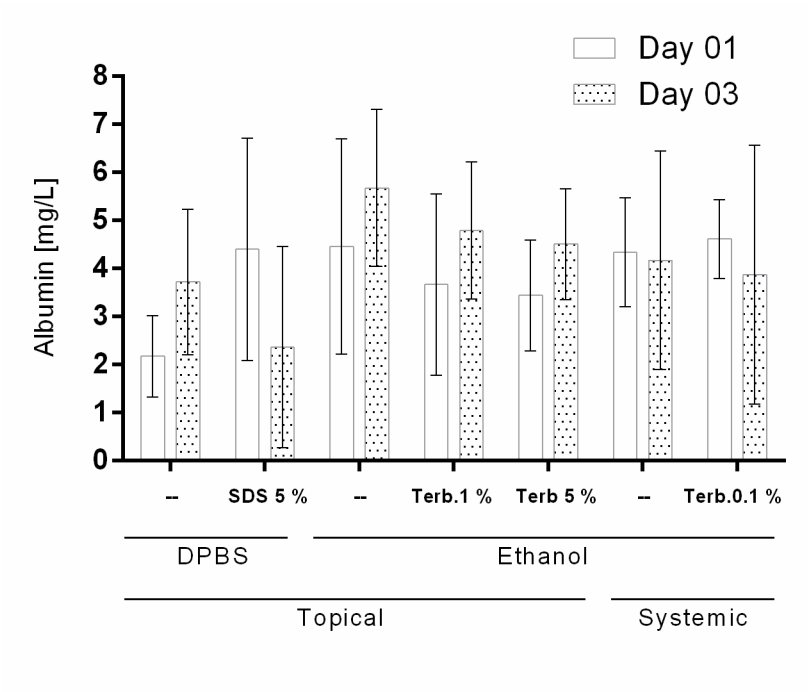

Figure 8. Substance effects on albumin production. Albumin produced by the liver on-chip before and after treatment (day 1, white bar; day 3, dotted pattern bar,). Mean ± SD, triplicates from three independent experiments resulting in n = 9 samples per group.

3.3. Enzyme immunoassay of inflammatory biomarker IL-6

We considered the amount of IL-6 released by cell units per 1 mL volume in order to compare the RHS static culture with the Chip2 circuits. We observed that less IL-6 was found in the medium in the Chip2 circuits (released by RHS and liver model) when compared to static ones (RHS) for topical applications of ethanol, 1% and 5% terbinafine, ($p < 0.05$) (**Figure 9**). Among Chip2 treatments, all of them released similar IL-6 concentrations. The reduction observed by SDS in the chip was not considered significant. On the other hand, in the static condition, SDS treatment provoked a significant reduction in the RHS IL-6 release when compared to all the other topical treatments, $p < 0.05$ (**Figure 9**). This small IL-6 release indicates that there was not enough time for IL-6 signaling in the tissues treated with SDS due to immediate death from necrosis. Since the IL-6 is quite stable from degradation (Graham et al., 2017), it could be also suggested that dead cells suppressed IL-6 release (Newby et al., 2000).

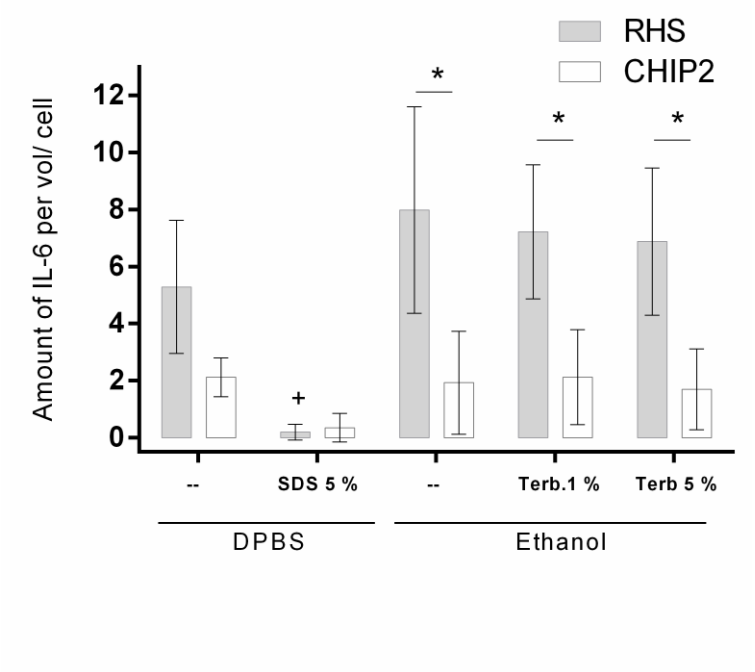

Figure 9. Substance effects on the release of interleukine-6 (IL-6). The amount of IL-6 released from RHS to the culture medium 42 h post-treatment in static (grey bar) and Chip2 (RHS+liver, white bar) culture. Values were normalized per volume culture medium and cell number per model. Where "*" means differences between the static and Chip2 and "+" means differences compared to all other static treatment ($p < 0.05$).

Mean ± SD, triplicates from three independent experiments resulting in n = 9 samples per group.

3.4. Skin gene expression

The topical terbinafine treatments (1 and 5%) did not dysregulate IL-6, IL-8 and EGFR genes in both RHS static or in the Chip2 (**Figure 10**). However, only in the Chip2, topical 5% terbinafine significantly upregulated IL-1α ($p < 0.05$) when compared to solvent control (defined as 1 fold change) and its expression was statistically different from systemic 0.1% terbinafine treatment in the Chip2 ($p < 0.05$) (**Figure 10a**). We also observed only in the Chip2 that systemic 0.1% terbinafine treatment upregulated EGFR significantly ($p < 0.05$) when compared to solvent control and when compared to static RHS expression, showing in the Chip2 to be more sensitive, activating the repair response (**Figure 10d**).

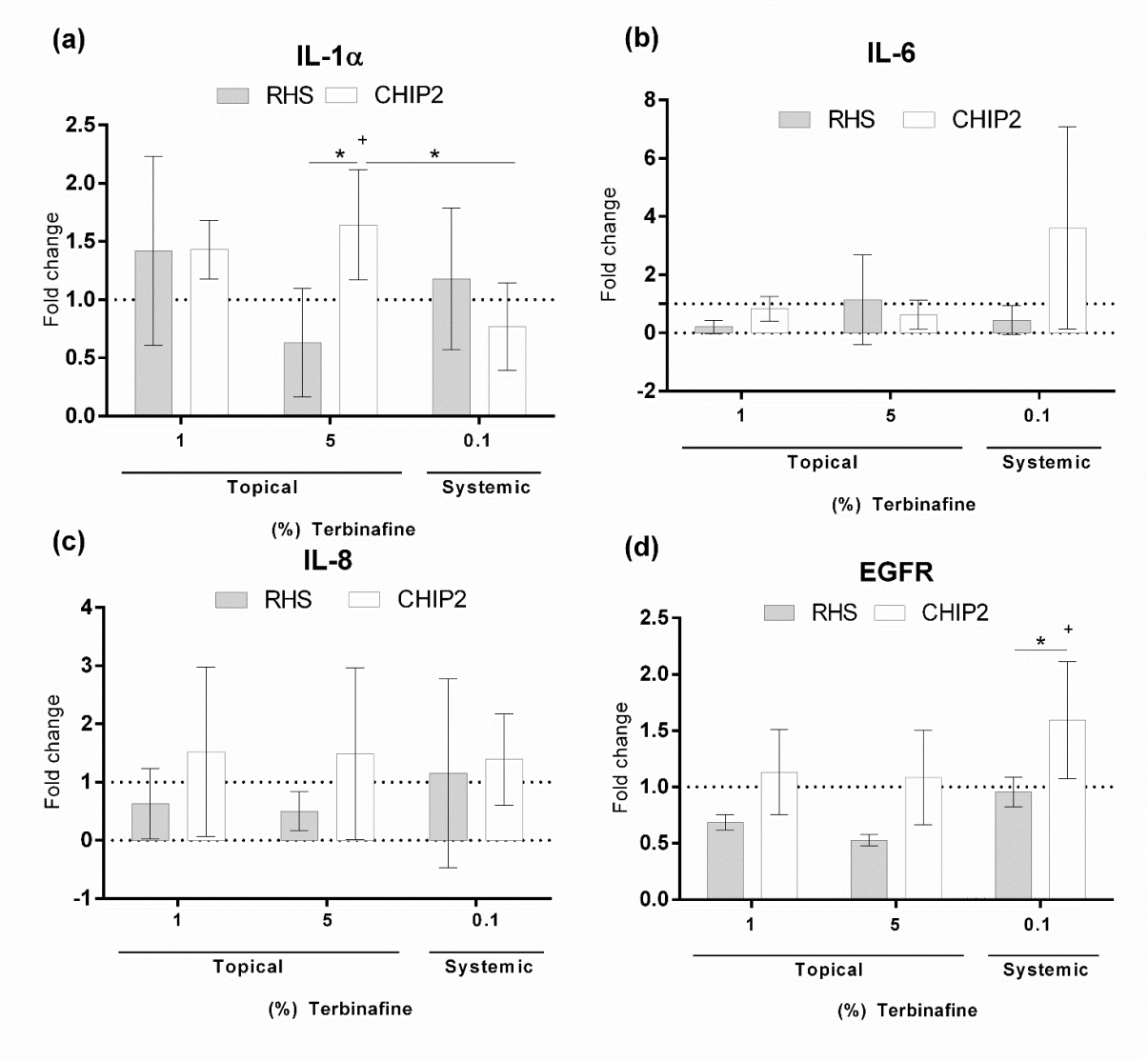

Figure 10. Substance effects on epidermal gene expression. Epidermal expression (from RHS or Chip2 RHS) of **(a)** IL-1α, **(b)** IL-6, **(c)** IL-8 and **(d)** EGFR; expressed as fold change to the ethanol solvent control (dotted line). Where "+" means significant difference from solvent control (defined as 1 fold change), $p < 0.05$, and "*" significant difference between treatments $p < 0.05$. Mean ± SEM; triplicates from three independent experiments resulting in n = 9 samples per group.

3.5. Liver gene expression

Downregulations of albumin and CYP1A2, 2C9, 2C19 and 3A4 are considered hepatotoxic signals, while upregulations of those CYPs and interleukins (IL-6 and IL-8) means metabolism of the drug and inflammation, respectively. Our findings shows that topical 1% terbinafine did not dysregulate CYPs, albumin or ILs (**Figure 11**). Moreover, topical 5 % terbinafine significantly upregulated the liver expressions of CYP1A2 (mean: 4.77-fold) and CYP3A4 (mean: 3.75-fold) ($p \leq 0.05$) (Figure 11a),

corroborating to immunofluorescence findings suggesting superior interaction of the drug with the liver than topical 1% terbinafine. The systemic treatment of 0.1 % terbinafine significantly downregulated albumin (mean 0.59-fold) ($p \leq 0.05$) (**Figure 11b**) which is a signal of hepatotoxicity, but it also significantly upregulated CYP2C9 (**Figure 11a**) ($p \leq 0.05$) suggesting also improved metabolism. None of the terbinafine treatments changed significantly interleukins expression in the liver spheroids (**Figure 11c**).

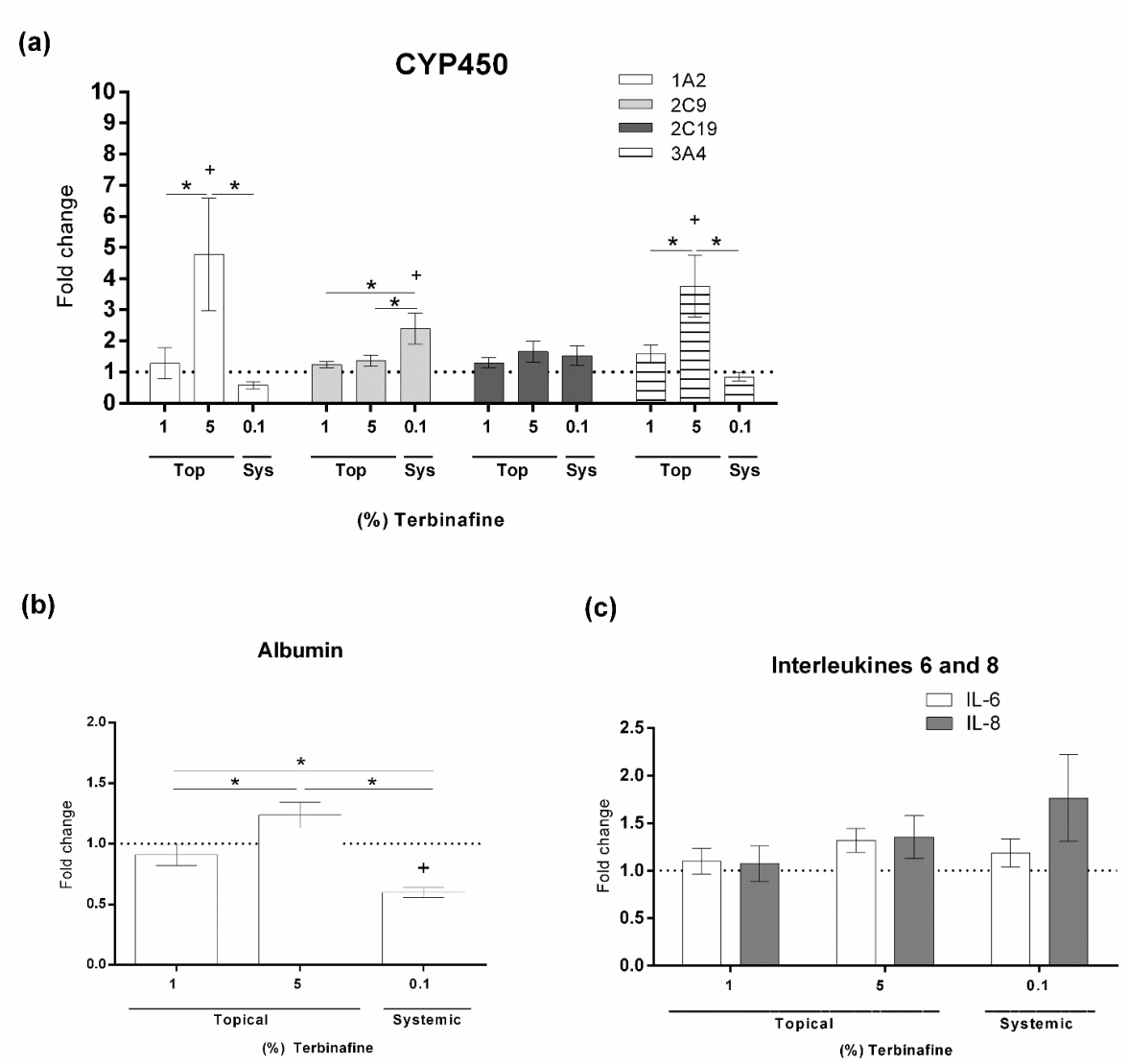

Figure 11. Substance effects on hepatic gene expression. Hepatic expression of **(a)** CYP 1A2, 2C9, 2C19, 3A4 **(b)** albumin and **(c)** IL-6 and IL-8 expressed as a fold change to the ethanol solvent control (dotted line). Where "+" means difference from solvent control (1), $p < 0.05$, and "*" means difference between treatments, $p < 0.05$. Mean ± SEM; duplicates or triplicates from three independent experiments resulting in n = 6 or 9 samples per group.

4. Discussion

Three-dimensional tissues are currently mostly cultivated and tested in static conditions (Ataç et al., 2013; Groeber et al., 2011; OECD, 2019; Shevchenko et al., 2010). The innovation of our skin irritation study, contrary to what usually happens, did not focus exclusively on the initial cascade event of skin viability but also analyzed other endpoints to evaluate the second and third events, related to the metabolism of xenobiotics, and the release or gene expression of cytokines. In addition, we included the skin models in a microphysiological circuit associated with a liver model to compare the events of toxicity after the topical and systemic exposure of substances.

First of all, instead of reconstructed human epidermal (RHE) model recommended for skin irritation test, we have chosen an in-house full-thickness RHS, since previous studies demonstrated that dermal fibroblasts play a pivotal role in epidermal differentiation, maturation, in the skin barrier formation, tissue homeostasis, and cutaneous wound healing (Jevtić et al., 2020). Our RHS efficiently mimics the morphology of human skin (Tavares et al., 2020) observed in Figure 2a, either cultured in static condition (**Figure 2b**) with 100% skin medium or in HUMIMIC Chip2 with 50% skin medium plus 50% liver medium (**Figure 2c**). While proliferative cells are located in the basal layers, apoptotic cells are located in the upper layers close to the stratum corneum as expected (**Figure 3 c and d**).

In our study, we constructed all the skin models with pool of three patients in every batch, aiming to reduce patient related variability; however, this procedure was not enough to obtain small standard deviations in the skin gene expression analyses, or in the IL-6 release. Even though *in vitro* assays offer a more controlled environment, primary cells are not representative of a larger pool of donors (Wikinson, 2019) and show individuals differences presenting a limitation concerning reproducibility. On the other side, in the liver model, consisting of the fully differentiated cell line HepaRG and primary HSC, the gene expression was much more reproducible between batches and among the nine replicates.

The liver model protocol was established previously (Wagner et al., 2013). It mimics the microenvironment of the liver and the flow is reported to prevent the necrosis in spheroids and upregulate cell activity back to levels observed in freshly isolated human primary cells (Vinci et al., 2011). (**Figure 4**). In addition, 3D liver

spheroids cultivated under flow condition are more predictive to human's toxicity than 2D liver primary cells (Eglen, 2017; Davidge, Bishop, 2017).

Analyzing each cell type used in our liver spheroid, HSCs are liver-specific mesenchymal cells that contribute to liver physiology and pathophysiology (Akbari et al., 2019). In a healthy liver, HSCs are quiescent at baseline, and their function is to store vitamin A lipid droplets. Following damage due to toxins or viral infections, HSCs become metabolically active resulting in the accumulation of cell–extracellular matrix in liver (Akbari et al., 2019). HSCs have limited proliferation capacity in 2D culture, cannot maintain the quiescent phenotype, and spontaneously lose key functional features in vitro (Akbari et al., 2019). In this study, HSCs were cultivated with differentiated HepaRGs, which is a tumor-derived cell line, that readily proliferates; but their functionality may be quite different from healthy tissue (Wilkinson, 2019). However, Coll and co-workers (2018) observed when grown as 3D spheroid co-cultures together with HepaRG cells, HSCs stored vitamin A and, more importantly, they switched from a quiescent state to an activated state in response to hepatic toxicity. Also, in a study done by Lübberstedt and co-workers (2010), they compared primary human hepatocytes (pHH) with HepaRG for hepatotoxicity studies (Hepatocyte-specific parameters like expression of five CYP450 and albumin release). They concluded that HepaRG cells could provide a suitable alternative to pHH in pharmaceutical research and development for metabolism studies such as CYP induction or sub-chronic to chronic hepatotoxicity studies. In another study conducted by Maschmeyer and co-workers (2015b), the liver equivalents (also made of HepaRG and HSC) responded properly to the respective troglitazone challenge, as demonstrated at the mRNA and immunohistochemistry level. These studies demonstrate how the use of HepaRG plus HSC is a good alternative instead of the gold standard, the human liver donor tissue, since it is limited due to the restricted living time demanding cryopreservation to match the time window for experiments (Wikinson. 2019; Lübberstedt et al.,2010). Besides that, it is difficult to isolate representative pools from different donors for every experiment in order to reduce patient-related responses.

In parallel, the focus of skin irritation is placed on IL-1α as an inflammatory mediator, since it is one of the primary cytokines secreted by the keratinocytes capable of initiating cutaneous inflammation (Newby et al., 2000). The disruption of the human skin barrier increases IL-1α release (Wood et al., 1997; Xiang and Yang, 1998) and

causes the production of tumor necrosis factor and IL-1α by fibroblasts, which stimulates the production of IL-6, firstly, by epidermal keratinocytes, whereas fibroblasts in the dermis represent a secondary source of this cytokine (Wang et al., 2004). In addition, full-thickness skin wound models produced IL-6 locally and released it within 30 min after injury; enhanced IL-6 levels have been described 24 h after treatment (Wang et al., 2004). For that reason, we selected IL-6 for the quantification in the medium, which, for instance, indicated that the Chip2 conditions presented the lowest IL-6 amounts for terbinafine, solvent control and DPBS treatments, probably due to medium circulation and liver clearance. Our liver model was made mainly by HepaRG cell, and those cells are reported to be involved in the clearance of recombinant human IL-6 through their IL-6 receptor (Heinrich et al., 1990). The SDS skin treatments released significant low amount for static RHS ($p < 0.05$) when compared to the other treatments in the static condition. In the Chip2, SDS treatments reduced the release, however, it was not considered significant when compared to the other treatments in the Chip2 condition. This was probably due to the reduced values in the IL-6 release observed for all the other Chip2 treatments. The reduction in the IL-6 release is expected by irritant compounds due to the early keratinocyte death right after substance application (necrosis), like we observed in the immunofluorescence slides (Figure 3a). IL-1α also stimulates a sequential release of IL-8, which is a potent neutrophil attractant stimulated by irritants or sensitizers due to skin damage (Mallampati et al., 2010). Also, Li and coworkers (2016) suggested that the differentiated production of IL-1α and IL-8 might be linked to the irritant or sensitizer potential of the agent, respectively, for that reason we analyzed IL-6 and IL-8 expressions beyond IL-1α. Finally, we analyzed the expression of the receptor involved in the skin permeability and repair and in the regulation of cytokine production, the EGFR. Terbinafine treatments did not affect epidermal expressions of the three ILs and EGFR in the skin static condition; however, in the Chip2, topical 5% terbinafine showed to be more sensitive than static one, upregulating IL1α significantly ($p < 0.05$) comparing to solvent control, and comparing with systemic terbinafine in the Chip2 (**Figure 10a**). The difference in the gene expressions of interleukins IL-6 and 8 in the terbinafine-treated skins were not significant **(Figure 10b, c)**.

The disruptive positive control, 5 % SDS, in the static condition was the only substance considered a skin irritant by MTT (1.81 %) and LDH (79 %) viability studies. The LDH assay was performed to validate the results obtained by the MTT assay (Li

et al., 2016). However, the LDH quantified in the Chip2 was very low (19 %) for the positive irritant control. The LDH activity was not suitable to measure early signs of toxicity due to the Chip2 medium perfusion or the irritant was applied too early before homeostasis of the chip system was reached. As observed by Wagner and co-workers (2013) who studied the LDH release by skin biopsies on-chip, a stable LDH concentration was obtained in the system after six days. It was maintained during the days of the experiment in the untreated models, while they observed an increase of LDH activity in response to the treatment of troglitazone from day four. The three days of our study were probably too short to observe a significant increase in the LDH activity induced by the acute irritation process; however they were chosen in order to follow OECD TG 439.

Looking at the metabolic data, SDS treatments represented the lowest glucose consumption and the lowest lactate production (**Figure 7**) when compared to DPBS. As mentioned previously, a healthy liver synthesizes albumin, which is a biomarker for liver functionality (Wagner et al., 2013). We observed a reduction in the albumin secretion in the medium of circuits treated with SDS (day 3) compared to the medium before treatment (day 1); however, it was not considered significant (Figure 8). This protein is reduced or downregulated in the liver acute phase response (Heinrich et al., 1990). In the fluorescence images, SDS reduced both proliferation and apoptosis, suggesting necrosis in the liver spheroids. Taken all together, we confirmed the toxic potential of 5 % SDS for the skin and suggests a potential hepatotoxic impact on the co-cultured liver spheroids.

Secondly, we chose a highly lipophilic substance to accumulate in the skin or to be able to pass it; terbinafine is a commercially available topical medicine (Lamisil AT® 1 % cream – containing 1 % terbinafine HCl) and is not reported as a skin irritant (FDA, 2012). Topical 1 % and 5 % terbinafine was detected as non-irritant in both static and dynamic conditions by the prediction model, even when dissolved in a permeation enhancer (ethanol) (Lachenmeier, 2008), since it did not reduce the cell viability to less than 50 % as specified by the ECVAM protocol (Miyani and Hughes, 2017; OECD, 2019). Nevertheless, the topical 5% terbinafine application reduced the cell viability significantly ($p < 0.05$) in comparison to topical 1% terbinafine application. In addition, those concentrations did not increase the LDH release by more than 50 %, establishing a parallel with the OECD prediction model of 50 % cutoff for MTT.

Besides the absence of skin irritation, topical 5 % terbinafine application significantly affected liver gene regulations in the Chip2, by the upregulation of CYP1A2 and 3A4. It shows that at this concentration terbinafine penetrated the RHS barrier, reached the circulation and was pumped to the liver spheroids, where it induced the metabolism of terbinafine by side-chain oxidation, dihydrodiols formation and deamination, the primary reactions promoted by these enzymes (Vickers et al., 1999). This was not observed for topical 1% terbinafine. Also, topical 5 % terbinafine treatment seems to reduce the number of proliferating liver cells and increased apoptosis, in the immunofluorescence slides, suggesting superior hepatic impact.

Finally, we observed in the systemic 0.1% terbinafine treatment, Chip2 RHS showed to be more sensitive than static ones, upregulating EGFR significantly ($p < 0.05$) comparing to solvent control (**Figure 10d**). It also caused liver gene dysregulations: significant ($p < 0.05$) downregulation of albumin (impairment of liver functionality) suggesting hepatotoxic signs as expected. Hence, we observed an increase in apoptotic cells in the liver immunofluorescence slides compared to the untreated liver spheroids. Additionally, CYP2C9 was significantly upregulated ($p < 0.05$) suggesting increased metabolism of this drug.

The evaluation of CYPs 1A2, 2C9, 2C19 and 3A4 enzymes in the liver reveal its regular metabolism functions. Terbinafine does not usually inhibit most major CYP enzymes at the clinically relevant concentration of 0.01 % (Vickers et al., 1999), which suggests its tenfold concentration (0.1 %) in plasma could present hepatic effect; since it has a small therapeutic index (FDA, 2012). However, taking all the results together, systemic 0.1 % terbinafine treatment was mild toxic for the RHS to liver spheroids, but this hepatic effect could not be detected by the LDH/glucose/lactate and albumin secretion analyses.

The liver mechanism of defense is usually related to IL-6 release, which then signals to release IL-8 (Orjalo et al., 2009). After IL-6 is synthesized *in vivo* in a skin lesion in the initial stage of inflammation, it moves to the liver through the bloodstream and reduces the production of fibronectin, albumin and transferrin (Tanaka et al., 2014). This correlation between IL-6 and albumin dysregulation was not observed in the gene expression analyses for terbinafine treatments.

Another limitation of the study observed is related to Chip2 metabolic analyses and IL-6 release in the Chip2, since we considered the Chip2 as one unit made of two “organs” interconnected, it was not possible to separate the contributions of each

“organ” in our medium analyses. One approach already used in the literature for more than one organ-on-a-chip, is to assess the cultivation of one organ at a time in the chip (only skin, and in parallel only the liver) as performed by Maschmeyer and co-workers (2015b) and Materne and co-workers (2015), the later has found the exposure of the co-culture to be more sensitive compared to respective single-tissue cultures in the multi-organ-chip. In our study, when we apply the substance topical on the skin, the substance needs to penetrate through the skin barrier and is then further transported to the liver compartment by active pumping, conversely than when we apply a known concentration fully in the medium (systemic). However, in order to solve the questions raised from organ- specific contributions, we followed many gene expressions of each “organ” to assess the effects of the test chemicals in the skin or in the liver. Microfluidic technology is being used to develop cost-effective in vitro models for lead compounds that can more reliably predict the efficacy, toxicity and pharmacokinetics of drug compounds in humans, as well as for novel screening assays (Cui, Wang, 2019). The added benefit of the multi-organ-chip is the addition of a second organ.

Herein, we showed the importance of the co-cultivation of the RHS and liver model in the skin irritation assay, since the additional hepatotoxic evaluation gives a clearer picture of toxicity. Our study suggests that these endpoints evaluated are suitable for extra irritancy/toxicity analyses in the detection of mild toxicants, since we measured the impact caused by those substances in the skin and the co-cultured liver model. Meanwhile, the combination of a skin and liver models allowed an assessment of toxic or metabolic responses in the liver caused by chemicals able to pass through the skin barrier. This would not have been measurable in the traditional static RHS culture. In other words, the conceptual advantage of skin-on-a-chip platform is not new. However, it was the first time that a work group takes profits of the microphysiological platforms to apply a published OECD guideline, to assess a specific endpoint (irritation) combined with other toxic and metabolic endpoints. This showed the increased complexity and also presents the limitations of the association of the skin model with another organoid like the liver model, to translate systemic toxic or metabolic missing effects not observed in the conventional static skin irritation assay. Therefore, the present study opens a more complex approach based on a microphysiological system to assess more than a skin irritation process.

Acknowledgments

This work was developed at TissUse GmbH, Berlin, Germany, within the framework of the National Institute of Science and Technology of Pharmaceutical Nanotechnology (INCT-Nanofarma), which is supported by “Fundação de Amparo à Pesquisa do Estado de São Paulo” (Fapesp, Brazil, grant #14/50928-2) and “Conselho Nacional de Pesquisa” (CNPq, Brazil, grant #465687/2014-8), and by the Bundesministerium für Bildung und Forschung (Berlin-Brandenburg Research Platform BB3R, grant number 031A262A). Renata Tavares thanks the call DAAD/CAPES/CNPq 15° 2017 for the fellowship grant 290281/2017-2 and grant 132062/2014-3.

Author contributions statements

Renata S N Tavares: Conceptualization; data curation; formal analysis; investigation; methodology; visualization; roles/writing – original draft. **Thi P Tao:** Investigation; formal analysis; roles/writing – original draft. **Annika Winter and Ilka Maschmeyer:** Project administration; resources; supervision; visualization. **Silvya S Maria-Engler**: Methodology. **Christian Zoschke and Monika Schafer-Korting**: Funding acquisition; roles/writing – original draft. **Roland Lauster**: Methodology; project administration; roles/writing – original draft **Uwe Marx:** Conceptualization, project administration; funding acquisition; resources. **Lorena R Gaspar**: Project administration; resources; roles/writing – original draft; supervision. **All the authors** approved the final version submitted.

Competing interests

Uwe Marx is a shareholder and CEO of TissUse GmbH, Germany, which is commercializing the microphysiological HUMIMIC chip platform. All other authors declare no competing interests.

Data availability

The datasets generated and/or analyzed during the current study are available from the corresponding author on reasonable request.

References

Abaci, H. E., Gledhill, K., Guo, Z., Christiano, A. M., Shuler, M.L., 2015. Pumpless microfluidic platform for drug testing on human skin equivalents. *Lab Chip*. 7, 15(3): 882–888. https://doi.org/10.1039/c4lc00999a.

Alexander Jr., F.A., Eggert, S., Wiest, J., 2019. Skin-on-a-Chip: Transepithelial Electrical Resistance and Extracellular Acidification Measurements through an Automated Air-Liquid Interface. *Genes*, 9, 114. https://doi.org/10.3390/genes9020114.

Akbari, S., Arslan, N., Senturk, S. and Erdal, E. 2019. Next-Generation Liver Medicine Using Organoid Model, *Front. Cell Dev*. Biol., 7:345. https://doi.org/10.3389/fcell.2019.00345.

Ataç, B., Wagner, I., Horland, R., Lauster, R., Marx, U., Tonevitsky, A.G., Azar, R.P., Lindner, G., 2013. Skin and hair on-a-chip: in vitro skin models versus ex vivo tissue maintenance with dynamic perfusion. *Lab Chip*. 13, 3555–3561. https://doi.org/10.1039/c3lc50227a.

Bacqueville, D., Jacques, C., Duprat, L., Jamin, E.L., Guiraud, B., Perdu, E., Bessou-Touya, S., Zalko, D., Duplan, H., 2017. Characterization of xenobiotic metabolizing enzymes of a reconstructed human epidermal model from adult hair follicles. *Toxicol. Appl. Pharmacol.* 329, 190–201. https://doi.org/10.1016/j.taap.2017.05.040.

Bal-Öztürk, A., Miccoli, B., Avci-Adali, M., Mogtader, F., Sharifi, F., Çeçen, B., Yaşayan, G., Braeken, D., Alarcin, E., 2018. Current strategies and future perspectives of skin-on-a-chip platforms: Innovations, technical challenges and commercial outlook. *Curr. Pharm. Des.* 24**,** 5437–5457. https://doi.org/10.2174/1381612825666190206195304.

Bauer, S., Wennberg Huldt, C., Kanebratt, K.P., Durieux, I., Gunne, D., Andersson, S., Ewart, L., Haynes, W.G., Maschmeyer, I., Winter, A., Ämmälä, C., Marx, U., Andersson, T.B., 2017. Functional coupling of human pancreatic islets and liver spheroids on-a-chip: Towards a novel human ex vivo type 2 diabetes model. *Sci. Rep.* 7, 14620. https://doi.org/10.1038/s41598-017-14815-w.

Coll, M., Perea, L., Boon, R., Leite, S. B., Vallverdu, J., Mannaerts, I., et al. 2018. Generation of hepatic stellate cells from human pluripotent stem cells enables in vitro modeling of liver fibrosis. *Cell Stem Cell* 23, 101–113.e7. https://doi.org/10.1016/j.stem.2018.05.027

Cui, P, Wang, S. 2019. Application of microfluidic chip technology in pharmaceutical analysis: A review. *Journal of Pharmaceutical Analysis* 9, 238–247.

Davidge, K.S. and Bishop, J. 2017. Improved IC50 Prediction Using Quasi Vivo®. Society of Toxicology Annual Meeting. Baltimore, MD.

Dehne, E.M., Hasenberg, T., Marx, U., 2017. The ascendance of microphysiological systems to solve the drug testing dilemma. *Future Sci. OA.* 3, FSO185. https://doi.org/10.4155/fsoa-2017-0002.

Eglen, R. 2017. The Use of Tumour Spheroids in Cancer Research. [video] Available at: https://www.youtube.com/watch?v=pQdiAhNNrfY [Accessed 06 June, 2020].

Jevtić, M., Lowa, A., Novačkovab, A., Kovačikb, A., Kaessmeyerc, S., Erdmannd, G., Vavrovab, K., Hedtricha, S. 2020. Impact of intercellular crosstalk between epidermal keratinocytes and dermal fibroblasts on skin homeostasis. *BBA - Molecular Cell Research* 1867:8. https://doi.org/10.1016/j.bbamcr.2020.118722.

Fabbrocini, G., Panariello, L., Caro, G., Cacciapuoti, S., 2015. Acneiform rash induced by EGFR inhibitors: Review of the literature and new insights. *Skin Appendage Disord.* 1, 31–37. https://doi.org/10.1159/000371821.

FDA: Food and Drug Administration, 2012. Lamisil (terbinafine hydrochloride) *Highlights of prescribing information.* https://www.accessdata.fda.gov/drugsatfda_docs/label/2012/020539s021lbl.pdf.

Gibbs, S., Vietsch, H., Meier, U., Ponec, M., 2002. Effect of skin barrier competence on SLS and water-induced IL-1alpha expression. *Exp. Dermatol.* 11, 217–223. https://doi.org/10.1034/j.1600-0625.2001.110304.x.

Graham, C., Chooniedass, R., Stefura, W.P., Lotoski, L., Lopez, P., Befus, A.D., Becker, A.B., Hayglass, K.T., 2017. Stability of pro- and anti-inflammatory immune biomarkers for human cohort studies. *J. Transl. Med.* 15, 53. https://doi.org/10.1186/s12967-017-1154-3.

Groeber, F., Holeiter, M., Hampel, M., Hinderer, S., Schenke-Layland, K., 2011. Skin tissue engineering--in vivo and in vitro applications. *Adv. Drug Deliv. Rev.* 63, 352–366. https://doi.org/10.1016/j.addr.2011.01.005.

Heinrich, P.C., Castell, J.V., Andus, T., 1990. Interleukin-6 and the acute phase response. *Biochem. J.* 265, 621–636. https://doi.org/10.1042/bj2650621.

Hryncewicz-Gwózdz, A., Wojciechowska-Zdrojowy, M., Maj, J., Baran, W., Jagielski, T., 2016. Paradoxical reaction during a course of terbinafine treatment of

trichophyton interdigitale infection in a child. *JAMA Dermatol.* 152, 342–343. https://doi.org/10.1001/jamadermatol.2015.4293.

Hübner, J., Raschke, M., Rütschle, I., Gräßle, S., Hasenberg, T., Schirrmann, K., Lorenz, A., Schnurre, S., Lauster, R., Maschmeyer, I., Steger-Hartmann, T., Marx, U., 2018. Simultaneous evaluation of anti-EGFR-induced tumour and adverse skin effects in a microfluidic human 3D co-culture model. *Sci. Rep.* 8, 15010. https://doi.org/10.1038/s41598-018-33462-3.

Kandarova, H., Liebsch, M., 2017. The EpiDerm™ Skin Irritation Test (EpiDerm SIT™), in Eskes, C., Van Vliet, E., Maibach, H. (Eds.), *Alternatives for Dermal Toxicity Testing.* Switzerland: Springer, Cham.

Lachenmeier, D.W., 2008. Safety evaluation of topical applications of ethanol on the skin and inside the oral cavity. *J. Occup. Med. Toxicol.* 3, 26. https://doi.org/10.1186/1745-6673-3-26.

Li, H., Toh, P.Z., Tan, J.Y., Zin, M.T., Lee, C.Y., Li, B., Leolukman, M., Bao, H., Kang, L., 2016. Selected biomarkers revealed potential skin toxicity caused by certain copper compounds. *Sci, Rep.* 6, 37664. https://doi.org/10.1038/srep37664.

Lübberstedt, M., Müller-Vieira, U., Mayer, M., Biemel, K.M., Knöspel, F., Knobeloch, D.; Nüssler, A. K., Gerlach, J.C., Zeilinger, K. 2011. HepaRG human hepatic cell line utility as a surrogate for primary human hepatocytes in drug metabolism assessment in vitro. *Journal of Pharmacological and Toxicological Methods,* 63, 59–68.

Mallampati, R., Patlolla, R.R., Agarwal, S., Babu, R.J., Hayden, P., Klausner, M., Singh, M.S., 2010. Evaluation of EpiDerm full thickness-300 (EFT-300) as an in vitro model for skin irritation: Studies on aliphatic hydrocarbons. *Toxicol. In Vitro* 24, 669–676. https://doi.org/10.1016/j.tiv.2009.08.019.

Maschmeyer, I., Lorenz, A.K., Schimek, K., Hasenberg, T., Ramme, A.P., Hübner, J., Lindner, M., Drewell, C., Bauer, S., Thomas, A., Sambo, N.S., Sonntag, F., Lauster, R., Marx, U., 2015a. A four-organ-chip for interconnected long-term co-culture of human intestine, liver, skin and kidney equivalents. *Lab Chip.* 15, 2688–2699. https://doi.org/10.1039/c5lc00392j.

Maschmeyer I, Hasenberg T, Jaenicke A, Lindner M, Lorenz AK, Zech J, Garbe LA, Sonntag F, Hayden P, Ayehunie S, Lauster R, Marx U, Materne EM. 2015b. Chip-based human liver-intestine and liver-skin co-cultures--A first step toward systemic

repeated dose substance testing in vitro. Eur J Pharm Biopharm. Sep;95 (Pt A):77-87. https://doi.org/10.1016/j.ejpb.2015.03.002.

Materne, E.M., Maschmeyer, I., Lorenz, A.K., Horland, R., Schimek, K.M., Busek, M., Sonntag, F., Lauster, R., Marx, U., 2015. The multi-organ chip--a microfluidic platform for long-term multi-tissue coculture. *J. Vis. Exp.* e52526. https://doi.org/10.3791/52526.

Miyani, V.A., Hughes, M.F., 2017. Assessment of the in vitro dermal irritation potential of cerium, silver, and titanium nanoparticles in a human skin equivalent model. *Cutan. Ocul. Toxicol.* 36, 145–151. https://doi.org/10.1080/15569527.2016.1211671.

Newby, C.S., Barr, R.M., Greaves, M.W., Mallet, A.I., 2000. Cytokine release and cytotoxicity in human keratinocytes and fibroblasts induced by phenols and sodium dodecyl sulfate. *J. Invest. Dermatol.* 115, 292–298. https://doi.org/10.1046/j.1523-1747.2000.00056.x.

OECD: Organisation for Economic Co-operation and Development. (2019). In vitro skin irritation: Reconstructed human epidermis test method, in *Chemicals*, O.G.F.T.T.O. (Ed.) Test No 439*.* Paris: OECD Publishing.

Orjalo, A.V., Bhaumik, D., Gengler, B.K., Scott, G.K., Campisi, J., 2009. Cell surface-bound IL-1alpha is an upstream regulator of the senescence-associated IL-6/IL-8 cytokine network. *Proc. Natl. Acad. Sci. U S A.* 106, 17031–17036. https://doi.org/10.1073/pnas.0905299106.

Ramadan, Q., Ting, F.C., 2016. In vitro micro-physiological immune-competent model of the human skin. *Lab Chip.* 16, 1899–1908. https://doi.org/10.1039/c6lc00229c.

Schimek, K., Hsu, H.H., Boehme, M., Kornet, J.J., Marx, U., Lauster, R., Pörtner, R., Lindner, G., 2018. Bioengineering of a full-thickness skin equivalent in a 96-well insert format for substance permeation studies and organ-on-a-chip applications. *Bioengineering (Basel).* 5. https://doi.org/10.3390/bioengineering5020043.

Schimek, K., Markhoff1, A., Sonntag, F., Blechert, M., Lauster, R., Marx, U., Lindner, G. 2015. Integrating skin and vasculature in a Multi-Organ-Chip Platform. *BMC Proceedings,* 9 (Suppl 9):P20. https://doi.org/10.1186/1753-6561-9-S9-P20

Shevchenko, R.V., James, S.L., James, S.E., 2010. A review of tissue-engineered skin bioconstructs available for skin reconstruction. *J. R. Soc. Interface.* 7, 229–258. https://doi.org/10.1098/rsif.2009.0403.

Sriram, G., Alberti, M., Dancik, Y., Al., E., 2018. Full-thickness human skin-on-chip with enhanced epidermal morphogenesis and barrier function. *Mater. Today*. 2*1*. https://doi.org/10.1016/j.mattod.2017.11.002.

Tanaka, T., Narazaki, M., Kishimoto, T., 2014. IL-6 in inflammation, immunity, and disease. *Cold Spring Harb. Perspect. Biol.* 6, a016295. https://doi.org/10.1101/cshperspect.a016295.

Tavares, R.S.N., Maria-Engler, S.S., Colepicolo, P., Debonsi, H.M., Schäfer-Korting, M., Marx, U., Gaspar, L.R., Zoschke, C., 2020. Skin irritation testing beyond tissue viability: Fucoxanthin effects on inflammation, homeostasis, and metabolism *Pharmaceutics.* 136, 1–12. https://doi.org/10.3390/pharmaceutics12020136.

Van Eijl, S., Zhu, Z., Cupitt, J., Gierula, M., Götz, C., Fritsche, E., Edwards, R.J., 2012. Elucidation of xenobiotic metabolism pathways in human skin and human skin models by proteomic profiling. *PLoS One.* 7, e41721. https://doi.org/10.1371/journal.pone.0041721.

Vickers, A.E., Sinclair, J.R., Zollinger, M., Heitz, F., Glänzel, U., Johanson, L., Fischer, V., 1999. Multiple cytochrome P-450s involved in the metabolism of terbinafine suggest a limited potential for drug-drug interactions. *Drug Metab. Dispos.* 27, 1029–1038.

Vinci, B., C. Duret, S., Klieber, S., Gerbal-Chaloin, A., Sa-Cunha, S., Laporte, B., Suc, P., Maurel, A., Ahluwalia and M. Daujat-Chavanieu 2011. Modular Bioreactor for Primary Human Hepatocyte Culture: Medium Flow Stimulates Expression and Activity of Detoxification Genes. *Biotechnology Journal*. 6(5), pp. 554–564.

Wagner, I., Materne, E.M., Brincker, S., Süssbier, U., Frädrich, C., Busek, M., Sonntag, F., Sakharov, D.A., Trushkin, E.V., Tonevitsky, A.G., Lauster, R., Marx, U., 2013. A dynamic multi-organ-chip for long-term cultivation and substance testing proven by 3D human liver and skin tissue co-culture. *Lab Chip.* 13, 3538–3547. https://doi.org/10.1039/c3lc50234a.

Wang, X.P., Schunck, M., Kallen, K.J., Neumann, C., Trautwein, C., Rose-John, S., Proksch, E., 2004. The interleukin-6 cytokine system regulates epidermal permeability barrier homeostasis. *J. Invest. Dermatol.* 123, 124–131. https://doi.org/10.1111/j.0022-202X.2004.22736.x.

Wood, L.C., Stalder, A.K., Liou, A., Campbell, I.L., Grunfeld, C., Elias, P.M., Feingold, K.R., 1997. Barrier disruption increases gene expression of cytokines and the 55

kD TNF receptor in murine skin. *Exp. Dermatol.* 6, 98–104. https://doi.org/10.1111/j.1600-0625.1997.tb00154.x.

Wufuer, M., Lee, G., Hur, W., Jeon, B., Kim, B.J., Choi, T.H., Lee, S., 2016. Skin-on-a-chip model simulating inflammation, edema and drug-based treatment. *Sci. Rep.* 6, 37471. https://doi.org/10.1038/srep37471.

Xiang, M., Yang, T., 1998. [A study of Nexin 1 of skin and hair follicle during postnatal development period of rat]. *Zhongguo Yi Xue Ke Xue Yuan Xue Bao.* 20, 127–132.

Yeganeh, M.H., Mclachlan, A.J., 2000. Determination of terbinafine in tissues. *Biomed. Chromatogr.* 14, 261–268. https://doi.org/10.1002/1099-0801(200006)14:4<261::AID-BMC983>3.0.CO;2-X.

Zoschke, C., Gonska, H., Kral, V., Kapfer, C., Schäfer-Korting, M. 2017. Isolation of keratinocytes and fibroblasts from human specimens. Available from: https://www.bb3r.de/forschungsplattform/Standardarbeitsvorschriften/SOP_cell-isolation_171109.pdf.

Zoschke C, Ulrich M, Sochorová M, Wolff C, Vávrová K, Ma N, Ulrich C, Brandner JM, Schäfer-Korting M. 2016. The barrier function of organotypic non-melanoma skin cancer models. *J Control Release*. 10;233:10-8. https://doi.org/10.1016/j.jconrel.2016.04.037.

5. DISCUSSÃO

Há um alto percentual de novos fármacos que falham em estudos clínicos, apesar de terem sido testados com sucesso em animais durante a pesquisa pré-clínica, o que indica que os testes em animais têm dificuldades em se correlacionar com os resultados em humanos (HARTUNG et al., 2012). Assim, para que o teste *in vitro* seja aprovado pela OECD como alternativo à experimentação animal, este deve apresentar maior correlação com humanos e o ensaio em animais.

Buscando essa alta correlação com humanos, a presente tese se baseou nos métodos alternativos *in vitro* desde os ensaios mais básicos em monocamadas aos mais complexos e inovadores como a microfluídica de órgãos em chip. Cada ensaio, seja ele mais simples ou mais complexo, contribuiu para a avaliação do potencial tóxico da substância em questão.

Foi desenvolvido um modelo de pele humana completa e posteriormente esse modelo foi reduzindo a um tamanho compatível com o chip microfluídico. Este modelo se apresentou mais vantajoso por ser realizado em menos dias, utilizando menor quantidade de material e células e ainda sim foi considerado reprodutível e adequado aos ensaios com ele propostos (fotoirritação, irritação e atividade antioxidante por meio da inibição de ERO). Os ensaios que utilizaram o modelo de pele foram comparados com resultados em monocamadas no primeiro capítulo, foram extrapolados com análises além viabilidade celular no segundo capítulo e, os modelos de pele foram cultivados tanto na forma estática quando em microfluídica associando-se ao modelo de fígado no terceiro e último capítulo. Todos os trabalhos desenvolvidos têm em comum a utilização dos ensaios *in vitro* utilizando tecidos 3D na avaliação de toxicidade e/ou eficácia de substâncias de uso tópico e/ou sistêmico.

No primeiro capítulo, abordamos a prospecção da alga marinha originária da Antártica *Desmarestia anceps* até o isolamento da fucoxantina. Esta parte do trabalho foi iniciada em colaboração com a professora Hosana Maria Debonsi e o professor Pio Colepicolo Neto durante o mestrado; entretanto, no doutorado, a substância isolada foi submetida a ensaios de fotoestabilidade quando incorporada em formulação fotoprotetora e sua fototoxicidade e atividade antioxidante avaliadas em modelo de pele humana reconstituída 3D (RHS).

Um dos resultados mais interessantes desse capítulo foi o controverso comportamento da fucoxantina que foi marcadamente fototóxica no ensaio em monocamadas, mas quando avaliada em modelo de pele 3D não apresentou potencial fotoirritante a 0,5% (p/v). Enquanto isso, a predição de fototoxicidade do controle

positivo cetoprofeno a 3%, foi confirmada uma vez que o modelo de pele 3D irradiado apresentou redução da viabilidade superior a 30 %, quando comparado ao não irradiado (KANDAROVA; LIEBSCH, 2017).

Este comportamento de fototoxicidade em fibroblastos 3T3 e ausência de fototoxicidade em modelo de pele ocorre devido ao teste 3T3 NRU-PT ser muito sensível e como consequência ele é superestimado podendo produzir resultados falso-positivos (GASPAR; KAWAKAMI; BENEVENUTO, 2017; KANDAROVA; LIEBSCH, 2017). Ainda, nos modelos de pele reconstituída, acima da derme que contém os fibroblastos, há a epiderme estratificada em camada viável (basal, espinhosa, granulosa) e o estrato córneo com a função barreira. Essa função também modifica a penetração da substância até camadas viáveis (mais profundas), influenciando a biodisponibilidade da mesma pela pele. Ainda, os modelos cutâneos são mais permeáveis que a pele humana (KEJLOVÁ et al., 2007), o que significa que dificilmente produzem resultados falso-negativos. Portanto, os ensaios de fototoxicidade sugeriram que a fucoxantina não apresenta potencial fototóxico para a pele humana na concentração estudada (0,5%). Após essa confirmação, buscou-se saber se a mesma era eficaz, ou seja, se a fucoxantina tem propriedades antioxidantes quando aplicada topicamente. Para tal, o potencial antioxidante foi avaliado nos queratinócitos HaCat e no modelo de pele; em ambos os ensaios foi utilizado a sonda fluorescente e permeável $DCFH_2$-Da. O resultado de inibição do ERO foi significativo tanto para a substância pura em monocamadas, quanto no modelo de pele a 0,5% incorporada em filtro solar, indicando que, mesmo em concentrações 50 vezes menores (no ensaio em monocamadas), a fucoxantina já apresenta ação protetora contra as ERO produzidas pela radiação UVA na pele. Ainda, a formulação contendo apenas filtros solares não reduziu significativamente a produção de ERO na pele 3D.

No capítulo 2, realizado durante o doutorado sanduíche em colaboração com o grupo da professora Dra. Monika Schäfer-Korting (Berlim, Alemanha), o comportamento da fucoxantina quanto ao potencial de irritação cutânea foi estudado. Primeiramente, a partir do protocolo desenvolvido no Brasil para modelos pele, o mesmo foi miniaturizado de 1,13cm^2 para 0.6 cm^2 para se adaptar aos estudos em microfluídica, além das vantagens relacionadas com economia de material, células e o aumento do número amostral.

O ensaio de irritação cutânea (OECD *Test Guideline* nº 439) foi concebido para prever e classificar o potencial de irritação de uma substância química através da

avaliação da viabilidade do tecido de RhE (OECD, 2017). A irritação aguda é uma resposta inflamatória local e reversível das células das camadas viáveis da pele em resposta à lesão direta causada pela aplicação de uma substância irritante (WORTH et al., 2014). O potencial para induzir irritação da pele é uma consideração importante incluída nos procedimentos para o manuseio, embalagem e transporte seguro de produtos químicos (WORTH et al., 2014).

Com o objetivo de obter uma análise detalhada sobre o comportamento da fucoxantina na pele, o guia de irritação cutânea foi seguido, no entanto, não somente visando a viabilidade dos tecidos pelo ensaio do MTT. A proposta de avaliar a capacidade da fucoxantina a 0,5% (p/v) provocar alterações na expressão de genes relacionados a inflamação (IL-1a,6,8), homeostase (EGFR, HSPB1) e ao metabolismo (NAT1) também foi considerada interessante, uma vez que estes são genes que podem estar desregulados frente a um agente irritante (TAVARES et al., 2020) sem que a viabilidade necessariamente seja alterada.

A fucoxantina provou ser não-irritante na pele 3D, embora tenham sido observadas alterações em genes relacionados à inflamação (regulação negativa) e metabolismo (regulação positiva) quando a mesma foi veiculada em etanol absoluto. Demonstrou tanto pela viabilidade dos tecidos quanto pela reduzida expressão gênica de IL-6 e 8 ter melhorado os sinais deletérios gerados pelo etanol absoluto nos modelos e ter tido superior biodisponibilidade pelo aumento na expressão de NAT1 em relação a fucoxantina em alqui benzoato. Esses resultados foram imprescindíveis para acrescentar a discussão sobre a escolha dos veículos ideais na solubilização de substâncias lipofílicas. Também foram úteis para definir o desenho experimental do último capítulo, que também se baseou no guia de irritação (OECD *Test Guideline* nº 439), porém avaliou a terbinafina, que é um fármaco muito utilizado e tem estudos em número suficiente para respaldar os achados do nosso trabalho. Incluímos alguns marcadores que foram mais promissores do estudo anterior, como as IL-1α, IL-6 e IL-8 e o EGFR, marcadores de viabilidade metabólicos (LDH, lactato e glicose), bem como marcadores específicos para o modelo de fígado (albumina e enzimas do CYP450).

Neste terceiro capítulo, a inovação do estudo foi a de realizar o guia de irritação cutânea, que foi desenvolvido para modelos de pele cultivados de forma estática, no chip dinâmico e microfluídico de dois compartimentos (Chip2), onde ainda foram adicionados os esferoides de fígado, aumentando a complexidade do sistema teste.

Neste artigo, além da avaliação da aplicação tópica de duas concentrações da terbinafina (1 e 5%), foram avaliados os efeitos causados pelas substâncias após permearem a pele até o meio de cultura e consequentemente até o segundo compartimento do modelo de fígado. Também foram avaliados os resultados de toxicidade por meio de uma aplicação sistêmica da terbinafina (0,1%), como um controle hepatotóxico.

O controle positivo, recomendado pelo guia, LSS 5% (p/v), também foi incluso e foi o único considerado irritante cutâneo por meio da viabilidade celular (abaixo de 50%), mudanças na morfologia dos tecidos, redução nos níveis de lactato e glicose e de liberação de IL-6. Na condição estática, o modelo de pele tratado com LSS liberou quantidades significativas de LDH (82%) ($p > 0.05$), corroborando com a redução na viabilidade observada pelo MTT. Entretanto, esse aumento não ocorreu no Chip2 e a teoria principal foi a falta de tempo para a homeostase dessa proteína de alto peso molecular (superior a 140 kDa). Ainda, em ambos os sistemas (cultivo estático ou dinâmico) as concentrações tópicas e sistêmica de terbinafina não foram consideradas irritante pelos níveis metabólicos. Entretanto, no Chip2 a concentração tópica aplicada de LSS bem como a concentração sistêmica 0,1% foram consideradas tóxicas para o fígado seja pelo aumento na expressão da enzima CYP2C9 pela redução na expressão de albumina, ou mudanças na proporção de células apoptóticas dos esferoides. Ainda, a concentração sistêmica de terbinafina aumentou a expressão do EGFR no RHS do Chip2. Ainda apenas no Chip2 a concentração tópica de terbinafina 5% aumentou a expressão de IL-1α no RHS e mostrou ter atravessado a pele, uma vez que esta concentração aumentou no número de células apoptóticas enquanto reduziu das células proliferativas nos esferoides de fígado e ainda aumentou na expressão das CYPs 1A2 e 3A4 de forma significativa ($p > 0,05$).

A vantagem da análise de toxicidade, como a irritação cutânea, associando outro “órgão” ao modelo de pele em microfluídica foi a superior sensibilidade do modelo de pele após a aplicação de terbinafina tópica a 5% e sistêmica a 0,1% detectada pelo aumento na expressão gênica de IL-1α e de EGFR, respectivamente. Além disso, foi observado aumento no metabolismo da terbinafina pelo modelo de fígado por expressão gênica após a aplicação tópica da mesma a 5%, bem como sinais de hepatotoxicidade após a aplicação tópica do irritante LSS, por imunofluorescência, o que constata efeitos hepáticos de substâncias que foram capazes de permear o modelo de pele.

O presente estudo abriu perspectivas para uma nova abordagem *in vitro*, mais complexa, baseada no sistema microfluídico para avaliar toxicidade de substâncias muito além do desfecho de irritação cutânea.

6. CONCLUSÃO

A fucoxantina foi isolada da alga *D. anceps* e identificada como all-*trans*-fucoxantina; nos estudos de fotoestabilidade ela foi considerada fotoinstável, mas quando veiculada em filtro solar, a formulação foi considerada fotoestável não reduzindo em mais de 20% a degradação após a irradiação e ainda aumentou em 72% a absortividade da formulação demonstrando efeito UV-*booster*.

A fucoxantina foi considerada fototóxica no ensaio em monocamadas e este resultado não se confirmou no ensaio em pele 3D na concentração de 0,5%, o que era esperado uma vez que este tipo de ensaio apresenta limitações tais como a superestimação dos resultados de toxicidade devido ausência do estrato córneo como barreira de permeação cutânea, o que aumenta muito a sua biodisponibilidade frente a condições reais de uso; quanto a atividade antioxidante, tanto no ensaio e monocamadas quanto em modelo de pele 3D, foi observada uma inibição significativa na produção de ERO induzidas pelo UVA, demonstrando propriedades fotoprotetoras que deverão ser melhor investigadas nos ensaios clínicos.

O modelo de pele humana reconstituída produzida *in house*, foi miniaturizada com sucesso, manteve as excelentes características morfofisiológicas emulando a pele humana;

O modelo miniaturizado foi adequado para predizer o potencial irritação e fototoxicidade dos controles positivos, negativos, das substâncias teste fucoxantina e da terbinafina; o modelo também considerado adequado para o cultivo em chip microfluídico de dois compartimentos.

Os biomarcadores IL1-α, IL-6, IL-8, EGFR e NAT1 utilizados no estudo de irritação cutânea contribuíram para confirmação da ausência de potencial irritante da fucoxantina; demonstrou também efeito anti-inflamatório da fucoxantina em relação aos efeitos deletérios do etanol nos tecidos (reduziu a expressão de gênica de IL-6 e IL-8) e superior biodisponibilidade quando neste veículo (aumento na expressão de NAT1), efeitos não observados para a fucoxantina em alquil benzoato.

O ensaio de irritação cutânea pôde ser realizado tanto em uma condição estática quanto dinâmica em chip microfluídico (Chip2).

Em ambos os ensaios de irritação (estático versus Chip2), a terbinafina não foi considerada irritante por meio dos resultados metabólicos, de liberação de IL-6 e ainda pela análise de viabilidade celular por LDH e MTT (nos tecidos estáticos), o controle positivo LSS foi considerado irritante e no cultivo no Chip2, o LSS demonstrou também efeitos deletérios nos esferoides de fígado, demostrando ter atravessado o RHS. No

entanto, a terbinafina tópica a 5% aumentou a expressão de IL-1α no RHS apenas do cultivo no Chip2 e aumentou a expressão das enzimas hepáticas CYP1A2 e CYP3A4, modificou a proporção de células proliferativas/apoptóticas nos esferoides, demonstrando ter permeado o RHS. Já a aplicação sistêmica de 0,1% de terbinafina aumentou a expressão de EGFR apenas no RHS do Chip2 e aumentou as células apoptóticas no fígado, além de regular negativamente o gene hepáticos de albumina e positivamente a enzima CYP2C9, agindo como um controle hepatotóxico de terbinafina. A combinação de RHS e fígado no Chip2 em microfluídica permitiu uma resposta mais sensível do RHS observada pela expressão gênica. O cultivo no Chip2 permitiu também a avaliação de efeitos hepáticos causados pelas substâncias capazes de atravessar o RHS.

Em geral e nas condições aplicadas, o aumento da complexidade dos ensaios *in vitro* ampliaram as análises de toxicidade e eficácia das substâncias corroborando com a hipótese de que quanto mais complexos e semelhantes ao microambiente nativo os sistemas *in vitro* forem, maior será a relevância para predizer a toxicidade em seres humanos.

7. REFERÊNCIAS

ALÉPÉE, N.; BAHINSKI, A.; DANESHIAN, M.; DE WEVER, B. *et al.* State-of-the-art of 3D cultures (organs-on-a-chip) in safety testing and pathophysiology. **ALTEX**, 31, n. 4, p. 441-477, 2014.

ANTONI, D.; BURCKEL, H.; JOSSET, E.; NOEL, G. Three-dimensional cell culture: a breakthrough *in vivo*. **Int J Mol Sci**, 16, n. 3, p. 5517-5527, Mar 2015.

ATAÇ, B.; WAGNER, I.; HORLAND, R.; LAUSTER, R. *et al.* Skin and hair on-a-chip: *in vitro* skin models versus ex vivo tissue maintenance with dynamic perfusion. **Lab Chip**, 13, n. 18, p. 3555-3561, Sep 2013.

BALLS, M. The History of Alternative Test Methods in Toxicology. *In*: BALLS, M.; ROBERT*, et al* (Ed.). 2018. cap. 1.1, p. 2-6.

BRASIL. **DECRETO Nº 6.899, DE 15 DE JULHO DE 2009.** Brasília, DF.

CANAVEZ, A. D. P. M.; SILVEIRA, T. M. T. P.; VITA, N. D. A.; WEIHERMANN, A. C. *et al.* Integrated Safety Strategy for the Development of Children's Cosmetic Products Using *In vitro* and Clinical Methodologies *In*: ESKES, C.;MAIBACH, H. I.*, et al* (Ed.). **Alternatives for Dermal Toxicity Testing**. Switzerland, 2017. cap. 41, p. 565-576.

CERIDONO, M.; TELLNER, P.; BAUER, D.; BARROSO, J. *et al.* The 3T3 neutral red uptake phototoxicity test: practical experience and implications for phototoxicity testing--the report of an ECVAM-EFPIA workshop. **Regul Toxicol Pharmacol**, 63, n. 3, p. 480-488, Aug 2012.

CURREN, R. D.; ESKES, C.; CHENG, S.; H., H. E. Contributions to the Development of Alternatives in Toxicology in China and Brazil. *In*: BALLS, M.;COMBES, R.*, et al* (Ed.). **The History of Alternative Test Methods in Toxicology**. Switzerland, 2018. cap. 2.9, p. 87-94.

D'ORAZIO, N.; GEMELLO, E.; GAMMONE, M. A.; DE GIROLAMO, M. *et al.* Fucoxantin: a treasure from the sea. **Mar Drugs**, 10, n. 3, p. 604-616, Mar 2012.

DE VECCHI, R.; DAKIC, V.; MATTOS, G.; RIGAUDEAU, A.-S. *et al.* Implementation, availability and regulatory status of an OECD accepted Reconstructed Human Epidermis model in Brazil. **Vigilância Sanitária em Debate**, 6, p. 64, 02/28 2018.

DEHNE, E. M.; HASENBERG, T.; MARX, U. The ascendance of microphysiological systems to solve the drug testing dilemma. **Future Sci OA**, 3, n. 2, p. FSO185, Jun 2017.

ESKES, C.; HOFMANN, M. Overview on Current Status of Alternative Methods and Testing Approaches for Skin Irritation Testing *In*: ESKES, C.;MAIBACH, H. I.*, et al* (Ed.). **Alternatives for Dermal Toxicity Testing**. Switzerland, 2017. cap. 1, p. 3-24.

EWART, L.; FABRE, K.; CHAKILAM, A.; DRAGAN, Y. *et al.* Navigating tissue chips from development to dissemination: A pharmaceutical industry perspective. **Exp Biol Med (Maywood)**, 242, n. 16, p. 1579-1585, 10 2017.

FDA: Food and Drug Administration, 2012. Lamisil (terbinafine hydrochloride) Highlights of prescribing information. https://www.accessdata.fda.gov/drugsatfda_docs/label/2012/020539s021lbl.pdf.

GASPAR, L. R.; KAWAKAMI, C. M.; BENEVENUTO, C. G. Overview on the Current Status of Available Test Methods and Additional Promising Methods for Assessing UV-Induced Effects. *In*: AL., C. E. E. (Ed.). **Alternatives for Dermal Toxicity Testing**. AG: © Springer International Publishing, 2017. cap. 33, p. 463.

HARTUNG, T. Perspectives on. **Appl *In vitro* Toxicol**, 4, n. 4, p. 305-316, Dec 2018.

_____.; VAN VLIET, E.; JAWORSKA, J.; BONILLA, L. *et al.* Systems toxicology. **ALTEX**, 29, n. 2, p. 119-128, 2012.

HASENBERG, T.; MÜHLEDER, S.; DOTZLER, A.; BAUER, S. *et al.* Emulating human microcapillaries in a multi-organ-chip platform. **J Biotechnol**, 216, p. 1-10, Dec 2015.

HEINONEN, T.; VERFAILLIE, C. Key Technologies and Tools. *In*: BALLS, M.;COMBES, R.*, et al* (Ed.). **The History of Alternative Test Methods in Toxicology**, 2018. cap. 5.1, p. 265-274.

ICH. International Council for Harmonisation of Technical Requirements for Pharmaceuticals for Human Use. Photosafety evaluation of pharmaceuticals. S10 Guideline 2013.

JENNINGS, P. "The future of *in vitro* toxicology". **Toxicol *In vitro***, 29, n. 6, p. 1217-1221, Sep 2015.

KANDAROVA, H.; LIEBSCH, M. The EpiDerm™ Phototoxicity Test (EpiDerm™ H3D-PT) *In*: AL., C. E. E. (Ed.). **Alternatives for Dermal Toxicity Testing**. Switzerland: Springer International Publishing, 2017. cap. 35.

KEJLOVÁ, K.; JÍROVÁ, D.; BENDOVÁ, H.; KANDÁROVÁ, H. *et al.* Phototoxicity of bergamot oil assessed by *in vitro* techniques in combination with human patch tests. **Toxicol *In vitro***, 21, n. 7, p. 1298-1303, Oct 2007.

LELIÈVRE, D.; JUSTINE, P.; CHRISTIAENS, F.; BONAVENTURE, N. *et al.* The EpiSkin phototoxicity assay (EPA): development of an *in vitro* tiered strategy using 17 reference chemicals to predict phototoxic potency. **Toxicol *In vitro***, 21, n. 6, p. 977-995, Sep 2007.

MARX, U.; AKABANE, T.; ANDERSSON, T. B.; BAKER, E. *et al.* Biology-inspired microphysiological systems to advance patient benefit and animal welfare in drug development. **ALTEX**, 02 2020.

_____.; ANDERSSON, T. B.; BAHINSKI, A.; BEILMANN, M. *et al.* Biology-inspired microphysiological system approaches to solve the prediction dilemma of substance testing. **ALTEX**, 33, n. 3, p. 272-321, 2016.

MATERNE, E. M.; MASCHMEYER, I.; LORENZ, A. K.; HORLAND, R. *et al.* The multi-organ chip--a microfluidic platform for long-term multi-tissue coculture. **J Vis Exp**, n. 98, p. e52526, Apr 2015.

OECD. Organisation for Economic Co-operation and Development. G**uidance document o**n using cytotoxicity tests to estimate starting doses for acute oral systematic toxicity tests. **OECD Publishing**, Paris, 2001.

_____. Organisation for Economic Co-operation and Development. *Guidance Document on an Integrated Approach on Testing and Assessment (IATA) for Skin Corrosion and Irritation*. **OECD Publishing**, Paris, 2014.

_____. Organisation for Economic Co-operation and Development. *In vitro* Skin Irritation: Reconstructed Human Epidermis Test Method. **OECD Publishing**, Paris, pp. 18, 2019.

_____. Organisation for Economic Co-operation and Development. Test No. 432: *In vitro* 3T3 NRU Phototoxicity Test, OECD Guidelines for the Testing of Chemicals. **OECD Publishing**, 2004.

TAVARES, R. S. N.; KAWAKAMI, C. M.; PEREIRA, K. C.; DO AMARAL, G. T. *et al.* Fucoxanthin for Topical Administration, a Phototoxic vs. Photoprotective Potential in a Tiered Strategy Assessed by *In vitro* Methods. **Antioxidants (Basel)**, 9, n. 4, Apr 2020.

_____; MARIA-ENGLER, S. S.; COLEPICOLO, P.; DEBONSI, H. M. *et al.* Skin Irritation Testing beyond Tissue Viability: Fucoxanthin Effects on Inflammation, Homeostasis, and Metabolism **Pharmaceutics**, 136, p. 1-12, 2020.

VICKERS, A. E.; SINCLAIR, J. R.; ZOLLINGER, M.; HEITZ, F. *et al.* Multiple cytochrome P-450s involved in the metabolism of terbinafine suggest a limited potential for drug-drug interactions. **Drug Metab Dispos**, 27, n. 9, p. 1029-1038, Sep 1999.

WORTH, A.; VIEGAS BARROSO, J. F.; BREMER, S.; BURTON, J. *et al.* **Alternative methods for regulatory toxicology – a state-of-the-art review**. 2014.

WORTH, A. P. Types of Toxicity and Applications of Toxicity Testing *In*: BALLS, M.;COMBES, R.*, et al* (Ed.). **The History of Alternative Test Methods in Toxicology**: Andre Wolff, 2018. cap. 1.2, p. 7-10.

WUFUER, M.; LEE, G.; HUR, W.; JEON, B. *et al.* Skin-on-a-chip model simulating inflammation, edema and drug-based treatment. **Sci Rep**, 6, p. 37471, 11 2016.

YEGANEH, M. H.; MCLACHLAN, A. J. Determination of terbinafine in tissues. **Biomed Chromatogr**, 14, n. 4, p. 261-268, Jun 2000.

YOON NO, D.; LEE, K. H.; LEE, J.; LEE, S. H. 3D liver models on a microplatform: well-defined culture, engineering of liver tissue and liver-on-a-chip. **Lab Chip**, 15, n. 19, p. 3822-3837, Oct 2015.

ANEXOS

Anexo 01

As Revistas *Antioxidants* e *Pharmaceutics*, onde estão publicados os artigos 1 e 2 da presente tese, são da base MDPI. A base MDPI possui a regra de acesso e de permissões que atesta que os artigos são de propriedade dos autores, podendo por eles ser reproduzido integramente, ao exemplo da reprodução integral em tese de doutorado. A seguir os dizeres do site e o email de confirmação do mencionado:

MDPI Open Access Information and Policy

All articles published by MDPI are made immediately available worldwide under an open access license. This means:

- everyone has free and unlimited access to the full-text of *all* articles published in MDPI journals;
- everyone is free to re-use the published material if proper accreditation/citation of the original publication is given;
- open access publication is supported by the authors' institutes or research funding agencies by payment of a comparatively low **Article Processing Charge (APC) (/about/apc)** for accepted articles.

Permissions

No special permission is required to reuse all or part of article published by MDPI, including figures and tables. For articles published under an open access Creative Common CC BY license, any part of the article may be reused without permission provided that the original article is clearly cited. Reuse of an article does not imply endorsement by the authors or MDPI.

Acesso em 25/04/2020 (https://www.mdpi.com/about/openaccess)

Anexo 02

Renata Spagolla Napoleão Tavares <renatasnt@usp.br>

copyright and licensing permission

Yilia Yu <yilia.yu@mdpi.com> 4 de março de 2020 11:07
Para: Renata Spagolla Napoleão Tavares <renatasnt@usp.br>
Cc: pharmaceutics@mdpi.com

Dear Renata,

Thank you for your message. As our journal is Open Access, the copyright belongs to the authors. More detailed information could be found at the below link:
https://www.mdpi.com/about/openaccess

Hope this is helpful for you.

Best,
Yilia

On 2020/3/3 22:46, Renata Spagolla Napoleão Tavares wrote:

> Dear Ms Yilia Yu,
>
> I would like to know how to get licensing permission to include the full papers "pharmaceutics-661030" and the submitted "antioxidants-736863" in my thesis.
> Could you help me with this?
>
> Thank you in advance.
> Best regards,
> Renata
> --
> *MSc **Renata Spagolla Napoleão Tavares*
> *Farmacêutica*
> *FCFRP - USP*
> *+55 31 995204718*

Anexo 03

Comprovante de publicação do Artigo 1: TAVARES, R. S. N.; KAWAKAMI, C. M.; PEREIRA, K. C.; DO AMARAL, G. T. et al. Fucoxanthin for Topical Administration, a Phototoxic vs. Photoprotective Potential in a Tiered Strategy Assessed by *In vitro* Methods. Antioxidants, 9, n. 4, 2020

antioxidants

an Open Access Journal by MDPI

Indexed in: PubMed | CITESCORE 4.88 SCOPUS | IMPACT FACTOR 4.520

CERTIFICATE OF PUBLICATION

Certificate of publication for the article titled:

Fucoxanthin for Topical Administration, a Phototoxic vs. Photoprotective Potential in a Tiered Strategy Assessed by In Vitro Methods

Authored by:

Renata Spagolla Napoleão Tavares; Camila Martins Kawakami; Karina de Castro Pereira; Gabriela Timotheo do Amaral; Carolina Gomes Benevenuto; Silvya Stuchi Maria-Engler; Pio Colepicolo; Hosana Maria Debonsi; Lorena Rigo Gaspar

Published in:

Antioxidants **2020**, Volume 9, Issue 4, 328

MDPI Academic Open Access Publishing since 1996

Basel, April 2020

Anexo 04

Comprovante de publicação do Artigo 2: TAVARES, R. S. N.; MARIA-ENGLER, S. S.; COLEPICOLO, P.; DEBONSI, H. M. et al. Skin Irritation Testing beyond Tissue Viability: Fucoxanthin Effects on Inflammation, Homeostasis, and Metabolism Pharmaceutics, 136, p. 1-12, 2020

pharmaceutics

an Open Access Journal by MDPI

Indexed in: PubMed | CITESCORE 4.58 SCOPUS | IMPACT FACTOR 4.773

CERTIFICATE OF PUBLICATION

Certificate of publication for the article titled:

Skin Irritation Testing beyond Tissue Viability: Fucoxanthin Effects on Inflammation, Homeostasis, and Metabolism

Authored by:

Renata Spagolla Napoleão Tavares; Silvya Stuchi Maria-Engler; Pio Colepicolo; Hosana Maria Debonsi; Monika Schäfer-Korting; Uwe Marx; Lorena Rigo Gaspar; Christian Zoschke

Published in:

Pharmaceutics **2020**, Volume 12, Issue 2, 136

MDPI Academic Open Access Publishing since 1996

Basel, April 2020

Anexo 05

Emails de comprovação de submissão do ARTIGO 3 a revista *"International Journal of Pharmaceutics"*, sob o número de referência: IJP-D-20-01177

International Journal of Pharmaceutics <eesserver@eesmail.elsevier.com> 28 de abril de 2020 22:26
Responder a: International Journal of Pharmaceutics <ijp@elsevier.com>
Para: renatasnt@usp.br

*** Automated email sent by the system ***

Dear Dr. Renata Spagolla Napoleão Tavares,

You have been listed as a Co-Author of the following submission:

Journal: International Journal of Pharmaceutics
Title: Toxicity of Topically Applied Drugs beyond Skin Irritation: Static Skin Model vs. Two Organs-on-a-Chip
Corresponding Author: Lorena Gaspar
Co-Authors: Renata Spagolla Napoleão Tavares, MSc; Thi P Tao, Master; Ilka Maschmeyer, Ph.D.; Silvya S Maria-Engler, Ph.D.; Monika Schäfer-Korting, Ph.D.; Annika Winter, Ph.D.; Christian Zoschke, Ph.D.; Uwe Marx, Dr;

To be kept informed of the status of your submission, register or log in (if you already have an Elsevier profile).

Register here: https://ees.elsevier.com/ijp/default.asp?acw=&pg=preRegistration.asp&user=coauthor&fname=Renata&lname=Spagolla Napoleão Tavares&email=renatasnt@usp.br

Or log in: https://ees.elsevier.com/ijp/default.asp?acw=&pg=login.asp&email=renatasnt@usp.br

If you did not co-author this submission, please do not follow the above link but instead contact the Corresponding Author of this submission at lorenagaspar@gmail.com;lorena@fcfrp.usp.br.

Thank you,

International Journal of Pharmaceutics

20/07/2020 E-mail de Universidade de São Paulo - Fwd: Your Submission IJP-D-20-01177

Renata Spagolla Napoleão Tavares <renatasnt@usp.br>

Fwd: Your Submission IJP-D-20-01177

Lorena Rigo Gaspar Cordeiro <lorena@fcfrp.usp.br> 30 de maio de 2020 20:50
Para: renatasnt <renatasnt@usp.br>

--------- Mensagem encaminhada ---------
De: **International Journal of Pharmaceutics** <eesserver@eesmail.elsevier.com>
Data: sáb, 30 de mai de 2020 às 20:42
Assunto: Your Submission IJP-D-20-01177
Para: <lorenagaspar@gmail.com>, <lorena@fcfrp.usp.br>

Ms. Ref. No.: IJP-D-20-01177
Title: Toxicity of Topically Applied Drugs beyond Skin Irritation: Static Skin Model vs. Two Organs-on-a-Chip
International Journal of Pharmaceutics or its open access mirror

Dear Dr. Gaspar,

Comments on your paper have now been received and are attached to this message. Please consider all the points made and upon returning your paper detail your responses and the actions taken.

Please submit the revised manuscript by Jul 30, 2020. Upon receipt of your revised paper, we will inform you of the outcome as soon as possible. Papers not received within that that time period will be considered to be withdrawn, you are welcome to resubmit your paper as a new submission at a later date.

NOTE: While submitting the revised manuscript, please double check the author names provided in the submission so that authorship related changes are made in the revision stage. If your manuscript is accepted, any authorship change will involve approval from co-authors and respective editor handling the submission and this may cause a significant delay in publishing your manuscript.

PLEASE NOTE: International Journal of Pharmaceutics or its open access mirror would like to invite you to enrich your article by including a list of up to 10 names of chemical compounds studied in the article.

Include interactive data visualizations in your publication and let your readers interact and engage more closely with your research. Follow the instructions here: https://www.elsevier.com/authors/author-services/data-visualization to find out about available data visualization options and how to include them with your article.

Thank you for submitting your work to the journal.

MethodsX file (optional)
We invite you to submit a method article alongside your research article. This is an opportunity to get full credit for the time and money you have spent on developing research methods, and to increase the visibility and impact of your work. If your research article is accepted, your method article will be automatically transferred over to the open

https://mail.google.com/mail/u/1?ik=066ebe44dd&view=pt&search=all&permmsgid=msg-f%3A1668161349338983395&simpl=msg-f%3A1668161349338983395 1/5

Anexo 06

Comprovante do Comitê de Ética em pesquisa aprovado para o projeto relacionado ao uso de células primárias humanas do ARTIGO 1.

29/04/2020 Plataforma Brasil

BRASIL

principal sair

Lorena Rigo Gaspar Cordeiro - Pesquisador | V3.2

Cadastros

Sua sessão expira em: 39min 36

DETALHAR PROJETO DE PESQUISA

DADOS DA VERSÃO DO PROJETO DE PESQUISA

Título da Pesquisa: Avaliação da fototoxicidade e performance de novos filtros solares de origem marinha.
Pesquisador Responsável: Lorena Rigo Gaspar Cordeiro
Área Temática:
Versão: 1
CAAE: 55438216.0.0000.5403
Submetido em: 25/04/2016
Instituição Proponente: Faculdade de Ciências Farmacêuticas de Ribeirão Preto - USP
Situação da Versão do Projeto: Aprovado
Localização atual da Versão do Projeto: Pesquisador Responsável
Patrocinador Principal: Financiamento Próprio

PLATAFORMA BRASIL COORDENADOR ORIGINAL PLATAFORMA BRASIL

Comprovante de Recepção: PB_COMPROVANTE_RECEPCAO_702407